DIVISION OF PORT AND OCEAN ENGINEERING
Alfred Getz vei 3
N 7034 Trondheim-NTH, NORWAY
Tlf. (075)94630

THESIS

TITLE	THESIS NO.
SAND WAVES IN FREE SURFACE FLOW.	P-1-84
A STUDY WITH EMPHASIS ON HYDRODYNAMIC ASPECTS.	**DATE** 08-08-84
STUDENT	**NUMBER OF PAGES**
Hermann Moshagen	**AVAILABILITY** Open

SUMMARY

The problem of sand wave generation in free surface flow has been presented and its engineering and scientific significance has been pointed out. A survey of the existing literature on the subject has been performed. The survey concludes with a need for improved understanding of the responsible instability mechanism.

An in detail study of depth effects on the classical Kelvin-Helmholtz instability, particularly in thin fluid layers, leads to a generalised version of the K-H stability model, which in turn is applied to a free surface flow with bed shear. This model is discussed theoretically and physically. As part of this some qualitative experiments are presented and commented on with a view to the theoretical model. The study shows that the actual K-H model contains several of the basic features of sand wave generation.

KEYWORD	SUPERVISOR
SAND WAVES	*Geir Moe*
SEDIMENT FLOW	Geir Moe, Professor, advisor
CHANNEL FLOW	
INSTABILITY	*Alf Tørum*
KELVIN-HELMHOLTZ	Alf Tørum, Professor, thesis supervisor

SAND WAVES IN FREE SURFACE FLOW

A STUDY WITH EMPHASIS ON HYDRODYNAMIC ASPECTS

BY

HERMANN MOSHAGEN

Preface

The present report is the documentation of a work that mainly was carried out while I was on a scholarship engagement at The Norwegian Institute of Technology, Division of Port and Ocean Engineering. This arrangement was made possible by a leave of permission from The Norwegian Hydrodynamic Laboratories. The experimental part was supported by Den norske stats oljeselskap a.s. My indebtedness to each of these bodies is hereby expressed.

Several individuals have been involved at different stages. With the following exceptions names are not mentioned. Professor Geir Moe backed up the arrangement initially and followed the work with continuous interest. Earlier inspiring collaboration with professor Alf Tørum at the River and Harbour Laboratory startet my interest in the challenging problems of dynamic interaction between flows and sediment beds. During the work I also had stimulating discussions with professor Bjørn Gjevik, University of Oslo, professor Torkild Carstens, River and Harbor Laboratory and Per Bruun, former professor in port and ocean engineering at The Technical University of Norway. Finally my family contributed with encouragement and patience during the whole work.

My thankfulness includes everybody involved.

Trondheim, August 1984

Hermann Moshagen.

CONTENTS

SYMBOLS

A_j – Determinantal terms in n – layer model, def. in eq. (8.18).

B_j – Determinantal terms in n – layer model, def. in eq. (8.19).

C – Sediment concentration, Engelund's theory.

C_b – Sediment concentration at bed level, Engelund's theory.

D – "Virtual" flow depth, Milne – Thomson theory.

F,F' – Hydraulic and shear Froude number resp.

G_0 – Surface wave coefficient in Reynolds' theory, def. in eg. (3.14)

K – Friction velocity coefficient in Engelund's theory.

$L=(1-m)q_s$ – Effective volume flux of sediments in Reynolds' theory.

U – Basic flow velocity. Indices count fluid layers downwards.

U_b – Basic flow at bed level, Engelund's theory.

ΔU – Velocity difference between neighbouring layers.

V – Average basic flow, Engelund's theory.

U_s – Shearing velocity field.

a – Perturbation amplitude. Indices count perturbed surfaces downwards.

$a_{j\pm1,j}$ – Amplitude ratio between neighbouring surfaceses.

$c=c+ic_i$ – Complex perturbation phase velocity of perturbation.

c_i – Growth velocity of perturbation.

$\bar{c}$ – Complex conjugate of c.

f – Perfurbed stream function, Engelund's theory.

$f_{1,2,3}$ – Functions used in discussion of K-H stability analysis results, def. in eq. (10.7)-(10.9).

h – Water depth. Indices count flow layers downwards.

h_s – Thickness of shearing layer.

k – Perturbation wave number.

k_c – Critical perturbation wave number.

m   – Sediment flow proportionality constant in Reynolds' theory.

n   – Sediment bed porosity.

q_b – Bed load sediment transport flow rate.

q_s – Transport rate of sediment flow.

q_t – Total sediment flow rate.

r   – Dimensionless density difference, def. in eg. (9.11).

t   – Time.

x   – Horizontal coordinate.

y   – Vertical coordinate.

u,v   – Perturbed velocity components.

w   – Sediment fall velocity.

α – Coefficient used in development of eigenvalue solutions, defined in App. A.

     – Sediment transport rate in Kennedy's analysis.

β – Coefficient used in eigenvalue analysis, def. in App.A.

     – Perturbation frequency in Anderson's theory.

     – Friction coefficient in Reynolds' theory.

γ – Coefficient used in development of eigenvalue solutions, defined in App.A.

δ – Do. Also long distance in Kennedy's theory.

κ – Coefficient used in eigenvalue analysis, def. in App.A.

ϵ – Diffusivity for turbulene and sediments in Engelund's theory.

     – Perturbation parameter in present stability model.

λ – Perturbation wave length.

λ_c – Critical perturbation wave length.

μ – Gravity coefficient in Fredsøe's analysis.

ξ – Eigenvalue in present theory, defined in eqns. (9.8) and (9.12).

ζ – Relative phase velocity, def. in eq. (9.8).

η – Perturbation of flow and bed. Indices count perturbed surfaces downwards.

σ – Complex angular frequency of perturbation.

τ – Shear stress on sediment bed.

ϕ – Perturbed sediment concentration in Engelund's theory.

         – Basic flow velocity potential in K-H theory.

Φ – Total flow velocity potential in K-H theory.

ϕ' – Perturbed flow velocity potential in K-H theory, def. in eq. (8.2.)

ρ – Fluid density. Indices count fluid layers downwards.

$\Delta\rho$ – Density difference between neighbouring layers.

ρ^* – Modified fluid density, def. in eq. (7.3).

$\Theta_{j\pm1,j}$ – Phase difference between neighbouring layers.

PART I

THE GRANULAR BED STABILITY PROBLEM

INCLUDING:

- AN INTRODUCTION TO THE SUBJECT

- A CLASSIFICATION OF BED FEATURES

- A SURVEY OF EXISTING STABILITY THEORIES

1. INTRODUCTION

1.1. An engineering and scientific subject.

The subject under study is related to the processes of erosion and sediment transport - both processes of paramount importance to human activities in many countries. They are met in a variety of civil engineering disciplines, thus mentioning

- structural protection against underscour offshore and on the coast, in harbours and rivers
- planning and management of waterways and navigation channels
- coastal and harbour engineering
- irrigation engineering
- flood control in rivers and reservoirs
- hydropower development in tunnels, rivers and canals.

Introductory books on the subject are for example the one by Engelund and Hansen and the one by Raudkivi. The books by Bruun and Gerritsen are written to meet more directly the needs of the coastal engineer. Several other books exist both for general purpose and for the various specialised application fields.

Be it also mentioned that basically the same or closely related processes are met in many other branches of engineering, such as the physical, chemical, metallurgical and agricultural branches.

Erosion and sediment transport are present as natural processes in the hydrologic, the coastal and the ocean environments. Even the movement of desert sand by wind is a similar process and - very likely - of the same basic nature as those found in wet environments. Thus researchers in both theoretical and descriptive natural sciences are also interested in the phenomena of erosion and sediment transport.

1.2. Erosion, Bed Forms and Stability

What is then the basic nature of erosion and sediment transport? More specifically we may ask:

- Under given flow and bed conditions when and where do
  we get erosion?
- How large will the sediment transport be?
- Where will the transported material settle down?
- What kind of dynamic processes are responsible for bringing
  heavy solid particles into suspension and kept suspended in a
  flowing fluid?
- What is the explanation for wave forms seen on a bed under
  erosion?

These and other questions have been asked and investigated by researchers from the fields of science and engineering mentioned. The work has gone on for several decades and the research activity at present is probably higher than ever. The amount of published literature on the subject is overwhelming as a consequence. Many questions have found their answers. Others remain partly or fully unanswered.

The question to be taken up in the following is the last one, and to a lesser extent the second last one:

- How do bed forms develop, and
- What is the connection between the erosion process and the
  generation of bed forms?

The important and interesting problems of suspension and transport of solid particles will then be left out of discussion. When a granular bed is eroded, wave forms, termed ripples, dunes or antidunes, are observed on the bed. In coastal areas and rivers also other forms (named shoals, bars, meanders etc.) are seen, but our concentration will be on the first three. A more comprehensive description and classification of granular bed wave forms will follow shortly. Before we do so we will address the question of the engineering significance of

the bed wave problem. We also regard somewhat closer the nature of the problem.

1.3. Engineering importance and hydrodynamic character of the bed form generation problem.

The wave forms enter the engineering problems in determining the flow conditions which in turn are needed to determine erosion and sediment transport.

Ripples act basically as roughness elements. However, as such they are several orders of magnitude larger than the grains that build them. So their influence on the flow is the more important. Adding to this is the fact that flow conditions that generate ripples are frequently occurring in engineering projects.

Dunes, being of the same extent and amplitude as the mean flow depth, on an order of magnitude scale, are as "roughness elements" of major influence on the flow. Their form drag influences the main flow as well as the free surface. And in addition a further influence comes from possibly coexisting ripples. Dunegenerating flows are also typical for those met in engineering.

Antidunes are less frequent both in nature and in engineering works since they occur only at supercritical flow conditions. However, when existing they interact strongly with flow and free surface and even cause the surface to break in some cases. So the flow can not be determined before the distribution and size of bed forms are known. On the other hand the bed forms are generated by the flow interacting with the bed. In other words: Flow and bed forms are parts of one and the same problem.

This is a situation very often met in hydrodynamics. But our problem is complicated further by the fact that the subjects under study - the granular materials - are composed of solid grains, i.e. particles not behaving as fluid elements. The particles themselves may vary by

density, size and shape. And when considering larger amounts one also may have to take the statistical distribution of the different qualities into account.

The laws of motion of single grains and grain ensembles are hard to establish. A large amount of the theoretical and empirical work confirms this. And in the attempt to handle the subject in hydrodynamic or hydraulic terms one also meets the question of relevance and usefulness of concepts and laws established for pure water flow. A general agreement, however, seems to exist between researchers on the subject: Bed waves are the result of a dynamic instability set up by water flowing over the bed.

A.J. Reynolds in 1974 gave a review paper at the Euromech 48 Symposium, where he placed the bed stability analysis in the general field of problems associated with erosion and transport of granular materials by the following figure.

The figure supplements earlier characterisation of the problem and emphasises the role of stability analysis as a central one. At the same time it pictures a more or less generally agreed opinion at that time about what type of principles or fields of knowledge that should form the basis of a granular bed stability analysis.

Thus, in summing up, we may state that we are facing a subject of wide engineering and scientific interest and of a high degree of descriptive and analytical complexity. In the following the most important contributions to the solution of the bed stability problem hitherto will be surveyed. First, however, the classification of bed forms as done by the ASCE Task Force on Bed Forms in Alluvial Channels will be reviewed and commented.
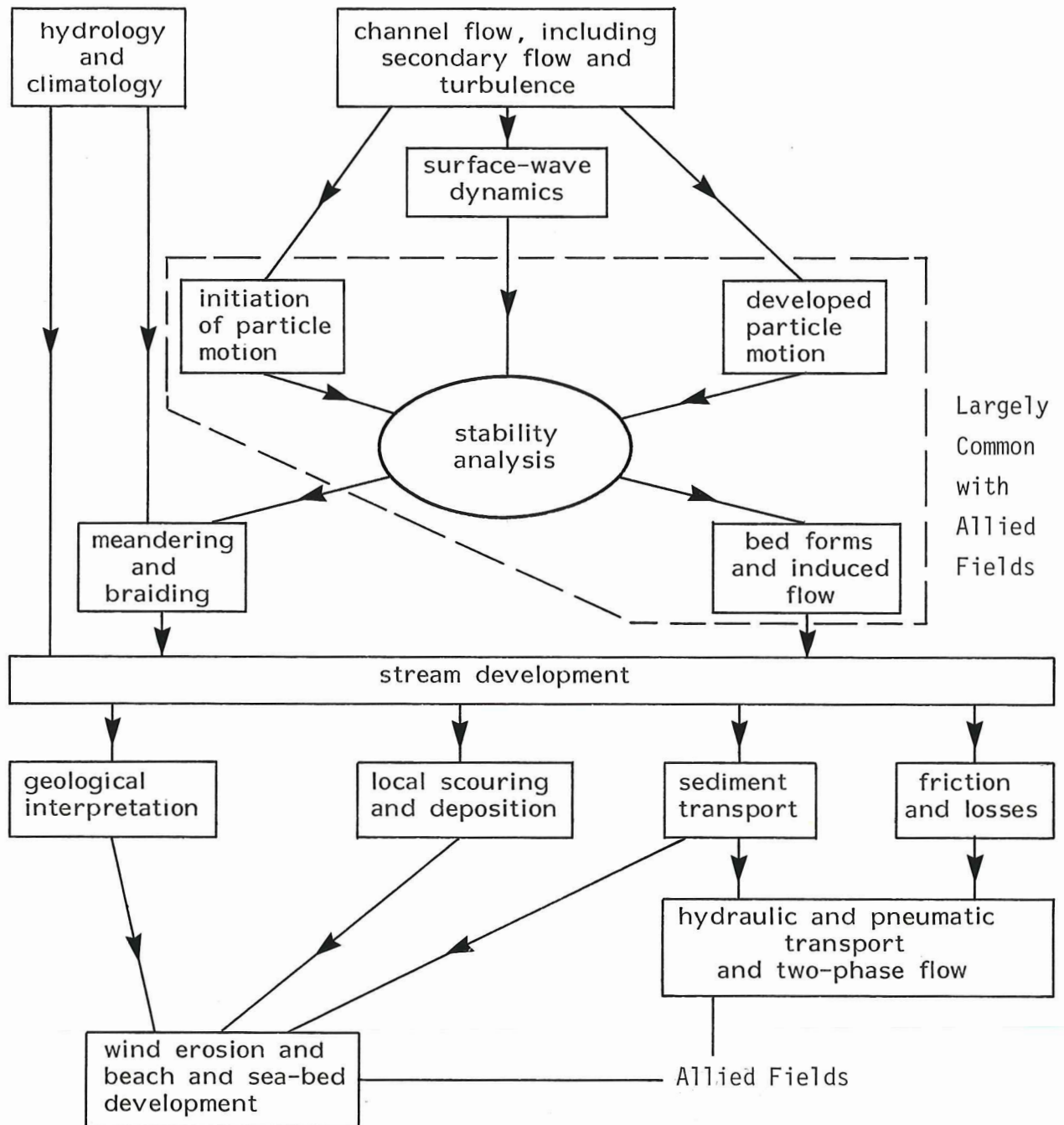
Fig.1.1. The place of bed stability analysis in the general field of problems associated with the erosion and transport of granular materials, after A.J. Reynolds, 1974.

2. CLASSIFICATION OF BED FORMS

2.1. The ASCE classification.

The classification of bed forms in this work is done according to the proposed nomenclature in the report of the Task Force on Bed Forms in Alluvial Channels of the ASCE Committee on Sedimentation, 1966:

Bed Form. – Any deviation, from a flat bed, that is readily detectable by eye or higher than the largest sediment size present in the parent bed material, generated on the bed of an alluvial channel by the flow.

Ripples. – Small bed forms with wave lengths less than approximately 1 ft and heights less than approximately 0.1 ft. Ripples occur at flow velocities slightly higher than those required for initiation of sediment motion, but at lower velocities than flat bed or antidunes. Parts of the upstream slopes of dunes are occupied by ripples under some flow conditions. In plan view, a ripple configuration can vary from an irregular array of three - dimensional peaks and pockets to a regular array of continuous parallel crest and troughs transverse to the direction of flow. In longitudinal section, ripple profiles vary from approximately triangular, with long gentle upstream slopes and downstream slopes approximately equal to the angle of repose of the bed material, to symmetrical nearly sinusoidal shapes. The triangular ripples commonly observed in alluvial channels move downstream with velocities that are small compared to the mean velocity of the generating flow. They are observed to occur only rarely in sediments coarser than approximately 0.6 mm.

Dunes. – Bed forms larger than ripples that are out of phase with any water surface gravity waves that accompany them. Dunes generally occur at larger velocities and sediment transport rates than ripples, but smaller velocities and transport rates than antidunes; however, ripples do occur on the

upstream slopes of dunes at the lower velocities in the dune regime. The lengths of dune crests are usually of the same order as the wave length. The longitudinal profiles of dunes are approximately equal to the angle of repose of the bed material. Dunes move slowly downstream with velocities that are small compared to the mean velocity of the generating flow. The large lee eddies that occur in dune troughs often cause surface boils of intense turbulence and high sediment concentration to occur above and slightly downstream from dune crests.

Transition. – A bed configuration consisting of a heterogeneous array of bed forms, primarily low-amplitude ripples or dunes and flat areas. The transition bed is a configuration generated by flow conditions intermediate to those producing dunes and flat bed. In laboratory flumes, the transition configuration has been observed in some cases to consist of dunes or ripples over a reach covering part of the channel length, and a flat bed over the remainder. The flow in the flat-bed reach is shallower than in the reach with ripples or dunes, and the discontinuity in the bed between the two reaches moves slowly downstream. In other instances, the bed configuration has been observed to consist of small, widely separated ripples or dunes over the entire bed.

Antidunes. – Bed forms that occur in trains and that are in phase with and strongly interact with gravity water surface waves. Antidunes can move upstream or downstream or can remain stationary, depending on the properties of the flow, fluid, and sediment. The free-surface waves have larger amplitudes than the antidunes. At higher velocities and Froude numbers, the surface waves usually grow until they become unstable and break in the upstream direction. The agitation accompanying breaking obliterates the antidunes, and the process of antidune initiation and growth is then repeated. At lower velocities, the antidunes will grow and then diminish in amplitude without the surface waves ever breaking. In longitudinal section, antidune profiles vary with flow and sediment properties from approximately triangular to sinusoidal, the latter occurring at larger

Froude numbers than the former. However, the sharp-crested, triangular-shaped antidunes have been observed only in laboratory flumes, and always move downstream. The crest lengths of antidunes are usually of the same order as the wavelength.

According to the description of the three classes of bed forms above we may illustrate the different flow states and associated bed forms by simplified twodimensional sketches as done in fig. 2.1. a-h.
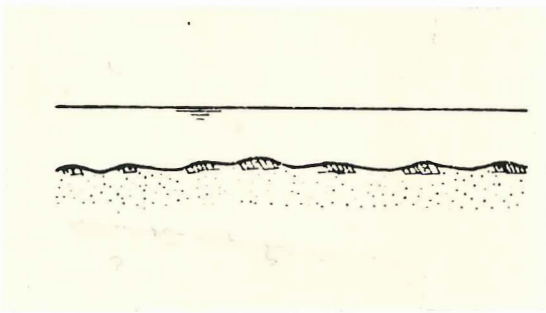
a.   F<<1. Ripples at weak flow. Surface unaffected.
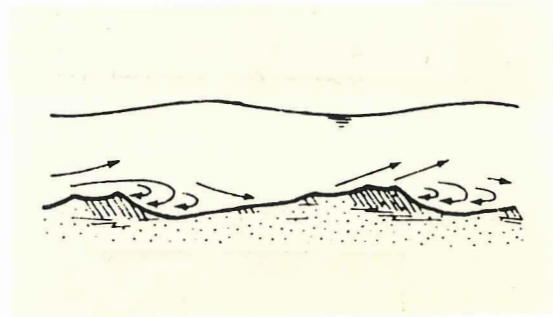
b.   F<1. Dunes with ripples on upstream slope. Surface out of phase with dune.
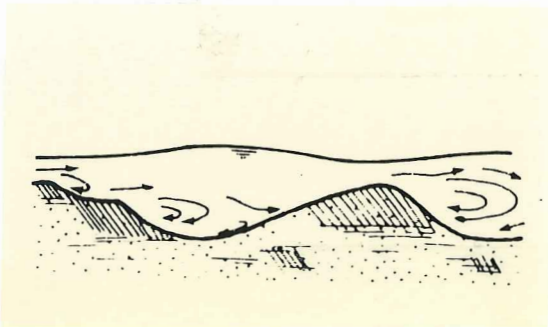
c.   F<1. Dunes of differing size. Surface out of phase with dunes.
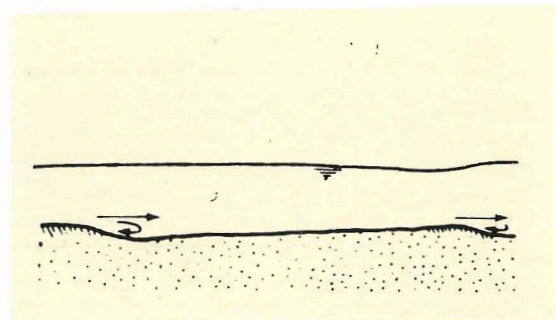
d.   F<1. Flow slightly subcritical. Dunes are washed out.
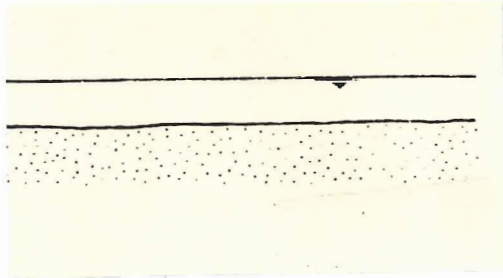
e.   F≅1. Plane bed or standing waves in phase with surface. Slightly supercritical flow.
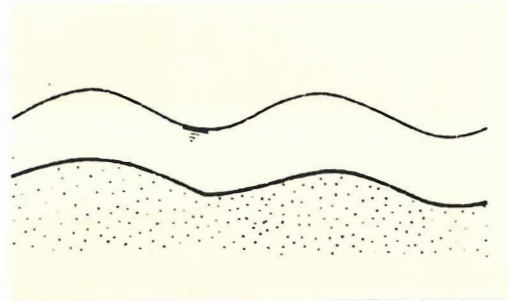
f.   F>1. Supercritical flow. Antidunes in phase with free surface.
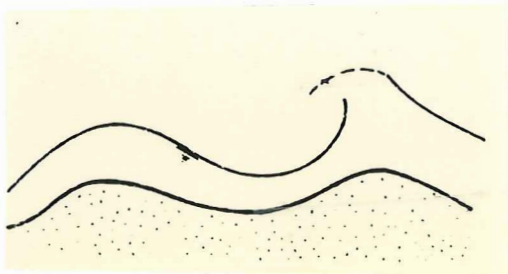
g.   F>1. Supercritical flow. Antidunes and inphase breaking surface wave.
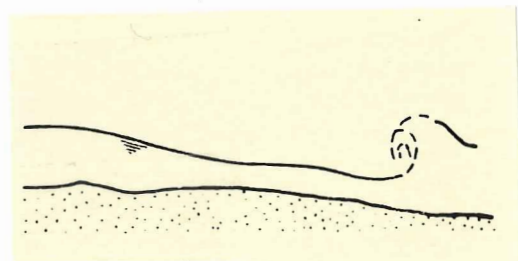
h.   F>>1. Strongly supercritical flow. Chutes and pools i.e. extreme antidune forms.

Fig. 2.1. Bed forms and associated surface wave pattern for increasing hydraulic Froude number according to a generally agreed classification.

Engelund and Hansen illustrate the occurrence of different bed forms and qualitatively the influence on the flow by a diagram of the following type
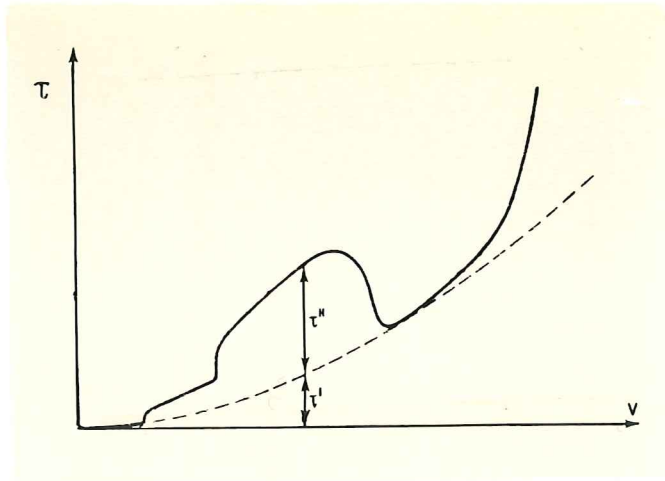
Fig.2.2. Bed forms affecting bed shear in different flow regimes, after Engelund and Hansen.

2.2. Some comments on the classification.

It appears from the preceding classification and illustrations that dunes and antidunes interact with the free surface but with different phase relationship. The two types are separated by a state where the bed as well as the surface is flat.

The distinction between dunes and ripples, however, is not so sharp. Engelund and Hansen indicate a transition between ripples and dunes for a certain flow condition. On the other hand dunes and ripples are observed coexisting, as shown in fig. 2.1.
A consensus exists between different authors that ripples are small, i.e. by wave length and amplitude compared to those of dunes. While the ASCE Task Force proposition is an upper wave length of 1 foot,

Engelund and Hansen propose a maximum wave length of 60 cm. Others allow ripple wave lengths up to 1.0 m. We thus seem to be left with a somewhat unsatisfactory characterisation of the ripples. It may even be justified to ask whether the ripples seen for flows just above the state of incipient motion – i.e. first grains movement – and the ripples seen superimposed on dunes are of the same type. Being characterised only by their size, relative or absolute, very little is in fact known so far about the physical nature and origin of ripples.

An interesting and comprehensive report was written by Guy, Simons and Richardson based on extensive laboratory research work on all three types of bed forms. It contains both a large amount of flow, sediment and bed form data and fascinating photographs and written descriptions of the observed bed and surface features. For a detailed and thorough description of bed forms and associated flow under laboratory conditions this is probably one of the best references available. A well known and authoritative source of descriptive information on bed forms observed in the field is the book by J.R.L. Allen.

3. A SURVEY OF THE LITERATURE ON SOFT BED STABILITY ANALYSIS.

3.1. Work before 1960

3.1.1. Early contributions

The interest in bed forms dates back to earlier centuries. Raudkivi mentions in his book an investigation by G.H. Darwin in 1883, and this was probably not the first one. It is interesting to note, however, that Darwin is reasoning along lines of hydrodynamic stability. And as such it is very likely to be one of the first attempts.

Raudkivi also refers to an empirical description of the nature of ripple formation by G.F. Deacon in 1892 "of a quality such that subsequent descriptions have added very little to it".

3.1.2. An early hydraulic approach. The erosion equation.

F.M. Exner (1925) is another early investigator working on the basis of hydraulics. The hydraulic way of attack has an inherent weakness in that it is developed for description of uniform flows i.e. phenomena of very long range in the flow direction. In terms of wave length λ and water depth h this means that the description is limited to cases where $2\pi h/\lambda = kh$ is small. An advantage of the hydraulic approach may be that it offers a possibility of taking friction and nonlinear accelerations to some extent into account.

Exners most important contribution was the establishment of the erosion equation

$$\frac{\partial \eta_2}{\partial t} + \frac{\partial q_s}{\partial x} = 0 \tag{3.1}$$

where q_s is the volume transport of sediments and η_2 is the bed elevation above a fixed level. This equation is obviously one of sediment

continuity. A slight improvement of (3.1) is needed, by inclusion of the bed porosity.

3.1.3. The first potential theory attempt.

A.G. Anderson (1953) applied potential theory for flow over a sinusoidal bed and Exner's erosion equation, considering bed load only, in a combined experimental and theoretical work. He seems, however, like Exner, to have missed the factor (1-n) on the term $\partial \eta_2 / \partial t$, where n is bed porosity. By further assuming $\partial q_s / \partial x$ to be proportional to $\partial u / \partial x$, u being mean horizontal velocity at bed level, he finds the analytical solution for the bed process as a bed wave

$$\eta_2(x,t) = 2a \cosh^{-1} kh \sin\beta t \cos(kx-\beta t) \qquad (3.2)$$

where k is the wave number $2\pi/\lambda$, a is the surface wave amplitude and β is a frequency given in terms of mean flow, surface wave and bed erosion parameters. He further argues that bed waves reach an equilibrium stage in phase with the surface wave and with maximum amplitude given by

$$\sin \beta t = 1 \implies \beta t = \pi/2 \qquad (3.3)$$

And by equating the resulting amplitude ratio to the one given by Milne-Thomson for stationary flow over a sinusoidal bottom, he arrives at a criterion to be satisfied by fully developed bed waves as

$$F^{-2} = kh (\tanh kh - 2 \sinh^{-1} 2kh) \qquad (3.4)$$

where

$$F = U/\sqrt{gh}$$

is the Froude number, U being the over all horizontal velocity of the flow, and h the water depth. Equation (3.4) with some experimental data is shown in fig. 3.1.
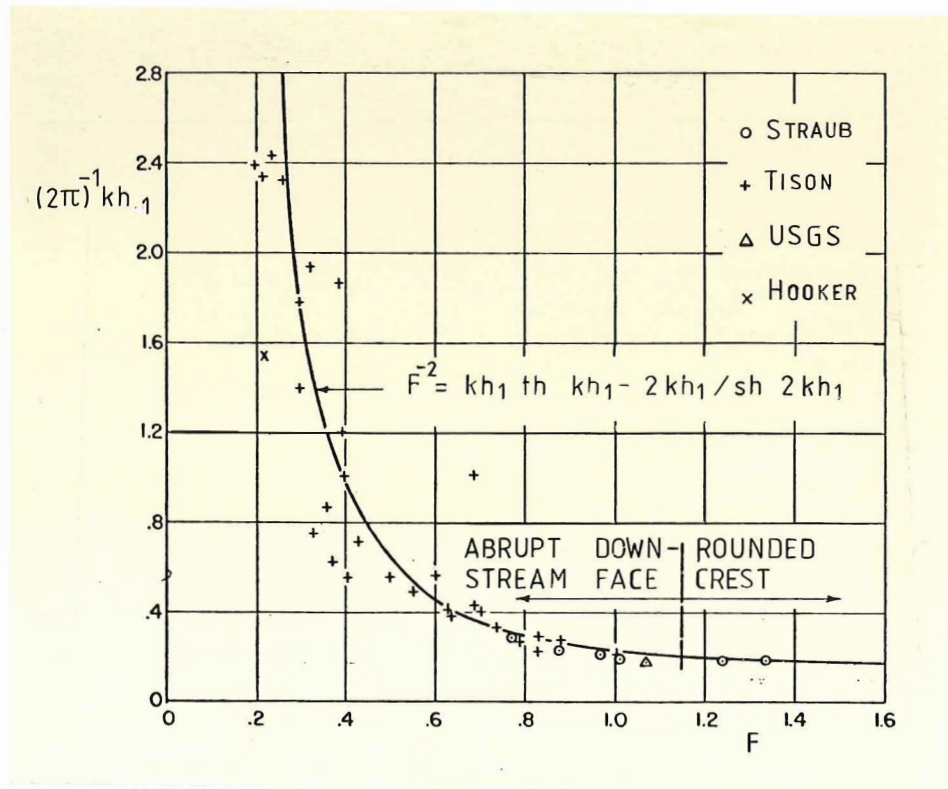
Fig. 3.1. - Relative wave length as a function of Froude number
according to A.G. Anderson (1953).

Even if the resulting formula shows a reasonable agreement with experi-
mental data, some remarks may be made on the analysis, in addition to
the porosity factor mentioned:

- Since the analysis is made on the development of dunes later
  experimental research has shown that fully developed dunes are
  out of phase rather than in phase with the surface wave.
- The theory says nothing about the transitional state and the
  specific nature of antidunes.
- Ripples, often seen coexisting with dunes are not mentioned in
  the analysis.
- The application of potentional theory results for the flow field
  close to the bed and in interaction with the bed material is from
  a physical point of view not convincing.

- The bed load transport relation saying that $\partial q_b / \partial x$ is proportional to $\partial u / \partial x$ is an analytically handy formulation. However, as is generally agreed to by researchers in this field, the bed load function is complex and cannot, even at present, be considered fully established.

3.1.4. Liu's work

H.-K. Liu (1957) in his doctoral thesis reviewed the work by Exner and Anderson and in addition the "classic" instabilities of hydrodynamics. In studying the bed instability in order to explain sediment ripple formation, he found experimentally that ripples formed for Froude numbers as low as 0.22. On this basis he concluded that ripples are not caused by surface waves. Further Liu states that a sediment-laden bed may be considered as a fluid since

a) a rigid boundary can be treated as a fluid of infinite viscosity, and

b) sediment density currents are usually accepted as being fluids, and a sediment-laden bed is an extreme case of a density current.

Both statements seem reasonable by themselves. But it does not appear to what extent they should have relevance to the bed stability problem. Liu in his further work does not seem to make any direct use of these ideas. His main contribution is on relating experimentally the beginning of ripple formation to Shields' criterion for incipient grain motion. Liu's resulting diagram is shown in fig 3.2.
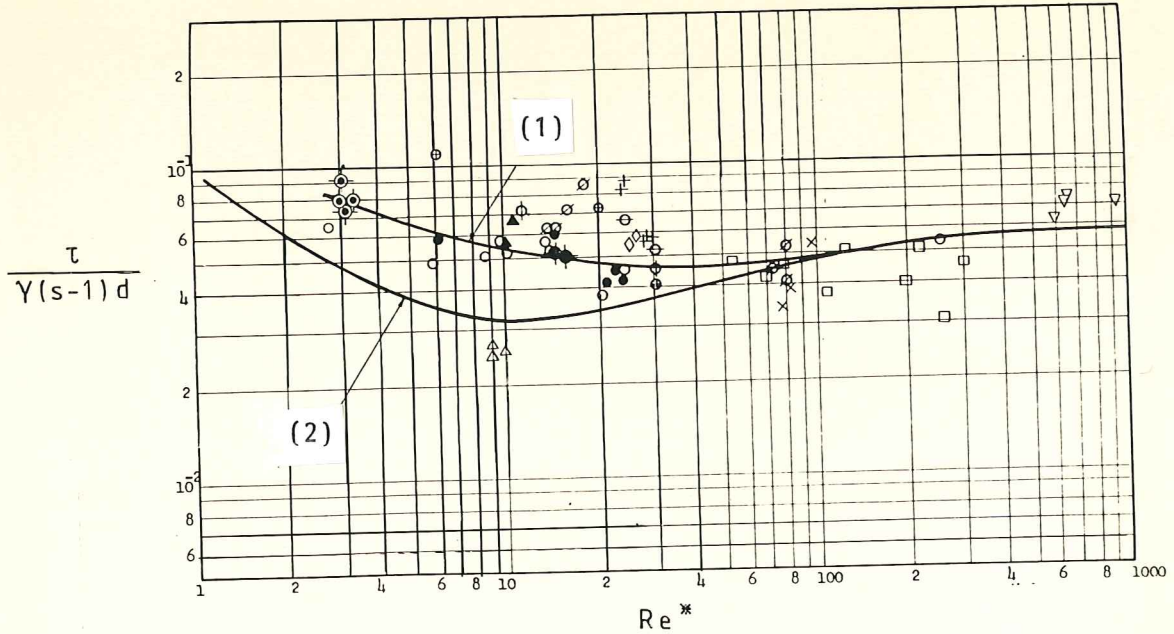
Fig. 3.2. Beginning ripple formation (1) and incipient grain motion (2), after H.- K. Liu.
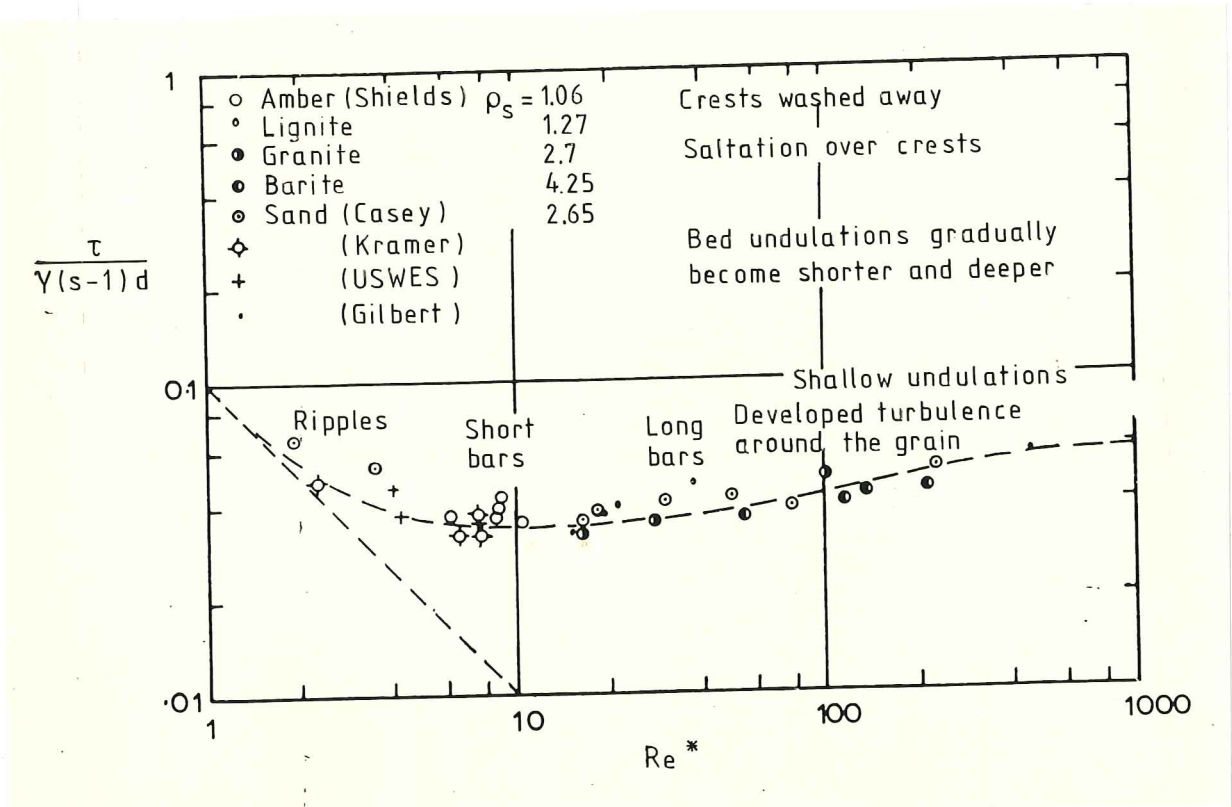
Fig. 3.3. Shields' critical shear stress diagram for incipient grain motion, after Raudkivi.

For comparison the same Shields' diagram with experimental data for incipient grain motion and domains of first occurring bed forms, as given by Raudkivi (1965), is shown in fig. 3.3.

The general impression of the early contributions to the study of granular bed stability is that the success in explaining the pertinent bed features was rather limited. This is readily understandable however when considering that we even today have important parts of the problem unsolved. We should also remember that the empirical knowledge and the amount of available high-quality physical data on the phenomena was much less than today.

3.2. A decade of high activity.

3.2.1. J.F. Kennedy's work. The potential theory approach.

Starting with the work by J.F. Kennedy (1963) on "The mechanics of dunes and antidunes in erodible - bed channels", the following decade showed an increasing number of publications on the subject. A strongly growing research activity took place which brought the subject from an initial stage to one of considerably improved knowledge. The development was empirical as well as theoretical. A summary of all experimental work is outside the scope of this work. Much of the empirical knowledge gained is reflected in the classification and description of section 2.1. For quantitative empirical information reference has to be made to the subject reports. The one by Guy et al. is, as said earlier, highly recommendable. Others are found in the list of references.

Kennedy continued on the line taken up by Anderson in applying potential theory for flow over a sinusoidal bed. In fig. 3.4 is shown his basic flow model.
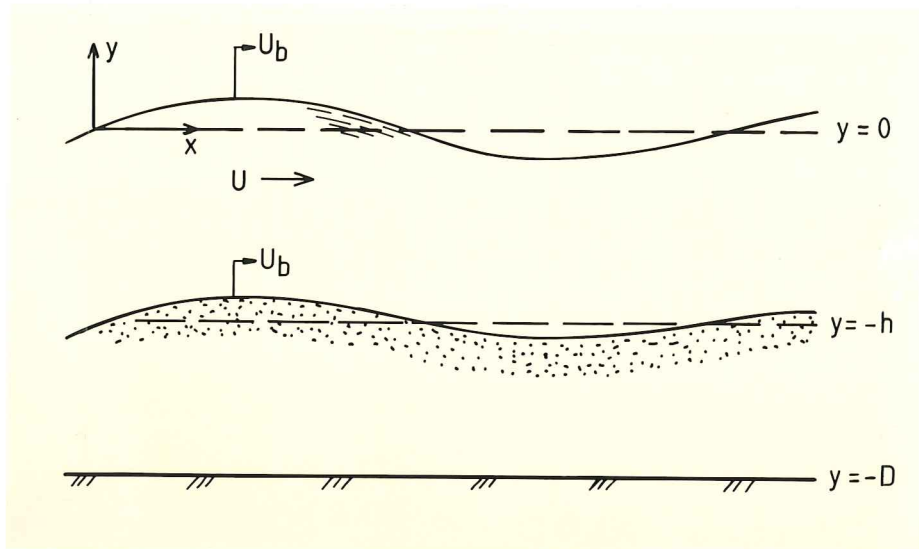
Fig. 3.4. Sketch of theoretical flow model used by J.F. Kennedy.

Kennedy restates a well known result of potential theory namely that the relation (given by Kennedy on a slightly different form)

$$a_2/a_1 = (F^2 - \tanh kh/kh) \, F^{-2} \cosh kh \qquad (3.5)$$

connects the bed and surface wave amplitudes. Equation (3.5) leads to the condition

$$F^2 = \tanh kh/kh \qquad (3.6)$$

separating in phase waves, i.e. antidunes, from out of phase waves i.e. dunes. F is the hydraulic Froude number $U/\sqrt{gh}$.

In analysing sediment transport as the cause of bed instability, i.e. growing bed waves, he arrives at the result

$$a_2(t)/a_1(o) = \{\sinh k(D-h)/\sinh kh\} \cdot$$

$$\cdot \exp \{\alpha k^2 t \coth k(D-h) \sin k\delta\} \qquad (3.7)$$

Here α is a sediment transport rate coefficient and δ is the length by which the local sediment transport rate at the bed lags the local velocity. If this lag is zero Kennedy's model is seen to give neither growth nor decay of bed perturbations. The depth parameter D, stemming from Milne-Thomson potential theory formulas, is artificial and serves the additional purpose of obscuring the physical content of the result (3.7). If D is removed through use of the linear wave theory stationarity condition

$$k U^2/g = \tanh kD, \qquad (3.8)$$

the resulting formula is

$$a_2(t)/a_1(o) = (F^2 - \tanh kh/kh) F^{-2} \cosh kh.$$

$$\cdot \exp\{-\alpha k^2 t \sin k\delta (F^2 - \coth kh/kh).$$

$$\cdot \tanh kh (F_2 - \tanh kh/kh)^{-1}\} \qquad (3.9)$$

This last form of Kennedy's stability result was used in the 1969 review paper. Equation (3.9) forms the basis of a detailed stability discussion in which the lag distance δ plays a central role. Kennedy suggests as part of this discussion the relation

$$F^2 = 1/kh \qquad (3.10)$$

as an upper boundary for the existence of antidunes, in spite of the fact that the relation

$$F^2 = \coth kh/kh \qquad (3.11)$$

is suggested by Kennedy's own result (3.9). As will be seen in the following (3.11) is in later stability analysis concluded to be the upper stability boundary.

Kennedy found the relation

$$c_r = \alpha \; k \; \cos k\delta \; \tanh kh \; (F^2 - \coth kh/kh).$$

$$. (F^2 - \tanh kh/kh)^{-1} \tag{3.12}$$

for the propagation rate of bed waves, which is seen to exist also for zero lag distance δ.

The following figure shows parts of Kennedy's theoretical results in the F – kh diagram including a considerable amount of experimental data on observed dunes and antidunes. The later upper regime boundary (3.11) is shown in stead of (3.10).
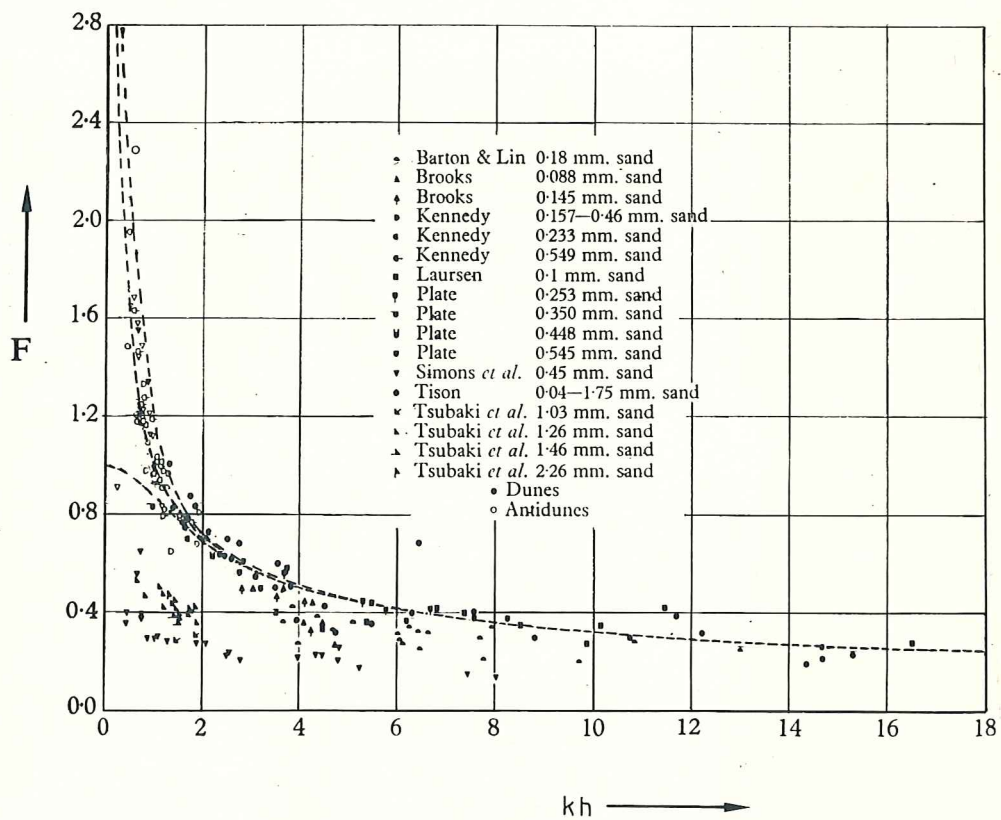
Fig. 3.5. Stability analysis results of J.F. Kennedy with empirical data on dunes and antidunes. The relation $F^2 = \coth kh/kh$ is also shown.

3.2.2. Reynolds' work.

A.J. Reynolds (1965) performed an analysis of the problem of erodible bed stability first along the lines of hydraulics and next using potential theory. The hydraulic analysis proceeds by use of the continuity and momentum equations

$$Uh = q \tag{3.13}$$

$$U \frac{\partial U}{\partial x} + g \left(\frac{\partial \eta_2}{\partial x} + \frac{\partial h}{\partial x} \right) + \beta \frac{U^2}{h} = 0 \tag{3.14}$$

where U is the flow velocity, h the water depth, q volum flux of water per unit width of channel, η_2 bed level, g acceleration of gravity and β a flow friction coefficient. Further he uses the erosion equation

$$\frac{\partial \eta_2}{\partial t} + \frac{\partial L}{\partial x} = \frac{\partial \eta_2}{\partial t} + m \frac{\partial U}{\partial x} = 0 \tag{3.15}$$

where m is a proportionality konstant and $L = (1-n)^{-1} q_s$ is effective volume flux of bed soil material per unit width of channel. The following figure shows Reynold's flow model.
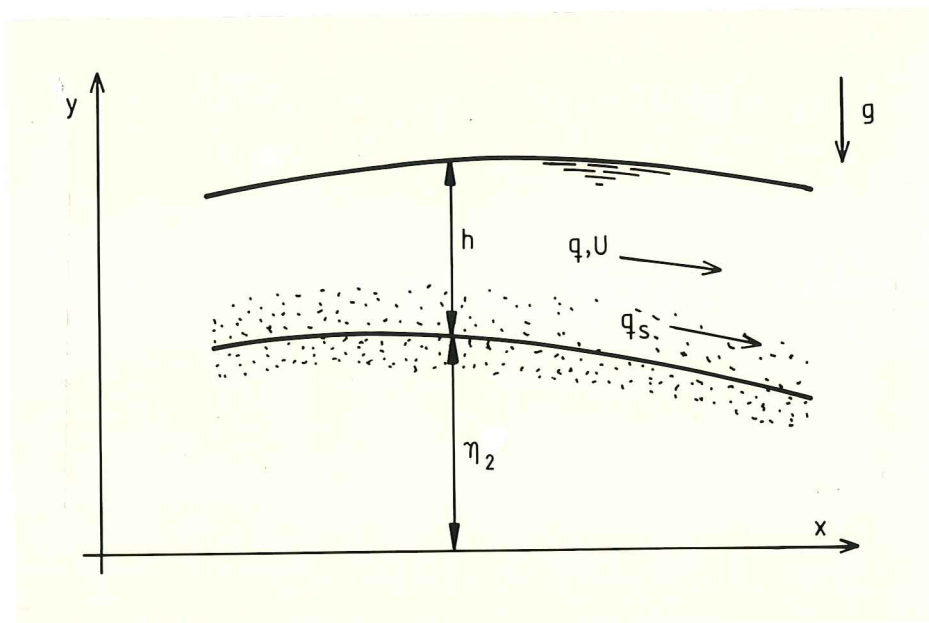
Fig. 3.6. Definition of flow parameters for hydraulic equations in Reynolds' analysis.

The inherent assumptions of this approach are:

- the velocity U is a cross sectional average,
- the vertical accelerations are small enough to be neglected,
- the pressure is hydrostatic,
- the frictional resistance obeys a "velocity squared law".

An implication of the neglect of vertical acceleration is that the longitudinal changes of flow have to be slow.

Reynolds found by a linear perturbation procedure on the above equations that without a phase difference δ between erosion and horizontal velocity gradient the bed was stable. Thus an unstable bed is described if the erosion equation is developed as

$$\frac{\partial \eta_2}{\partial t}\bigg|_x + m \, \frac{\partial U}{\partial x}\bigg|_{x - \delta} = 0 \qquad\qquad (3.16)$$

Reynolds' finding on this point is then essentially the same as Kennedy's. In considering the effect of bed friction Reynolds concluded that friction was generally not sufficient to explain phase shift and instability.

In revising Kennedy's potential theory Reynolds arrives at the expression

$$\frac{c}{U}\rho = - \, mk \, (1 - G_o^2 \, \tanh \, kh)(G_o^2 - \tanh \, kh)^{-1} \qquad\qquad (3.17)$$

for the velocity of propagation of bed waves, where $G_o^2 = kU^2/g$. If G_o is allowed to be larger than one – Kennedy considered $G_o < 1$ – one gets a limiting condition for upstream propagating antidunes as

$$F^2 = \coth kh/kh \qquad\qquad (3.18)$$

He stated further that (3.18) marks also the boundary of the region of instability of bed waves of small amplitude.
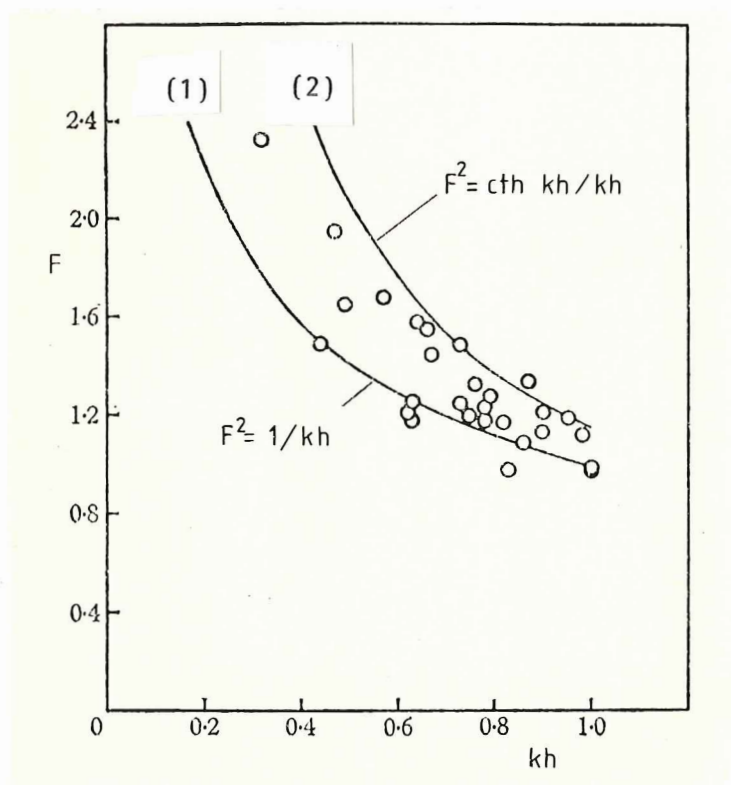
Fig. 3.7. Upper range stability limited curves according to Kennedy (1) and Reynolds (2), with data plotted for observed antidunes.

We note that as Kennedy based his criterion on water wave considerations Reynolds applied the erosion equation.

3.2.3. A detailed empirical description.

A.J. Raudkivi in 1966 published a work where he stresses the importance of the wake formed behind bed wave peaks and also the

importance of bed shear stress and sediment transport for the understanding of bed form generation. He states his doubt about an instability mechanism being responsible saying that

> "The development of bed forms from a flat bed is a progressive process and not a spontaneous growth of amplitude of a bed disturbance".

Raudkivi's remark seems in fact to be directed towards the use of a maximum growth rate criterion, leading to one specific or preferred wave length, more than towards the instability idea itself.

3.2.4. The Boussinesq refinement of the hydraulic approach.

F. Engelund and E. Hansen (1966) made an effort to generalise the hydraulic model by applying the Boussinesq method, which allows to some extent for changes in the direction of flow. Additionally an empirical "delay distance" was applied. They arrived at a criterion for unstable bed and also succeeded in describing some threedimensional effects. However, the Boussinesq method complicates the hydraulic analysis considerably. On the other hand the principal weaknesses of the hydraulic approach, mentioned earlier, are conserved. Thus the Boussinesq refinement does not seem to be a penetrating improvement of bed stability analysis.

3.2.5. Time varying hydraulic equations.

M.H. Gradowczyk (1968) worked with the nonstationary hydraulic equations or the unidirectional first order shallow water equations, reading

$$\frac{\partial U}{\partial t} + U \frac{\partial U}{\partial x} + g \frac{\partial(\eta_2 + h)}{\partial x} + \beta \frac{U^2}{h} = 0 \tag{3.19}$$

$$\frac{\partial h}{\partial t} + \frac{\partial(Uh)}{\partial x} = 0 \tag{3.20}$$

The flow variables are defined as in fig 3.6. In addition the erosion equation

$$\frac{\partial \eta_2}{\partial t} + \frac{\partial q_b}{\partial x} = 0 \qquad (3.21)$$

was used where q_b is the bed - load part of the sediment transport, i.e. that part of the sediment transport which occasionally touches the bed.

Gradowczyk analyses both the propagation and stability of surface and bed waves, the mathematical techniques being the method of characteristics and that of channel flow linear stability analysis as used earlier by Jeffreys. The analysis leads to an instability of the surface for high Froude numbers ($F > 2.0$), and, interesting enough, the bed was concluded to be unstable without use of the artificial phase shift δ.

The model used by Gradowczyk meets the same objections as all other work on this problem along the lines of hydraulics, even when, as here, allowance is made for nonstationarities. The basic restriction in this kind of theoretical flow modelling i.e. when vertical flow and horizontal pressure variations are suppressed, may exclude essential parts of an existing instability mechanism. The porosity factor (1-n) in the erosion equation seems to be overlooked also by Gradowczyk.

3.2.6. A study on the lag distance.

T. Hayashi in 1970 concentrated specifically on analysing the lag distance δ. He found the limit for antidunes to lie beyond the curve $F^2 = \coth kh/kh$ found by Reynolds. Hayashi's analysis also put significance on the role played by gravity. It is interesting to note that the same conclusion came out of laboratory tests on sand transport in tunnels by D.K. Lysne (1969) at just about the same time.

3.2.7. Engelund's shear model.

A new line of theoretical analysis of the bed stability problem was taken up by F. Engelund in 1970 by using the two-dimensional vorticity transport equation.

$$\frac{d\omega}{dt} = \varepsilon \nabla^2 \omega \qquad (3.22)$$

where the vorticity is defined by

$$2\omega = \frac{\partial v}{\partial x} - \frac{\partial u}{\partial y} \qquad (3.23)$$

The mean flow and concentration profiles used are shown in the following figure. We note that both profiles start with finite values U_b and C_b at bed level. The velocity profile is parabolic while the concentration varies exponentially.
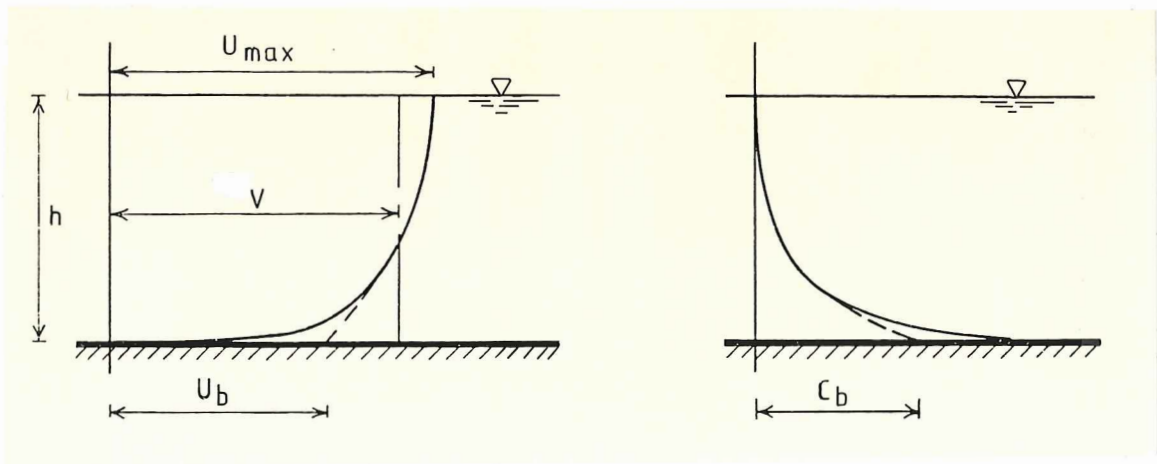
Fig. 3.8. Engelund's basic flow and sediment concentration profiles used in vorticity transport stability theory.

The continuity equation for the suspended sediment is taken as

$$\frac{dC}{dt} = w \frac{\partial C}{\partial y} + \varepsilon \nabla^2 C \qquad (3.24)$$

where the first right-hand term expresses changes due to the falling of grains, w being the single grain fall velocity, while the last term is one of diffusion. The diffusion coeffient ε is taken to be the same here as in (3.22) for diffusion of vorticity. And more specifically ε is assumed to be the channel flow eddy viscosity, of constant value througout the flow region.

Engelund further included the bed load by the Meyer-Peter & Müller formula. The connection between the total load q_t, the bed load q_b and the suspended load was formulated by

$$q_t = q_b + \int_{\eta_2}^{h+\eta_1} U\,C\,dy, \tag{3.25}$$

where the integration is over the actual water depth. And the erosion equation, or total sediment continuity equation

$$\frac{\partial q_t}{\partial x} + (1-n)\frac{\partial \eta_2}{\partial t} = 0 \tag{3.26}$$

connects the bed perturbation η_2 to the flow and sediment transport field.

Boundary conditions at the bed were formulated by requiring continuity of the vertical velocity component, a horizontal velocity squared relation for bed shear and a relation between the nominal bed sediment concentration C_b the bed shear τ and the fall velocity w:

$$\frac{\partial \eta_2}{\partial t} + U_b\frac{\partial \eta_2}{\partial x} = v \tag{3.27}$$

$$\tau/\rho_w = (U_b - c_r)^2/K^2 \tag{3.28}$$

and $\quad C_b = 13\alpha(\tau/\rho_w)^{3/2}w^{-3}$ $\qquad$ (3.29)

respectively. K and α are constants. The ration τ/ρ_w is recognised as the friction velocity (squared). The bed slip velocity U_b is set proportional to the friction velocity.

At the free surface the requirements were no vertical sediment flux, no normal or shear stress and a kinematic relation of the same type as at the bed.

A linearisation procedure based on small amplitude, harmonic perturbations of the flow and sediment variables then leads to an Orr-Sommerfeld equation for the perturbed stream function $f(y)$:

$$(U-c)\{f''-(kh)^2f\}-U''f = \{f''''-2(kh)^2f''+(kh)^4f\} \varepsilon/ikh^2 \qquad (3.30)$$

and a second order coupled equation for the perturbed sediment concentration $\phi(y)$:

$$\phi''+(wh/\varepsilon)\phi'-\{(kh)^2+(U-c)i\ kh^2/\varepsilon\}\phi$$

$$= \{i\ kh^2(V/\varepsilon)dC_o/dy\}f \qquad (3.31)$$

In the above formulas h is the unperturbed water depth, $U(y)$ the parabolic basic flow velocity profile of which V is the vertical average and k is the perturbation wave number.

The asymptotic boundaries of the instability region, i.e. the limit of zero fall velocity, were found to be

$$F^2 = coth\ kh/kh \qquad (upper) \qquad (3.32)$$

and $\qquad F^2 = tanh\ kh/kh \qquad (lower) \qquad (3.33)$

the first one in agreement with Reynolds' result. The interpretation of (3.33) as a stability boundary was a new result of Engelund's analysis.
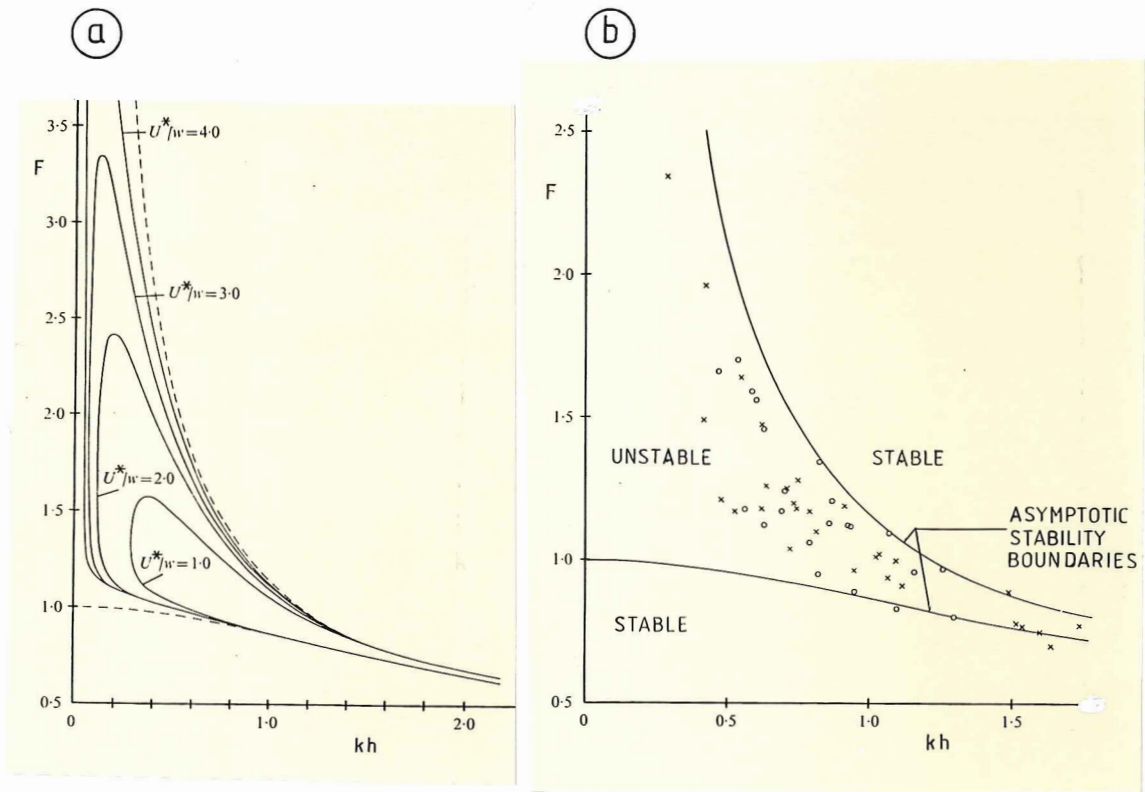
Fig. 3.9. Engelunds stability analysis result for the case of suspension load only, a: parametric stability boundaries from theory, b: experimental data and asymptotic stability boundaries.

Solving for complete sediment transport, i.e. both suspended load and bed load, Engelund finds stability diagrams of the type shown in fig. 3.10 for fine sediment (a) and coarser sediment (b).
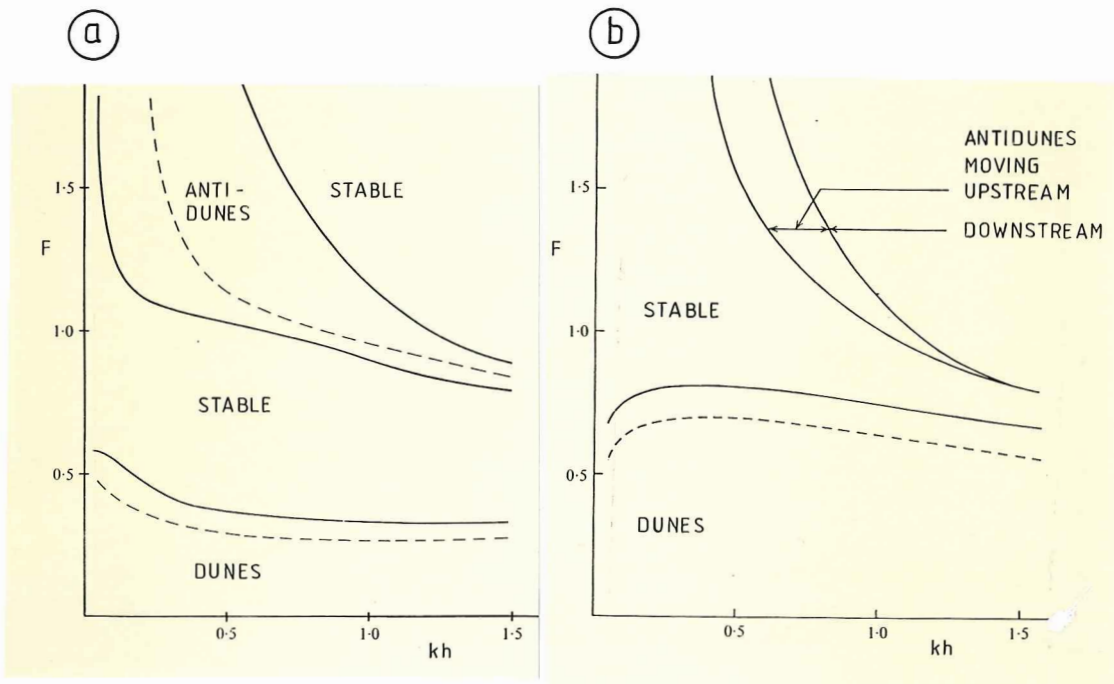
Fig. 3.10 Stability solutions for bed load and suspended loadaccording to F. Engelund, a: fine sediment, b: coarse sediment. Dashed curves indicate maximum growth rate.

As can be seen, the inclusion of bed load implies a lower range of instability as well. The stability region picture also changes strongly from the fine to the coarse sediment case, in particular the upper boundary of antidunes.

Engelund's stability model invites some remarks:

- The use of a bed slip velocity is favourable from the point of view of solving the Orr-Sommerfeld equation. However, it appears as a rather drastic simplification in a theoretical model that otherwise is unusually refined.
- Applying an eddy diffusivity coefficient constant over flow depth, the same coefficient used for diffusion of vorticity and sediment concentration, and in magnitude of mean size for pure water channel flow, is another rough point in the analysis.
- The grain fall velocity is known to depend on sediment concentration. This effect is not considered in the model.
- The distinction between a suspended sediment load and a bed load may be hard to justify in a refined stability analysis which aims at finding the basic mechanics behind specific sediment flow phenomena at the bed.
- The Orr-Sommerfeld equation is formulated for fully developed turbulent flow. Thereby the hydrodynamic stability problem is decoupled from the bed stability problem. This point might be worth wile some discussion.
- The eigenvalue problem formulated contain other eigenvalues not presented or commented on.

In spite of the above remarks the analysis represents an improved insight into the upper range bed behaviour, particularly the effect of suspended load and grain fall velocity. The most prominent of earlier hydraulic and potential theory results are retained. The subcritical instability found with bed load included is definitely a new result.

However, as Engelund himself points out:
"the agreement between the theoretical stability analysis and the observations does not necessarily imply that the model is in accordance with the actual mechanism of instability."

Thus we have to conclude that the upper regime improvement is gained at the cost of a considerable increase in analytical complexity, and that the lower regime new instability rests on questionable "laws" of flow and sediment transport. Then we are still left with a considerable uncertainty about the instability mechanism.

3.2.8. A three-dimensional study.

The three-dimensional character of upper regime bed waves was studied by F. Engelund and J. Fredsøe (1971) using potential theory and a nonuniform suspended flow of sediments. Earlier findings of Reynolds were essentially confirmed, while the transition curve between upper and lower range in Reynolds' analysis was interpreted as a stability boundary by Engelund and Fredsøe.

3.3 More recent work

3.3.1. J. Fredsøe's work on lower range instability.

J. Fredsøe (1974) worked along the same lines as Engelund in studying further the lower range instability. A new aspect in Fredsøe's analysis was the inclusion of the effect of gravity along a sloping bed on the sediment transport. It is also interesting to note that Fredsøe, studying the effect of the basic flow vorticity, concluded that a constant velocity profile gave only a very small change of the stability result when compared to a "correct" rotational profile. The following figure shows some of Fredsøe's findings. The effect of a gravity component along the bed, represented by the parameter μ, is seen to be of some importance.

In a second order development, in terms of the ratio between bed wave amplitude and flow depth, Fredsøe finds that dunes develop with a steepening downstream face, in accordance with what is seen in reality.
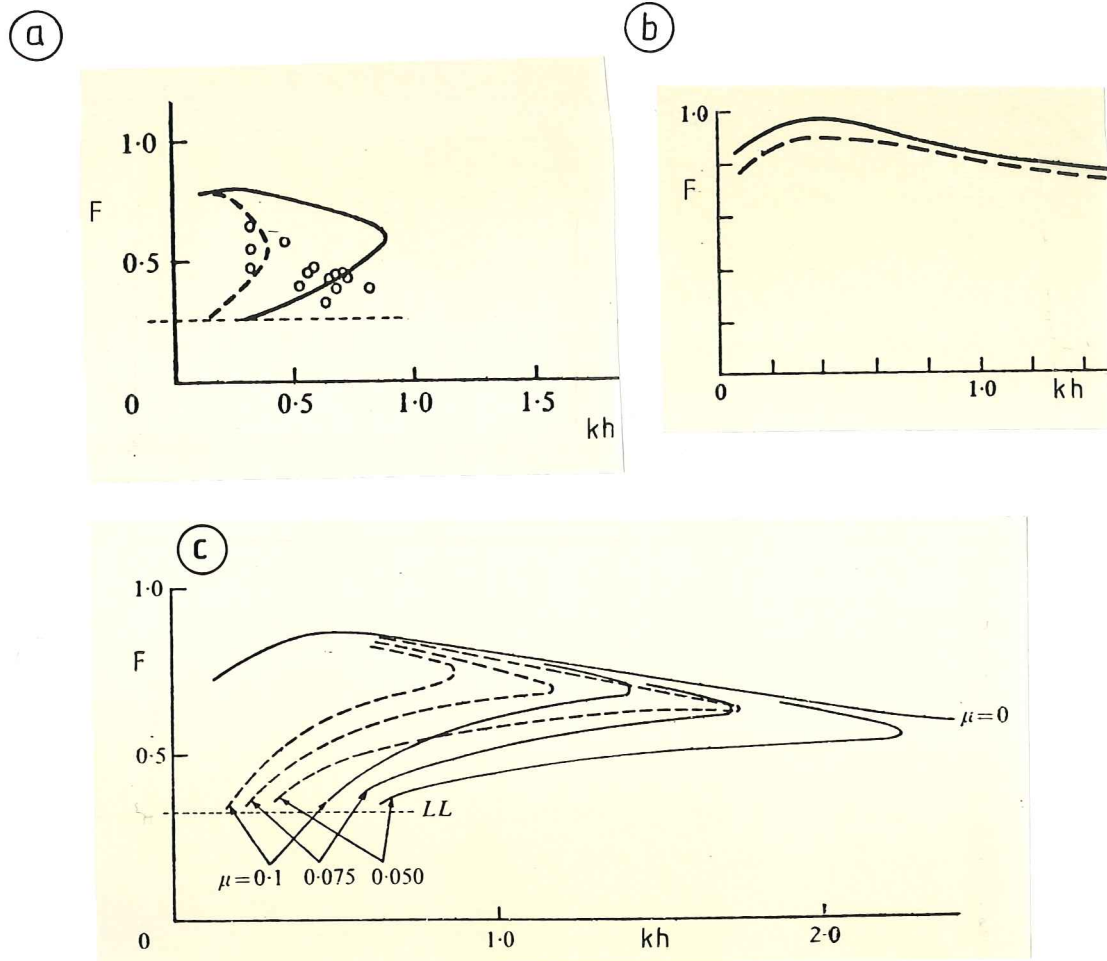
Fig.3.11. Dune generation analysis results by J. Fredsøe, a: theory
          compared with fully developed dunes studied experimentally
          by Guy et al., b: Influence of constant (——) and rotational
          (---) basic flow velocity profile, c: influence of gravity
          component along the bed, parametrised by μ in the figure.

3.3.2. A two-layer shearing interface model.

T. Shirasuna (1973) worked with two potential flow layers of different
densities flowing over a sinusoidal sediment bed with different basic
velocities. He argues for his model saying:

> "A close observation of sand waves shows us that the motion of
> erodible beds is composed of the translation of a sand wave
> whose travelling velocity is far smaller than that of the flow
> above it and the movement of a fluidified thin surface layer
> which flows as a fluid".

His analysis includes both the free surface and the fixed plane upper
boundary cases.

It might be argued against this type of stability model that the result depends on an unknown velocity ratio between the main flow and the bed layer, and also an unspecified bed layer porosity (or sediment concentration) is involved. The model is thus to some extent inconclusive. Shirasuna's potential flow description is further made unnecessarily indirect by using two "virtual" depths. Once again Milne-Thomson is the source.

Despite these remarks the fact remains, no erosion equation or other sediment transport relation being used, that Shirasuna's model seems to give stability limits of the same type as given by earlier potential theory or even the refined shear analysis in the upper regime. The lower regime stability limits found by Shirasuna resemble those of the refined shear model and are not even indicated by earlier potential theory. The most serious remark to be made about Shirasuna's work is that due to a highly condensed presentation his analysis can hardly be followed, leading to a bed wave velocity of the same order of magnitude as the mean flow velocity in opposition to a reality showing completely different orders of magnitude on the two.

3.3.3. A study with improved turbulence modelling.

K.J. Richards (1980) also worked along the lines of Engelund, considering bed load and lower flow regime only. He generalised the approach by including a turbulent basic flow energy equation and a varying eddy diffusivity. Richards' findings were two modes of instability in the theoretical solution, one interpreted as a dune mode and the other as a ripple mode.

The free surface was allowed only a very small or no deformation in Richards' theoretical model. This, of course, limits the validity of the results seriously. Another remark may be made on the bed roughness, playing an important role in the model. Since the bed roughness is dominated by the phenomena under study, this adds a second unsatis-factory property to Richards' theory. Thus in spite of a strong effort in representing flow turbulence, the results are likely to be indicative only.

3.3.4. Modification of dunes in unsteady flow.

In two interesting papers Fredsøe (1979 and 1981) discusses the changes in dune properties due to a sudden change in the water discharge, the changes in weakly oscillating flow and the effect of suspended sediments under weakly unsteady basic flow conditions. In the last paper the transition from dunes to plane bed was considered in particular.

This type of analysis, dealing with the modification of already existing dunes, is related to the bed stability problem and gives valuable additional knowledge about the dynamic interaction between flows and sedimentary beds. However, as they do not address the stability problem itself the two contributions by Fredsøe will not be discussed further here.

3.3.5. Related topics.

Along with and partly interacting with the ongoing research on soft bed stability there has been an increasing activity seen in the research work on the turbulent structure of pure fluid shearing flow. As early as in 1956 H. A. Einstein and Huon Li focused on the periodic growth and decay of the bed sublayer. Considerable interest has been paid to the "bursting" phenomenon originating in the flow region close to the bed. The line of development is represented by the Von Kármán Lecture of Mollo-Christensen (1971), and the experimental work of Nychas, Hershey and Brodkey (1973), Grass (1974) and others. Jackson (1975) and Yalin (1977) attempted to make sediment flow interpretations by use of the turbulent shear flow ideas and results.

Without going into a detailed discussion of this subject we note some points of resemblance between shear flow and sedimentary flow pheno-mena. One is the intermittent character of shear flow boundary layer instabilities while intermittency is a typical feature of antidunes. Anot-her remarkable point is the "ordering principle" appearantly acting both in boundary layer instabilities and in the formation of soft bed waves.

Sumer and Deigaard (1981) particularly stress the experimental fact that the mean periodicity of the quasicyclic events scales with the outer main flow variables. Their work was directed towards the suspension mechanism by observing the trajectories of single grains. Several researchers emphasise the deterministic character of these quasicyclic events. Both Nychas et al. and Grass stress the role of a Helmboltz type instability forming a "key element in the turbulence generation cycle".

A basic difference between the development of bed waves and the development of strong turbulent vortices in shear flow is found on the time scale for development of the phenomena. While bed waves develop very slowly the shear flow instabilities develop with a rate given by the outer flow. The other basic difference is of course that between the "ultimate" result of instability i.e. a flow vortex versus a bed wave.

4. THREE REVIEWS

4.1. Introductory remarks.

A complementary type of information to the one found in the scientific publications surveyed in chapter three, is given by the review papers on the same subject. The review papers to be considered are written by persons with up to date knowledge of the subject, and who have themselves given strong contributions in the actual field of research. The following three reviews written on the soft bed stability problem are considered for the purpose of giving direct expressions for the "state of the art" at the time of writing: How the problem is conceived, and to what extent the physical phenomena under study are explained and understood.

4.2. J.F. Kennedy, 1969.

In characterising the nature of the soft bed phenomena Kennedy says:

"Although there is no consensus about the details of mechanisms responsible for any of these bed forms, some aspects of their occurrence appear to be self-evident and common to all of them.

First, all sedimentary bed forms are the result of an orderly pattern of scour and deposition. Their growth occurs by material being scoured from trough regions and deposited over the crests; this process continues until the forms attain their equilibrium amplitude, after which there is no further net deposition on the peaks or scour from the bottoms of the troughs. Ripples, dunes, and some antidunes move downstream because of a net transport of material from the upstream to the downstream faces, and upstream motion of antidunes results from the sediment transport rate being greater on downstream than on upstream slopes. The flat bed, on the other hand, accompanies flow conditions that cause scour from the crests and deposition in the troughs of bed forms of any

length that might be initiated. It should be clearly borne in mind that the pattern of scour and deposition responsible for the growth and migration of bed forms is generally only a perturbation imposed on the gross downstream transport of material, and not all of the transported sediment necessarily participates in the process.

A second obvious conclusion is that periodic bed forms result from an instability phenomenon. A small disturbance on an otherwise initially flat bed, for example, can perturb the longitudinal distribution of sediment transport capacity in such a way that deposition and scour occur over the crests and troughs, respectively, of the initial disturbance, causing it to increase in amplitude. The increased amplitude of the disturbance enhances the rate of differential scour and deposition, thereby promoting a still faster rate of growth of the bed waves, and so on until other factors associated with the finite amplitude intervene and fix their equilibrium height. The flow disturbance downstream from a bed-form train of finite extent induces the formation of additional downstream bed waves, thereby causing the length of the train to increase. Hence, under some flow conditions a flat bed is unstable in that any bed disturbance, whether fortuitous or induced, modifies the longitudinal distribution of sediment-transport capacity in such a way that the bed deformation grows and propagates. Under other flow conditions, any bed disturbance influences the local transport so as to diminish its own amplitude; whence the flat-bed configuration.

A final observation of sufficient generality that it warrants recording here is that there is, at least in a statistical sense, a characteristic wavelength and equilibrium amplitude for the bed forms accompanying a given flow over a specified granular material. Small aeolian ripples and wave-generated ripples are ex-tremely regular in shape and spacing. Alluvial ripples or dunes formed on an artificially flattened bed are initially very regular in shape and spacing and are also long-crested, often extending across the full width of a laboratory flume. It is only some time after initiation of formation, when the bed forms have approached

or achieved their equilibrium dimensions, that their shapes become somewhat random and short-crested and their arrangement becomes disordered."

And in reviewing the analytical treatments seen at that time Kennedy classifies the different approaches in four categories:

"The first has proceeded from classical mechanics and has sought predictions of the conditions for occurrence and characteristics of various bed forms by introducing the continuity equation for sediment movement, together with assumed or generalized empirical relations for the local sediment transport rate, into the equations of motion for the fluid. Exner's contribution was the first effort in this category. The major stumbling block encountered in this approach has been the lack of a concisely formulated, generally applicable sediment transport law to couple with the fluid-flow equations in order to express the local sediment transport as a function of the local boundary geometry and flow properties.

The second approach, typified by Liu's analysis, has argued that bed forms result from an instability of the Helmholtz type, the sediment bed behaving as a fluid of very high viscosity. This model is rendered invalid by two obvious considerations, 1) sedimentary bed forms are the result of a scour-and-deposition process, not a shear deformation of the bed, and 2) a granular bed will not deform under the action of pressure distributions realizable in ordinary flows.

A third school has overlooked the details of the responsible mechanisms and instead has sought only to obtain from experimental data relationships for the occurrence, dimensions, and kinematics of bed forms. A good example of the numerous papers in this class is that of Shinohara & Tsubaki. This avenue can be properly classed with the regime approach utilized in predicting the transport properties of alluvial channels on the basis of data obtained from other channels which had been judged to be in equilibrium.

The fourth and most recent line of inquiry has sought to describe ripples and dunes in terms of their statistical properties, and has attempted by means of spectral analysis to make deductions about the processes involved in their formation.

Among these approaches the first and last appear to hold the most promise. An adequate understanding of the formation and properties of bed forms can be expected only from a detailed analysis of the kinematics and dynamics of the interaction between the flow and the bed. Moreover, various dimensionless renderings of experimental data will continue to be of limited value until a successful theory yields a logical framework for their presentation and interpretation. Description and examination of fully developed aqueous ripples and dunes by means of spectral analysis has merit because of the inherently random geometry and kinematical behavior of these bed forms."

It is remarkable that Kennedy does not adress the hydraulic way of analysis in this connection as a school of its own, or at least as an analytical approach distinctly different from the potential theory approach.

The Kelvin-Helmholtz type of approach as proposed by Liu is agreeably concluded to be invalid. One should, however, make it clear that the arguments, and thereby the conclusion, apply to Liu's model and not to the K-H mechanism as such.

4.3. A.J. Reynolds, 1976.

Reynolds surveyed the complete work in the western world that had been done up to and including 1974 on the soft bed stability problem. An interesting cut from his summing up of the current understanding reads as follows:

"The best understood bed features are the least important – antidunes. These are of less importance because they are rather

uncommon in nature and never appear under a flow lacking a free surface. We have a good understanding of the mechanism of instability - namely, the finite time required for the suspended sediment to adapt to changed conditions - and of the role of the free surface, both in providing the overall conditions for instability and in introducing an important mechanism of growth limitation. The appearance of antidunes corresponds quite well to the predictions of the linearized theories (Kennedy 1969) and the role of three-dimensional flows is understood in general terms (Reynolds 1965, Engelund and Fredsøe 1971).

A significant feature of antidunes is the adherence of the adjacent flow, even for quite large amplitudes, to the sinusoidal pattern assumed in the usual stability analyses. Dunes and ripples do not have this happy characteristic, the fluid motion downstream of each crest being dominated by separating and reattaching flows, in general of three-dimensional character. Although a good deal is known about these recirculating motions (see, for example, Raudkivi 1966 and Allen 1968) it has not been possible to introduce this information into the stability analysis in a convincing way. Moreover, the irregular character of these bed features is not closely approximated by the sinusoidal cross-stream variations which have been adopted in analytical models.

The general nature of the transitions between dunes and antidunes is understood (Engelund and Fredsøe, 1974), but detailed predictions are not easy, since the stability boundaries are critically dependent on the balance between suspended load and bed load, among other factors. What is more, the nature of the bed in this region is often observed to vary in time. It is widely conceded that ripples - dune-like features much smaller than the channel dimension - are associated with the boundary layer on the perturbed channel bed, that their size is determined by the dimensions of the region of rapid velocity variation, and that the mechanism of instability presumably involves this variation. However, no analysis based on these ideas has been advanced. The case of wind ripples has been treated, it is true, but in the hydraulic environment the transport of particles is predominantly as bed load, unlike the aeolian situation where saltation is of great importance.

It is a privilege to have seen the subject of stream-bed stability develop within a period of little more than a decade. While we may hope that the expectation will prove to be incorrect, there is some reason to fear that progress will be less rapid in the future. The available mathematical techniques have revealed the general features of the interaction between flow and bed material. But it is apparent that our understanding decreases as the role of bed load becomes more dominant, because our insight into the interaction between the fluid and the particles on and near the bed is not sufficiently penetrating to allow the construction of simple, yet realistic models of the processes occurring there."

The remarkable thing about the "best understood bed features" is that they are explained by the action of the suspended load. This indeed raises the question about the distinction between bed load and suspended load. If the suspended load is allowed to take part in bed processes the concept seems to be strained beyond justification.

It is not obvious that separating and reattaching flow effects should be included in a stability analysis, at least not a linear one, since these effects are connected with the developed, i.e. finite amplitude, stages of the bed features.

4.4. F. Engelund and J. Fredsøe, 1982.

In their paper entitled "Sediment Ripples and Dunes" Engelund and Fredsøe review the more recent work on the generation of bed wave forms. The subject is reviewed in a wider context of sediment transport and flow resistance and, in spite of the title, antidunes are also given some space. In addition the discussion of antidunes is suffering from a slight misconception of the amplitude ratio result in potential theory. (see fig. 11.1)

The work on formation of dunes is reviewed with emphasis on effects demonstrated to have influence, in descending order of importance:

- fluid friction,
- rate of sediment transport as bed load or suspended load,
- gravity and inertia of sediment particles,
- percolation of permeable bed.

And, since Richards' analysis is the only attempt made towards explaining the generation of ripples, that topic occupies only a minor part of the whole paper (in fact less than a half page).

The state of the art in 1982 very much seems to confirm Reynolds' (1976) pessimism concerning further progress. The situation is strikingly characterised by Engelund's and Fredsöe's introductory statements:

"Many of the aspects are far from being clarified in a satisfactory way, and it has not been possible to avoid controversial issues. In such cases the authors have tried to state the situation objectively, but without trying to hide their own point of view."

5. SOME ESSENTIALS, AND A WORKING HYPOTHESIS.

5.1. Free surface dynamics.

Few items in the stability discussion of soft bed wave forms are subject to such a degree of general agreement as the significance of the free surface in the generating mechanism of dunes and antidunes. Even if one should distinguish sharply between an approximately stationary free surface flow interacting with a fully developed undulatory bed on the one hand and the dynamics responsible for its generation on the other, there seems to be a firm theoretical and experimental basis for the significance of the free surface. In fact free surface relations play a dominating role in the most successful stability results up to now. And quite logically the $F - kh$ plane is the most meaningful interpretation space for the theoretical and experimental results.

5.2. Bed shear.

Another effect generally agreed to be important is the bed shear. However, its role in the instability mechanism becomes indirect by its coupling to sediment transport relations. The formulation of a stability model with "correct" modeling of shear flow and sediment behaviour at the bed is of course the hard part of the problem.

It is a remarkable fact, however, that the boundary layer concept, very successfully applied in other branches of hydrodynamics, has so far not been applied in the stability analysis of soft beds. There is one place in the literature where a "boundary layer way of thinking" is met, and that is in the argumentation (or speculation) about the origin of ripples.

Two further observations should be made here. One is that the sediment transport mainly occurs as a bed load i.e. in the bed boundary layer, especially in the lower regime. Another observation is Engelund's experience that inclusion of a bed load in the stability analysis has a strong influence on his stability results. The bed load has also formed a basic part of Fredsøe's later work on dunes.

5.3. Sediment transport.

It has been emphasized by earlier stability analysts and reviewers that the main difficulty met is the lack of "generally valid sediment transport laws". This is of course the immediate consequence once we have said that the sediment transport is an á priori prosess in our problem. And this is again an almost obvious assumption. A couple of remarks, however, seem appropriate at this stage.

If we accept that the ultimate purpose of a stability theory is to establish a rational mechanical model to explain causality in the behaviour of the subject system, we also have to accept that use of empirisism in such a theory generally is undesirable. Agreeing that this ultimate goal may be hard to attain and that quite often there will be no choice between empirisism or not, it remains though that in this sense the quality of a stability analysis decreases with the amount of empirisism involved.

It may further be remarked that by basing stability theories for soft beds on empiric sediment transport "laws", such theories will hardly be suitable for explaining how the sediment transport itself is established. And this should be a problem at least as important as the sand wave generation problem. What appears intuitively evident, however, is that the sediment transport is established through an erosional prosess where the flowing water is the agent and the sediment bed is the reagent. In bed wave stability theories the erosion equation is used only as a tool to deal with the bed wave problem. It appears not self-evident that one type of erosion is responsible for the sediment transport while another type generates bed waves. Could it be that a more fundamental purely hydrodynamic instability is responsible for both types of sediment motion and that erosion and sediment transport then is the result when this instability is strong enough while bed waves are generated by a weak action of the same instability?

5.4. Basic flow.

The requirement to be met by the basic flow relations used in a rational hydrodynamic stability theory is that the fundamental equations of motion, state and continuity plus all boundary conditions should be satistied. Using empiric or semiempiric relations for the flow field which are approximations to "reality" is then again undesirable but usually unavoidable.

If an instability is involved, basic flow modelling is not a question of modelling a flow "reality" but rather of modelling an á priori flow. In practical terms this means finding a complete solution to the same hydrodynamic boundary value problem as in the stability model but now assuming the solution to be stationary. The basic flow solution should in general account for the nonlinear character of the basic equations or boundary conditions. As is well known, very few such exact solutions to hydrodynamic boundary value problems are known. And stability analysis is for this reason at present strichtly possible only for a limited number of cases.

We finally recollect the most important result up to now on basic flow modelling in granular bed stability analysis, namely Engelund's and Fredsøe's finding that the basic flow velocity gradient had only a very small influence on the stability results.

5.5. A basic feature of sand wave development.

Before closing this chapter it seems justified to emphasize a feature of the sand wave development not very much discussed in earlier stability analysis, but pointed out by experimentalists. In particular Raudkivi in his (1966) work emphasizes this phenomenon.
It is a striking observation, when following the lower regime sand wave development, that it is a progressive prosess from shorter towards longer waves. The final dunes seen in a constant flow experiment have a much larger wave length than the ripple like wave forms seen in the beginning of the experiment. And there is a more or less gradual

transition during the experiment from the one to the other. There is, in other words, experimental evidence for the existence of a range of unstable wavelengths with a gradual transition from shorter to longer waves. The transition is in general slow, as is the propagation velocity and growth rate of the sand waves. None of the existing stability theories are able to explain this.

5.6. A hypothesis for an alternative stability model.

On the background of the preceding discussion it appears rather obvious that there is a need for a different way of attack on the problem of soft bed stability. However, it is not a matter of evidence how such an attack should be made. The following is a set of requirements, more or less justified by the preceding discussion, wich will be sought implemented in an alternative stability model to be developed and discussed in the remaining part of this work.

A. Free surface dynamics should be accounted for, at least as far as linear theory can do it.

B. Flow shear should be modelled in the near-bed region. In the remaining part of the main flow field the shear is assumed to be of minor importance.

C. Fluid viscosity and grain roughness are of minor importance to the main flow.

D. Sediment transport as suspended and bed load should be roughly modelled by average fluid densities. The purely hydrodynamic character of the flow system should instead be placed in the center of the discussion.

PART II

THE K - H INSTABILITY

INCLUDING:

- A DISCUSSION OF DEPTH EFFECTS, IN PARTICULAR SMALL
  DEPTHS

- A GENERALISATION OF THE K - H STABILITY MODEL

- A STABILITY DISCUSSION OF A FREE SURFACE FLOW WITH
  BED SHEAR

6. INTRODUCTORY REMARKS AND A LOOK BACK ON A "CLASSI-CAL" STABILITY RESULT.

6.1. On the subject.

6.1.1. Remarks on hydrodynamic instability

The subject under study is one of hydrodynamic stability and instability. Even if the whole of Part 1 of this report is on stability models, it seems appropriate, before starting a detailed stability analysis in the following, to point out some basic aspects of hydrodynamic stability analysis in general. As an indicative statement of what the stability problem is about we may take the following:

> "A hydrodynamic system is in a state of dynamic instability if it from an initial nonoscillatory state of motion by itself generates growing oscillatory motion when given a slight disturbance (perturbation). If such a perturbation disappears with time the system is said to be stable. And finally the system is dynamically indifferent or neutral if its perturbed motion goes on with no change."

The initial nonoscillatory motion as well as the total motion after introduction of the perturbation should satisfy the basic principles of dynamics and continuity. Further an equation of state and all conditions on the boundary of the system have to be satisfied.

In mathematical terms a perturbation η is usually specified as a small amplitude wave with a time dependence expressed by

$$\eta \sim e^{-i \sigma t}$$

σ being a complex angular frequency

$$\sigma = \sigma_r + i \, \sigma_i \tag{6.1}$$

In linear stability analysis terms of second and higher order in per-
turbed quantities are considered small and disregarded throughout the
analysis. A solution of the linear stability problem is thus classified as
follows

$$\sigma_i > o \quad \text{unstable}$$
$$\sigma_i = o \quad \text{neutral} \qquad\qquad (6.2)$$
$$\sigma_i < o \quad \text{stable}$$

Inherent in the formulation of a linear stability problem as sketched
above is that conclusions on the system's stability are valid only with
respect to small perturbations. And a possibly unstable solution
describes the behaviour of the system only for a short time interval
from the onset of the instability. Full account for nonlinear effects is
necessary to describe further development into an eventual final state
of motion.

A second order solution to the mathematical problem of a linear instabil-
ity generally improves somewhat on the linear solution but by no means
approaching a description of the state of motion for large values of the
time t. And it is usually gained at the expence of a considerable
increase in analytical complexity. This being said it should be pointed
out that there exist many examples of mechanical systems that are
stable with respect to a small perturbation but unstable when the
perturbation is larger. In such a case the solution must account for the
finiteness of the perturbation in order to detect the instability.

Another point to observe is concerning the formulation of stability
problems: If the problem is formulated with too strong restrictions one
may conclude with stability in spite of dealing with a reality which is
linearly unstable. A trivial example of this is a sliding or rolling mass
at a saddle-point, being stable with respect to perturbations in one
particular range of directions while generally unstable.

Some consequences concerning physical experiments and observations on
hydrodynamic instabilities may now be seen. Firstly, if the idea is to
check a stability theory by experiment, it is clear that establishing the

correct basic flow conditions may be difficult. One reason for this may be that the theoretically applied basic flow meets strong restrictions set by the actual laboratory equipment to be used.

Secondly it appears difficult to do measurements on instabilities, once basic flow conditions are established, since they usually exist over a range of wave numbers. They may develop simultaneously and possibly with high growth rate, leaving a very short time interval from the onset available for measurement and comparison with linear theory results.

Thirdly we understand form this that visual observations on flow processes in general will be on "fully developed"phenomena i.e. usually very far from conditions at the initial stages of the instability. The risk for misinterpretations may under such circumstances be high.

6.1.2. Some examples of hydrodynamic instabilities.

Perhaps the most well known example of a hydrodynamic instability is the transition from laminar to turbulent flow in a viscid fluid. The theoretical work by Tollmien, Schlichting and others on the transition to turbulence in a boundary layer over a flat plate and the later experimental confirmation by Schubauer and Skramstad is reported in Betchov and Criminale's book (among others) and stands as one of the most successful works in this branch of hydrodynamics.

Another well known and strongly investigated instability is the generation of surface waves on water by a blowing wind. An early proposed mechanism to explain wind generated waves was the Kelvin – Helmholtz instability. However, it soon became clear that it could at best be only a part of the explanation since waves were found to be generated for only a small fraction of the wind velocity predicted by the K-H mechanism. Later work has shown considerable improvements. The most important work in this area is presented in LeBlond and Mysak (1978) and in Yih (1980).

The Kelvin - Helmholtz instability already mentioned dates back to a work by Helmholtz in 1868 and one by Lord Kevin in 1871. It is recognised as an important basic hydrodynamic instability playing an essential role both in large scale geophysical flows and in small scale flow phenomena.

6.2. The classic Kelvin-Helmholtz instability

6.2.1. Basic model

The original Kelvin-Helmholtz (K-H) theory deals with the hydrodynamic stability of the interface between two shearing, ideal fluid layers of infinite extent horizontally and vertically in a gravity field. The situation is sketched in fig. 6.1, where η is a small amplitude perturbation of length $\lambda = 2\pi/k$.
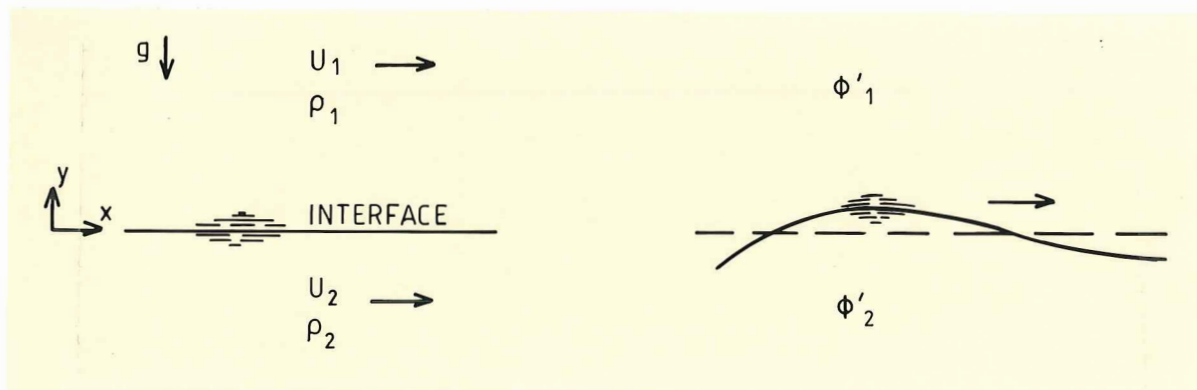

Fig. 6.1. The classic Kelvin-Helmholtz stability model, a: basic flow, b: perturbed flow.

The fluids are of different densities ρ_1 and ρ_2, and the velocity shear is represented by a Dirac delta-function being infinitely large along the interface and zero elsewhere. The formulation of the hydrodynamic problem in terms of potentials and linearized boundary conditions as

well as the solution of the problem is straight forward and may be found in standard textbooks on theoretical hydrodynamics f. ex. Lamb (1945) or Yih (1980).

6.2.2. The stability criterion

The final dynamic relation for the perturbed interface may be solved explicitly with respect to the phase velocity, giving

$$c = \sigma/k = (\rho_1 U_1 + \rho_2 U_2)(\rho_1 + \rho_2)^{-1}$$

$$\pm i\{(\rho_1 + \rho_2)^{-2} \rho_1\rho_2\Delta U^2 - (\rho_1 + \rho_2)^{-1}\Delta\rho g/k\}^{\frac{1}{2}} \quad (6.3)$$

where $\Delta U = U_2 - U_1$ and $\Delta\rho = \rho_2 - \rho_1$. By use of the definition (6.1) for the complex angular frequency, we readily find the relation

$$\sigma_i(k) = \pm \{(\rho_1+\rho_2)^{-2}\rho_1\rho_2\Delta U^2 k^2 - (\rho_1+\rho_2)^{-1}\Delta\rho g k\}^{\frac{1}{2}} \quad (6.4)$$

for the imaginary part of the growth rate. This shows then that, for a perturbation in the given flow system making the formula (6.4) real, one solution grows exponentially in time expressing instability, and another decays exponentially to zero for large values of the time. The stability solution then appears as a complex conjugate pair of angular frequencies. Since an unstable solution exists the flow is concluded to be unstable. The result (6.4) is shown sketched in fig. 6.2.

We observe that the growth rate is high for large k-values i.e. for short perturbation wave lengths, and in fact no maximum growth rate exists. Another observation to be made from the figure is that σi grows from zero at $k = k_c$ to a finite value over a very short interval of k-values, indicating that unstable perturbations of wave number close to k_c may be observable. The limiting value k_c defines the transition between unstable and neutral solutions, called the critical wave number. It is given by requiring (6.4) to be zero, whereby we get

$$k_c = (\rho_1\rho_2)^{-1}(\rho_1 + \rho_2) \Delta\rho \, g \, \Delta U^{-2} \quad (6.5)$$
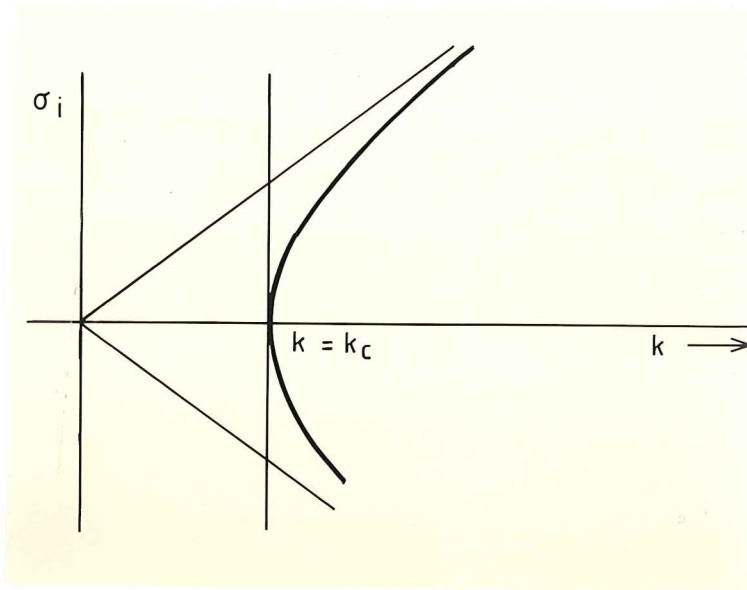
Fig. 6.2. Growth and decay rate according to the classic K-H solution.

The corresponding critical wave length then follows as

$$\lambda_c = 2\pi\rho_1\rho_2(\rho_1+\rho_2)^{-1} \Delta U^2(\Delta\rho \ g)^{-1} \tag{6.6}$$

Perturbations of wave length larger than λ_c give real angular frequencies. They are in other words neutral progressive gravity waves at the interface for which (6.3) is the dispersion equation. These waves may be regarded as indifferent solutions of the stability problem.

6.2.3 Remarks on the original K-H theory.

The fluid model used in the K-H theory includes fluid heterogeneity but disregards compressional as well as diffusional (thermal or viscous) processes. The relevance of such a fluid model is then restricted to phenomena that are much slower than compressional ones and at the same time much faster than the diffusional phenomena occurring in the same flow system.

The basic flow modelling is of course an idealisation. Representing flow shear by a Dirac δ-function as done in K-H theory is preferable by its analytical convenience. Its relevance depends, however, on the á priori shear profile in the actual flow case. The δ-function representation may be an acceptable approximation to flow zones with high flow shear over a limited thickness while neighbouring zones have low shear and are wider.

Besides the restrictions already mentioned the original K-H theory assumes infinite flow depths. This restricts in reality the perturbation wave length to being much smaller than the existing depths, since the assumption is never realised in actual flow systems. The original K-H stability result is in this sense a short wavelength result. If this now is combined with the basic flow shear modelling, we also see that the wavelength has to be larger than the shear zone thickness. On this scale the K-H result is a long wave length result.
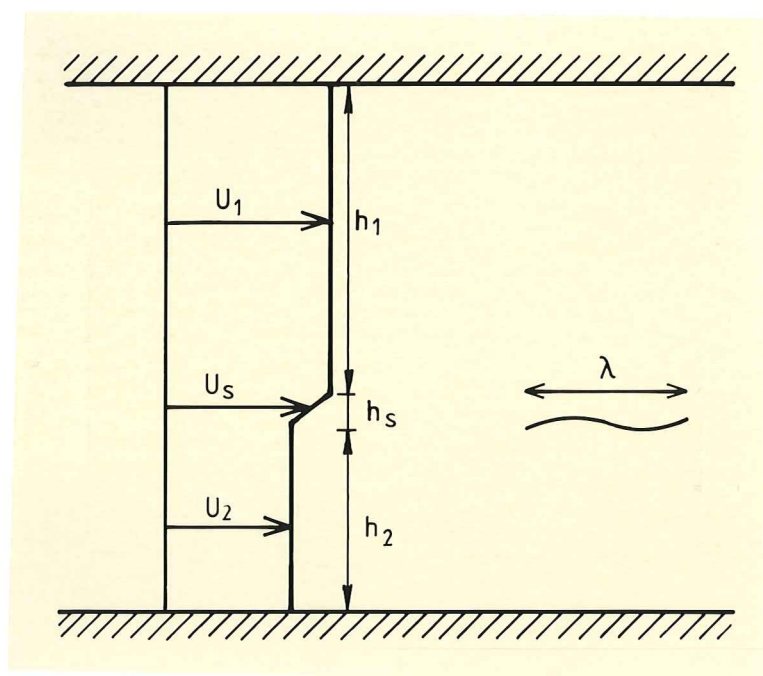
Fig. 6.3. Two layered flow with finite depths and with transitional shear zone of thickness h_s perturbed by a wave of length λ.

If h_1 and h_2 are the depths of an upper and a lower fluid layer respectively and h_s is the shear layer thickness, the requirement on the original K-H result is thus that λ should satisfy the relation

$$h_s \ll \lambda \ll \min (h_1, h_2) \tag{6.7}$$

a requirement that generally may be hard to satisfy. The preceding figure illustrates the situation under consideration. Shear zones at the upper and lower boundaries are in this connection disregarded.

In conclusion the original K-H stability result is valid only under very strong restrictions. It will consequently be of use in only a very limited number of flow cases. These restrictions are not always, but should indeed be, considered when attempting applications of it.

On the other hand it should be emphasized that the K-H instability mechanism still is an important one and that the critisism above is directed towards the mathematical restrictions imposed on it. One restriction is entirely unnecessary namely that the wave lengths should be short compared to flow depths. Generalising the K-H result on this point is a triviality from a mathematical point of view. From the applications point of view the inclusion of finite depths and thereby long wave instabilities is essential. The finite depth K-H result is therefore considered in particular in the following.

7.   THE K-H INSTABILITY IN FINITE AND SMALL DEPTH SYSTEMS.

7.1. Finite depth case.

7.1.1. Stability criterion.

The development of a K-H criterion for finite depth of the fluid layers is straight forward. The solution procedure will be omitted since it is similar to the one for infinite depths and may be found in the same text books as referred to in chapter 6. The only difference between the two cases is the kinematic condition of no vertical motion at bed and top level. The flow system is then modelled as shown in fig. 7.1.
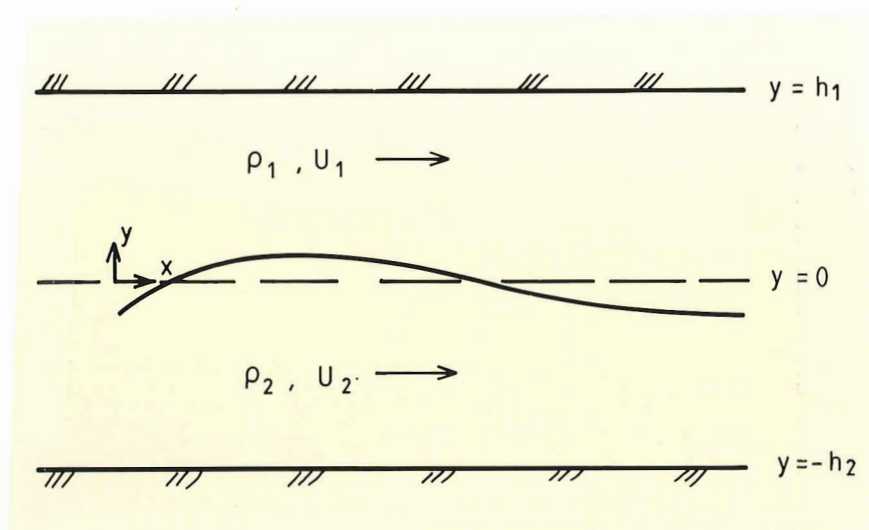
Fig. 7.1. K-H stability model for finite fluid depths.

The dynamic condition at the interface, as in the infinite depth case, requires continuous pressure, which upon application of linearized interface equations gives the new depth-modified dispersion or stability equation

$$\rho_1 \, (c-U_1)^2/\tanh \, kh_1 + \rho_2 \, (c-U_2)^2/\tanh \, kh_2 = \Delta\rho \, g/k \quad (7.1)$$

Equation (7.1) shows that the finite depth requirement affects the inertia terms only.

From now on we use the following short notation for the hyperbolic functions

$$sh \equiv sinh$$
$$ch \equiv cosh$$
$$th \equiv tanh$$
$$cth \equiv cotanh$$

The phase velocity solution is formally identical to (6.3)

$$c = c_r + ic_i$$

$$= (\rho_1^* U_1 + \rho_2^* U_2)(\rho_1^* + \rho_2^*)^{-1}$$

$$\pm i \{\rho_1^* \rho_2^* (\rho_1^* + \rho_2^*)^{-2} \Delta U^2 - \Delta\rho(\rho_1^* + \rho_2^*)^{-1} g/k \}^{\frac{1}{2}} \qquad (7.2)$$

where we for compactness have written

$$\rho_1^* = \rho_1/th\ kh_1, \quad \rho_2^* = \rho_2/th\ kh_2 \qquad (7.3)$$

The critical wave length formula is now

$$\lambda_c = 2\pi\rho_1\rho_2(\rho_1 th\ k_c h_2 + \rho_2 th\ k_c h_1)^{-1}(\Delta\rho g)^{-1}\Delta U^2 \qquad (7.4)$$

Equation (7.4) is transcendental and not solvable in terms of an explicit formula for λ_c or k_c. On the other hand there should be no problem in solving it numerically. However, the general nature of the solution is easily outlined analytically and is shown in the following. First we may note that it is symmetric in the sense that subscripts 1 and 2 may be interchanged, except, of course, in $\Delta\rho$. Formula (7.4) may be rewritten as

$$\Delta U^2/gh_2 = (\rho_1\rho_2)^{-1}(\rho_1 th\ k_c h_2 + \rho_2 th\ k_c h_1)\Delta\rho/k_c h_2 \qquad (7.5)$$

from which two special cases are easily derived:

$$k_c h_1 \ll 1, \quad h_1/h_2 \ll 1:$$

$$\Delta U^2/gh_2 = \Delta\rho \cdot \rho_2^{-1} \; \text{th} \; k_c h_2/k_c h_2 \tag{7.6}$$

and

$$k_c h_1 \gg 1, \quad h_1/h_2 \gg 1:$$

$$\Delta U^2/gh_2 = \Delta\rho(\rho_1 k_c h_2)^{-1} + \Delta\rho\rho_2^{-1} \; \text{th} \; k_c h_2/k_c h_2 \tag{7.7}$$

The following figure is an illustration of relations (7.5 - 7.7). Because of the mentioned formal symmetry a similar figure exists with subscripts interchanged.
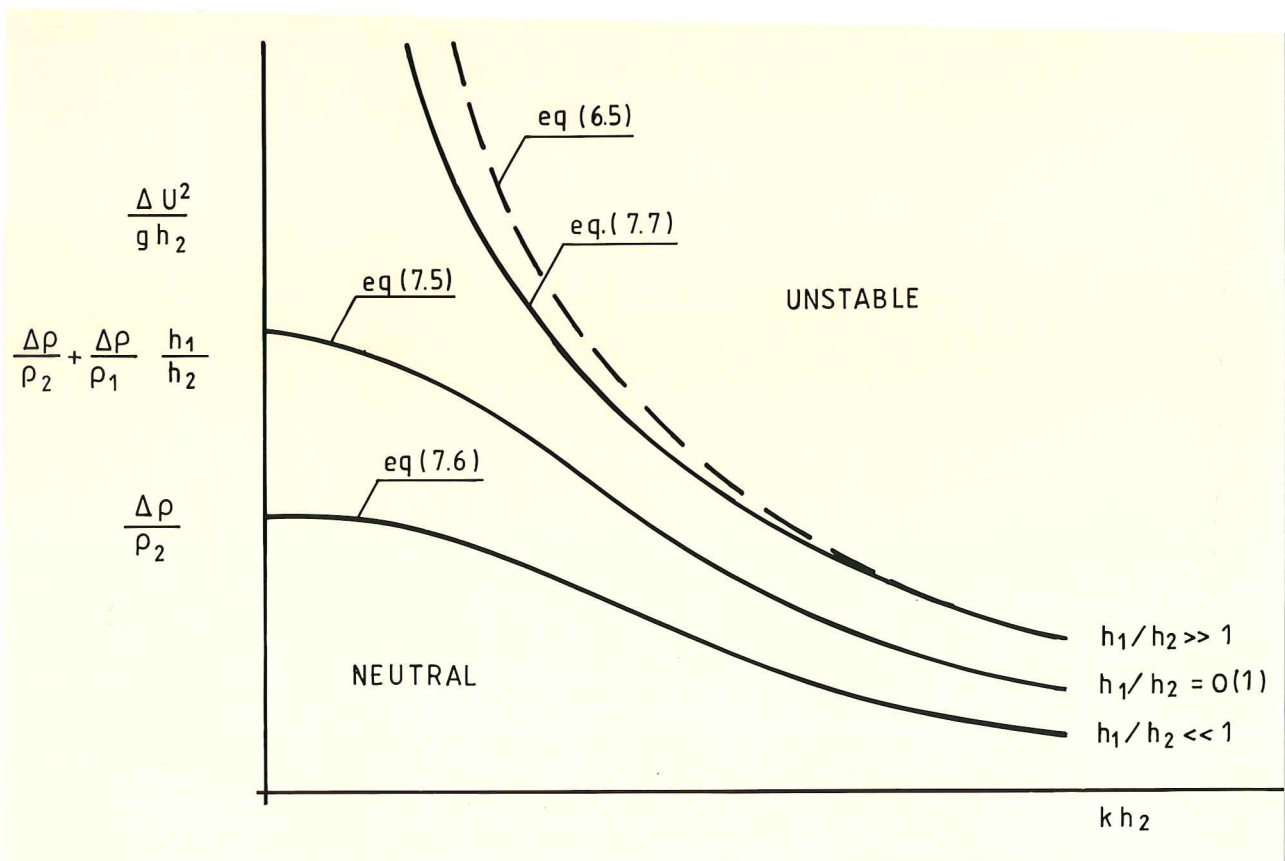
Fig. 7.2. Finite depth K-H stability boundaries.

From this we see that an important effect of finite depth on the K-H instability is a long - wave limit on the shearing flow conditions above which all waves are unstable. We also note that the infinite depth K-H result cannot be interpreted in this type of diagram.

7.1.2. Finite depth effect on instability region.

By noting that the tanh (kh) function for all positive real arguments has values in the interval $\langle 0,1 \rangle$, the critical wave number k_c, implicitly given by equation (7.5), is easily seen to be less than k_c for the infinite depth case given by (6.5). The corresponding critical wave length is consequently larger than in the infinite depth case:

$$\lambda_c(h_1,h_2) > \lambda_c(\infty,\infty) \tag{7.8}$$

Finite depths destabilises the interface according to the K-H criterion in the sense that the interval of unstable wave lengths is increased compared to the infinite depth case. And in general, since tanh is a monotonic function, the interface between two ideal fluids is destabilised in this sense when the depths are reduced.

7.1.3. Finite depth effect on growth rate.

The shape of the function $\sigma_i(k;h_1,h_2)$ is very much the same as that of $\sigma_i(k; \infty,\infty)$ shown in fig. 6.2. Since we get from (7.2) that

$$\sigma_i(k;h_1,h_2) = \{\rho_1{}^*\rho_2{}^*\Delta U^2 k^2 (\rho_1{}^*+\rho_2{}^*)$$

$$- \Delta\rho gk(\rho_1{}^*+\rho_2{}^*)^{-1}\}^{\frac{1}{2}} \tag{7.9}$$

it is clear that σ_i starts with vertical tangent at $k = k_c$. The asymptotic behaviour for large values of k is the same as in the infinite depth case. Thus the general behaviour of the function $\sigma_i(k;h_1,h_2)$ may be sketched as follows
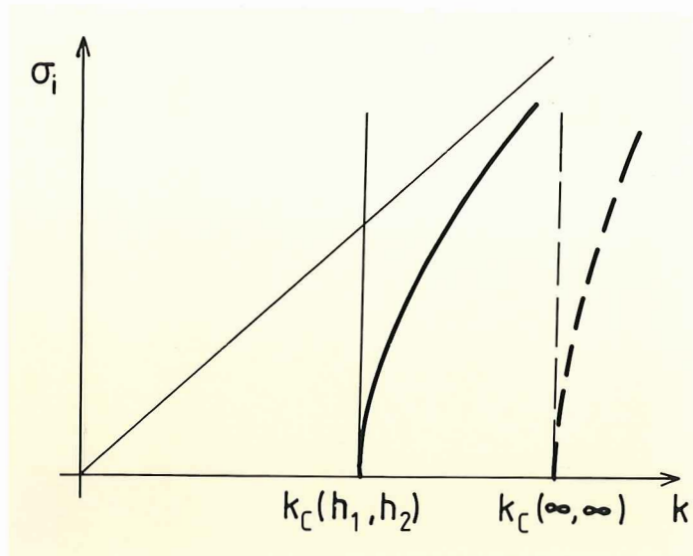
Fig. 7.3. Unstable wave growth rate according to the finite depth K-H
    model.

In the following we investigate in more detail the finite depth effects on
the growth rate of unstable waves. First (7.9) is rewritten as

$$\sigma_i^2(k; h_1, h_2) = \rho_1^* \rho_2^* (\rho_1^* + \rho_2^*)^{-2} \Delta U^2 k^2$$

$$- (\rho_1^* + \rho_2^*)^{-1} \Delta \rho g k \qquad (7.10)$$

The case $h_1 = h_2 = h$ gives

$$\sigma_i^2 (k; h, h) = \rho_1 \rho_2 (\rho_1 + \rho_2)^{-2} \Delta U^2 k^2$$

$$-(\rho_1 + \rho_2)^{-1} \Delta \rho g k \ \text{th} \ kh$$

$$= \sigma_i^2(k; \infty, \infty) + (\rho_1 + \rho_2)^{-1} \Delta \rho g k (1 - \text{th} \ kh) \quad (7.11)$$

And we see that even the limiting case of $kh \ll 1$, under the
restriction of same depth in the two layers, gives the finite and slightly
increased growth rate

$$\sigma_i^2(k;h,h) \rightarrow \sigma_i^2(k;\infty,\infty) + (\rho_1 + \rho_2)^{-1} \Delta\rho g k \qquad (7.12)$$

$$kh \ll 1$$

On the other hand it is easily shown that the growth rate goes to zero if one of the layers is allowed to approach zero depth while the other depth is kept finite:

$$\sigma_i^2(k;h_1,h_2) = (\rho_1^* \Delta U^2 k^2 - \Delta\rho g k) \cdot kh_2/\rho_2 + H.O.T. \qquad (7.13)$$

$$kh_2 \ll 1$$

The growth rate of an unstable wave in a finite depth system then may be larger than, equal to or smaller than that for the infinite depth system.

A more complete investigation of this point is done by independent variation of the two depths. This is most easily performed by derivation:

$$\left.\frac{\partial\sigma_i^2}{\partial h_1}\right|_{h_1=h_2=h} = -\rho_1\Delta\rho k^2\{\rho_2\Delta U^2 k + (\rho_1+\rho_2)g \text{ th } kh\}.$$

$$\cdot\{(\rho_1+\rho_2)^3 \text{ ch}^2kh \text{ th } kh\}^{-1} \qquad (7.14)$$

and

$$\left.\frac{\partial\sigma_i^2}{\partial h_2}\right|_{h_1=h_2=h} = \rho_2\Delta\rho k^2\{\rho_1\Delta U^2 k - (\rho_1+\rho_2)g \text{ th } kh\}.$$

$$\cdot\{(\rho_1+\rho_2)^3 \text{ ch}^2kh \text{ th } kh\}^{-1} \qquad (7.15)$$

An upper layer depth increment is seen to give a reduced growth rate for all unstable waves. On the other hand a lower layer depth increment gives an increased, unchanged or reduced growth rate according to the condition

$$\Delta U^2/gh \gtreqless (\rho_1+\rho_2)\rho_1^{-1} \text{ th } kh/kh \qquad (7.16)$$

While the conclusion based on (7.11) was limited to the case $h_1 = h_2 = h$, the above results are valid for any pair (h_1, h_2) of depths. And we note in particular that the lower layer only may give rise to a growth rate increment by altering the depth.

7.1.4. Propagation velocity of unstable waves.

The velocity of propagation of unstable waves is given by formula (7.2) as

$$c_r(k;h_1,h_2) = (\rho_1^* U_1 + \rho_2^* U_2)(\rho_1^* + \rho_2^*)^{-1} \qquad (7.17)$$

An immediate consequence of (7.17) is that the propagation rate in an equal-depths system is given by

$$c_r(k;h,h) = (\rho_1 U_1 + \rho_2 U_2)(\rho_1 + \rho_2)^{-1}$$

$$= c_r(\infty,\infty) = \text{const.} \qquad (7.18)$$

This result indicates that a depth difference between the layers is more determining for the propagation rate than the depths themselves. According to (7.18) c_r does not vary with depth at all as long as the two depths are kept the same, nor does in this case c_r vary with wave length.

Further insight into the influence on c_r of depth variations is gained by establishing the derivatives as follows

$$\frac{\partial c_r}{\partial kh_1} = \rho_1^* \rho_2^* (\rho_1^* + \rho_2^*)^{-2} \Delta U \, (\ln \text{th } kh_1)' \qquad (7.19)$$

$$\frac{\partial c_r}{\partial kh_2} = - \rho_1^* \rho_2^* (\rho_1^* + \rho_2^*)^{-2} \Delta U \, (\ln \text{th } kh_2)' \qquad (7.20)$$

where the dash signifies derivation. While c_r is depending on the basic velocities the depth derivatives are seen to depend on the velocity

shear. Another interesting point is this: While an upper layer depth increment adds to the propagation velocity a depth increment in the lower layer acts oppositely. And in particular we get

$$\frac{\partial c_r}{\partial kh_1} + \frac{\partial c_r}{\partial kh_2} \Bigg|_{h_1=h_2} = 0 \tag{7.21}$$

confirming (7.18).

The formal limit of disappearing depth of one layer gives

$$c_r(h_1,0) = U_2, \quad c_r(0, h_2) = U_1 \tag{7.22}$$

The limiting case is certainly meaningless and from a physical point of view without any interest. However, conceiving (7.22) as an approximative result for small but not disappearing depths, we have a result that seems much more interesting

$$c_r(h_1, \Delta h_2) = U_2 + \Delta U_2 \text{ and } c_r(\Delta h_1,h_2) = U_1 + \Delta U_1 \tag{7.22a}$$

where ΔU_2 and ΔU_1 are small compared to U_2 or U_1. This will be investigated further in the following. First we sum up the finite depth results.

7.1.5. Summary of finite depth results.

On the basis of the preceding analysis we may sum up the main results as follows:

- The F' – kh plane is the natural plane for interpretation of the one mode finite depth K-H stability.
- Finite layer depths affect only the inertia part of the interface dynamics.
- The critical wave length is increased compared to the infinite depth case, i.e. the region of unstable wave lengths is larger in a finite depth than in an infinite depth system.

- In a finite depth system all wave lengths are unstable for sufficiently strong shear ΔU.
- The growth rate of an unstable wave close to the critical one has finite value and increases monotonically with kh. No maximum growth rate exists.
- The growth rate of an unstable wave in a finite depth system may be larger than, equal to or smaller than that of an infinite depth system.
- The propagation velocity of an unstable wave in an equal-depths system is unaffected by the depth. In a one-thin-layer-system the propagation velocity approaches the flow velocity of the thin layer.

7.2. K-H instability in a thin sublayer system.

7.2.1. Why thin bed layers?

Having considered so far the infinite depth and the finite depth cases we now turn to systems where the lower layer thickness is very small. The reason for doing this lies in the fact that natural systems do have bed layers set up by viscosity, gravity or other effects. The modelling done here allows the bed layer to be heavier than the fluid above to account for internal gravity effects.

The model thus established will be purely hydrodynamical in spite of the fact that we have sedimentary flows in mind. This point will be discussed further in the later parts of this report. The hydrodynamic analysis will be continued along the lines of K-H theory, this being the main subject of the present part. Thus no use of traditional viscous or turbulent boundary layer theory will be made.

The limiting case of very small lower layer depth was considered at the end of the last section. This is also the starting point for our thin bed layer analysis.

7.2.2. Growth rate in thin bed layer system.

The growth rate formula for a finite depth system was established by (7.10), where from one should recall the definitions (7.3). Divided through by k^2 we have

$$c_i^2 = \rho_1^* \rho_2^* (\rho_1^* + \rho_2^*)^{-2} \Delta U^2 - (\rho_1^* \rho_2^*)^{-1} \Delta \rho g / k \qquad (7.23)$$

Assuming now that kh_2 is very small i.e.

$$kh_2 \ll 1 \qquad (7.24)$$

while the upper layer depth is kept finite, we may develop (7.23) in series of ascending powers of kh_2 as

$$c_i^2 = \rho_1 \rho_2^{-1} (\Delta U^2 / \text{th } kh_1 - \rho_1^{-1} \Delta \rho g / k) kh_2 + O\{(kh_2)^2\} \qquad (7.25)$$

Generally we then have

$$c_i = O\{(kh_2)^{\frac{1}{2}}\} \qquad (7.26)$$

However, 7.25 shows that when the relation

$$F'^2 = \Delta U^2 / gh_1 = \Delta \rho \, \rho_1^{-1} \, \text{th } kh_1 / kh_1 \qquad (7.27)$$

is satisfied, i.e. the first paranthesis in (7.25) is zero, then

$$c_i = O\{kh_2\} \qquad (7.28)$$

This shows that unstable waves on an interface close to a bed, i.e. (7.24) satisfied, grow slowly, and proportionally to $(kh_2)^{\frac{1}{2}}$. Again this means that if h_2 is fixed, the shorter waves in general grow faster than the longer waves.

7.2.3. Stability criterion.

Equation (7.25) also serves as a first order stability criterion since the first order term generally dominates the expansion. And, as pointed out already, the paranthesis associated with kh_2 may become zero. Relation (7.27) then in fact is, to first order, the stability criterion and may as such be written

$$F'^2 = \Delta U^2/gh_1 = \Delta\rho\rho_1^{-1}\text{th } k_c h_1/k_c h_1 \qquad (7.29)$$

k_c now being the critical wave number. With a view towards later discussion we have introduced the F' symbol for the ratio between the shear velocity ΔU and the long wave velocity of the upper layer ($\sqrt{gh_1}$). It should be noted that h_1 is introduced as a dummy parameter in the denominator of both (7.27) and (7.29). The reason is again our view towards a description and interpretation of results in terms of main flow variables and the ordinary hydraulic Froude - number.

Relation (7.29) now is seen, by inspecting (7.25), to separate the region in the F'-kh_1 plane where c_i^2 is positive, and perturbations consequently unstable, from the region where c_i^2 is negative and only neutral perturbations exist. Figure 7.4 illustrates this.
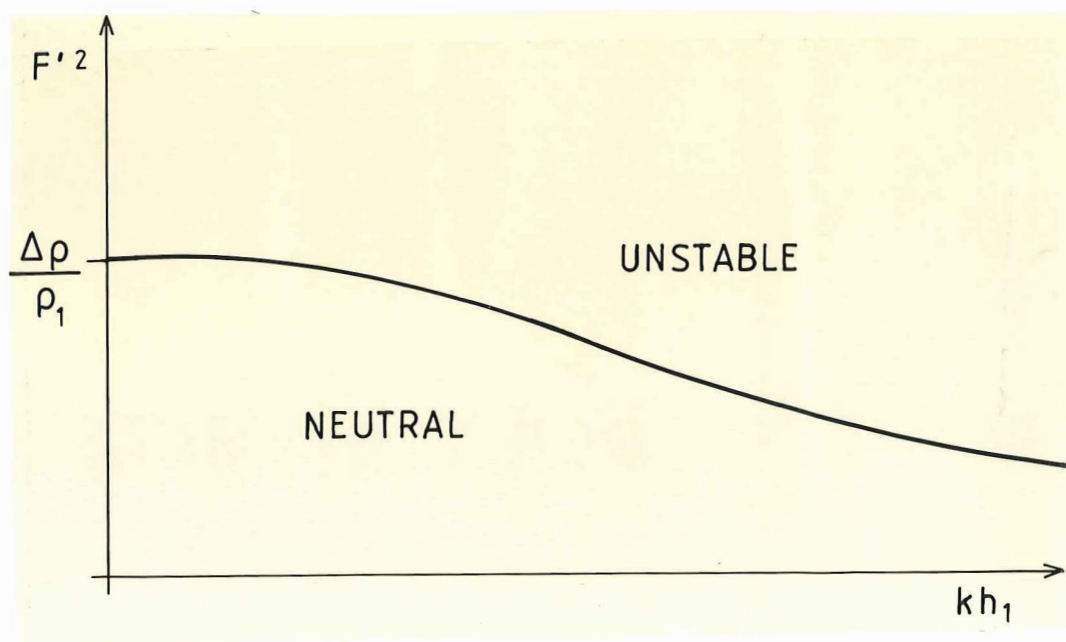
Fig. 7.4. One mode first order K-H stability criterion for a thin sub-layer system.

It is important to note that the criterion (7.29) in general defines a finite critical wave length. For a shear velocity of high enough strength waves of all lengths are still unstable.

It should also be remarked that assumption (7.24) - the "thinness assumption" - holds only for waves that are long enough when the depth h_2 is given as the case will be in a real system. And when interpreting results here and in the following based on (7.24) - this limitation should be kept in mind. When we express the finiteness of the upper layer by saying

$$kh_1 = O\{1\} \qquad (7.30)$$

this has the consequence that

$$h_2 \ll h_1 \qquad (7.31)$$

7.2.4. Propagation of unstable waves on a thin sublayer.

The starting point for our development of the propagation velocity of unstable thin sublayer waves is relation (7.17)

$$c_r(h_1,h_2) = (\rho_1{}^*U_1 + \rho_2{}^*U_2)(\rho_1{}^* + \rho_2{}^*)^{-1}$$

$$= (\rho_1{}^*U_1 \text{th } kh_2 + \rho_2 U_2)(\rho_1{}^* \text{th } kh_2 + \rho_2)^{-1} \quad (7.32)$$

When we develop th kh_2 as before we get

$$c_r (h_1, h_2 \ll h_1) = U_2 + \rho_1{}^*\rho_2{}^{-1}\Delta Ukh_2 + O\{(kh_2)^2\} \qquad (7.33)$$

or the alternative statement:

$$c_r - U_2 = O\{kh_2\} \qquad (7.34)$$

The present result (7.33) is a more precise statement of the comment to (7.22) where we considered the zero limit of the lower layer depth.

It is interesting now to go back to the basic interface equation (7.1) and apply the results (7.25) and (7.34) in a development of (7.1) for a thin sublayer interface. We get after straight forward development the relation

$$\rho_1^* \Delta U^2 = \Delta\rho g/k + O\{kh_2\} \tag{7.35}$$

which is exactly the stability limit (7.29) and illustrated in fig 7.4.

7.2.5. The homogeneous fluid limit.

We may go to the limit $\Delta\rho\to0$ in both the infinite, the finite and the small sublayer depth cases considered. Such a limiting process is from a mathematical point of view a trivial matter, so we simply state the most important findings:

- Neutral or indifferent waves no longer exist, irrespective of depths being infinite, finite or small.
- All wave lengths are unstable for $\Delta U \neq 0$
- The growth rate is given by

$$\sigma_i = \pm (\text{th } kh_1 \text{ th } kh_2)^{\frac{1}{2}} (\text{th } kh_1 + \text{th } kh_2)^{-1} k\Delta U \tag{7.36}$$

any depth case being included. In particular

$$\sigma_i (k;h,h) = \pm \tfrac{1}{2} k\Delta U \tag{7.37}$$

- The propagation velocity of unstable waves for a general depth system becomes

$$c_r = (U_2\text{th } kh_1 + U_1\text{th } kh_2)(\text{th } kh_1 + \text{th } kh_2)^{-1} \tag{7.38}$$

approaching

$$c_r = U_2 + O\{kh_2\} \tag{7.39}$$

for

$$kh_2 \ll 1$$

It may be remarked that an interpretation of the stability criterion in the $F' - kh_1$ diagram of fig. 7.4 still may be done as we go to the limit $\Delta\rho\to o$. The stability boundary itself eq. (7.29) degenerates into the horizontal axis, which means that the whole $F' - kh_1$ quadrant is a region of instability. We therefore conclude that the main flow $F' - kh_1$ plane is suitable also for interpretation of the weak instabilities of the shear interface close to the bed.

7.2.6. Summary of thin sublayer results.

The main results found for the thin sublayer may be summarised as follows

- The thin sublayer model leads to the existence of a weak K-H instability which is suitably interpreted in terms of the main flow variables, i.e. in a $F' - kh_1$ diagram.
- The stability criterion is expressed by the relation

$$F'^2 = \Delta U^2/gh_1 = \Delta\rho\rho_1^{-1} \text{ th } kh_1/kh_1$$

which for a finite Froude number F' generally determines a finite value of the critical wave length $\lambda_c = 2\pi/k_c$.
- The growth rate of unstable waves is small and of order given by

$$c_i = O\{(kh_2)^{\frac{1}{2}}\}$$

- The propagation velocity of unstable waves approaches the flow velocity close to the bed

$$c_r - U_2 = O\{kh_2\}$$

7.3. The thin superlayer system. Remarks.

The results gained in the preceding sections for a thin sublayer all have their counterpart in a thin upper layer (or superlayer) system.

This is obvious from the symmetry pointed out for finite depth systems, (see equations (7.2) - (7.5) and comment to fig. 7.2). Results for the thin superlayer are therefore not stated explicitly as they are deducible directly from the given sublayer results by replacing subscript 2 by subscript 1. An immediate consequence is that propagation velocity and growth rate of unstable waves are both small, to the orders given by

$$c_r - U_1 = O\{kh_1\} \tag{7.40}$$

$$c_i = O\{(kh_1)^{\frac{1}{2}}\} \tag{7.41}$$

The dimensionless depth kh_1 of the superlayer is here assumed much smaller than one. And the critical wave length will again generally be finite.

The preceding discussion of the K-H mechanism in a system with one finite depth and one small depth fluid layer of course meets the objection that such a system is hardly met in practice. We always have to do with more than one dynamic surface, be it internal shear surfaces or free surfaces without shear but with strong gravity effects. In order to meet this serious objection to the application of K-H theory to real systems the K-H model has to be generalised to cope with multidegree of freedom systems. This is the subject of the following chapter.

8. A GENERALISED DISCRETE INVISCID STABILITY MODEL FOR SHEARING FLOWS.

8.1. Theoretical model.

We consider an inviscid two-dimensional hydrodynamic system consisting of a high number of incompressible, homogeneous fluid layers of finite thickness and different densities in a gravitational field.
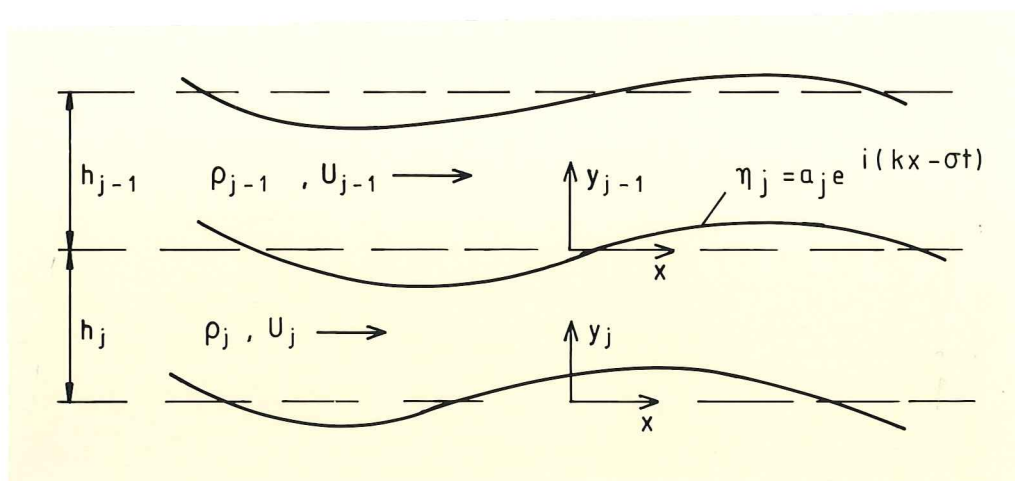
Fig. 8.1. Perturbed system of inviscied shearing fluid layers. Definition sketch.

The system is given a perturbation as shown in fig. 8.1. The flow within each layer is considered as potential flow. We define conventionally the velocity components in layer j by

$$v_{i,j} = -\partial\phi_j/\partial x_i, \quad \begin{aligned} i &= 1,2 \\ j &= 1,2, \text{ --- } \end{aligned} \tag{8.1}$$

Here ϕ_j is the velocity potential in the j – th layer and x_i is any of the coordinates x or y.

We may now formulate the stability problem as follows:

The total flow field is taken as the sum of the basic flow and a perturbed flow

$$\bar{\phi}_j = \phi_j + \phi_j' \tag{8.2}$$

where the meaning of the symbols is obvious. For the basic flow we define

$$\phi_j = U_j x \tag{8.3}$$

And for the perturbed flow

$$\phi_j' = C_{j,1} \, \text{sh} \, k(y_j - h_j) + C_{j,2} \, \text{ch} \, k(y_j - h_j) \tag{8.4}$$

$C_{j,1}$ and $C_{j,2}$ are integration constants to be determined by the kinematic conditions for layer j. In linearized form they appear as

$$\frac{\partial \eta_j}{\partial t} + U_j \frac{\partial \eta_j}{\partial x} = - \frac{\partial \phi'_j}{\partial y_j}, \quad y_j = h_j \tag{8.5}$$

and

$$\frac{\partial \eta_{j+1}}{\partial t} + U_j \frac{\partial \eta_{j+1}}{\partial x} = - \frac{\partial \phi'_j}{\partial y_j}, \quad y_j = o \tag{8.6}$$

After straight forward development we find

$$C_{j,1} = i \, a_j (c - U_j) \tag{8.7}$$

and

$$C_{j,2} = i \, (a_j / \text{th} \, kh_j - a_{j+1} / \text{sh} \, kh_j)(c - U_j) \tag{8.8}$$

For layer j – 1 the formulation and reasoning is entirely similar, and we find a corresponding pair of integration constants for this layer determined as

$$C_{j-1,1} = i \, a_{j-1}(c - U_{j-1}) \tag{8.9}$$

and

$$C_{j-1,2} = i(a_{j-1} / \text{th} \, kh_{j-1} - a_j / \text{sh} \, kh_{j-1})(c - U_{j-1}) \tag{8.10}$$

The amplitudes are generally allowed to be complex - valued by defining

$$a_j = |a_j| \, e^{i\theta_j} \qquad (8.11)$$

The velocity fields of layers j and j-1 are now completely determined by the basic flows and the perturbed flow potentials

$$\phi'_j = i(c-U_j)\{a_j \, \text{sh} \, k(y_j-h_j) \, +$$

$$(a_j/\text{sh} \, kh_j - a_{j+1}/\text{sh} \, kh_j)\text{ch} \, k(y_j-h_j)\}e^{i(kx-\sigma t)} \qquad (8.12)$$

and

$$\phi'_{j-1} = i(c-U_{j-1})\{a_{j-1} \, \text{sh} \, k(y_{j-1}-h_{j-1}) \, +$$

$$(a_{j-1}/\text{sh} \, kh_{j-1} - a_j/\text{sh} \, kh_{j-1}).$$

$$.\text{ch} \, k(y_{j-1}-h_{j-1})\}e^{i(kx-\sigma t)} \qquad (8.13)$$

We may now enter the dynamic condition at interface j requiring continuity of pressure across the interface, which in linearized form reads

$$\rho_{j-1} \{ \frac{\partial \phi'_{j-1}}{\partial t} + U_{j-1} \frac{\partial \phi'_{j-1}}{\partial x} - g \, y\}$$

$$= \rho_j \{ \frac{\partial \phi'_j}{\partial t} + U_j \frac{\partial \phi'_j}{\partial x} - g \, y\}, \quad y = \eta_j \qquad (8.14)$$

After substitution of potentials and some rearrangement of terms we arrive at the generalised interface condition

$$\rho_{j-1}(1/\text{th} \, kh_{j-1} - a_{j-1,j}/\text{sh} \, kh_{j-1})(c - U_{j-1})^2$$

$$+ \rho_j(1/\text{th} \, kh_j - a_{j+1,j}/\text{sh} \, kh_j)(c - U_j)^2 \qquad (8.15)$$

$$= (\rho_j - \rho_{j-1}) \, g/k, \qquad j = 1,2, - - -,n$$

The symbol $a_{j-1,j}$ is a short notation for the amplitude ratio a_{j-1}/a_j, and correspondingly for $a_{j+1,j}$. And since mostly the phase difference and not the phases themselves is the information of interest in this context we may also introduce the notation $\theta_{j+1,j}$ for the phase difference $\theta_{j+1} - \theta_j$, and similarly for other phase differences.

8.2. Some comments on the generalised condition.

8.2.1. Decoupling

The essential result of the generalisation is the presence of the two coupling terms containing the amplitude ratios and a depth dependence. The system may be decoupled in two ways,

- by letting the depths of the layers be large compared to the perturbation wavelength, or
- by requiring no deformation of the neighbouring faces (i.e. plane rigid walls).

In the decoupled cases we are back to the classical K-H results, for infinite or finite depths, respectively.

8.2.2. Coupled system without basic flow.

A check on the coupling terms is achieved by reducing the model to one without stability aspects i.e. by setting the shearing flow out of discussion ($U_j = U_{j-1} = 0$).
Eq. (8.15) should then be the general eigenvalue equation for free oscillation in an n-layer system. Rewriting it as a homogeneous amplitude equation, we have

$$- \rho_{j-1} kc^2 / \text{sh } kh_{j-1} \cdot a_{j-1}$$

$$+ \{ (\rho_{j-1}/\text{th } kh_{j-1} + \rho_j/\text{th } kh_j) kc^2 - (\rho_j - \rho_{j-1}) g \} a_j$$

$$-\rho_j kc^2/\text{sh } kh_j \cdot a_{j+1} = 0 \qquad (8.16)$$

$$j = 1,2, - - -, n-1$$

The eigenvalues are determined by the determinantal equation

$$
\begin{vmatrix}
A_1 & -B_2 & & & 0 \\
-B_2 & A_2 & -B_3 & & \\
& -B_3 & A_3 & -B_4 & \\
& & \text{----------} & & \\
0 & & & -B_{n-1} & A_{n-1}
\end{vmatrix}
= 0 \qquad (8.17)
$$

where

$$A_j = (\rho_{j-1}/\text{th } kh_{j-1} + \rho_j/\text{th } kh_j)k - (\rho_j - \rho_{j-1})g \qquad (8.18)$$

$$B_j = \rho_{j-1} kc^2/\text{sh } kh_{j-1}, \quad j = 1,2, - - -, n - 1 \qquad (8.19)$$

and this is exactly the n-layer eigenvalue equation of R.R. Webb as reported by A.G. Greenhill and later applied in theoretical considerations on the critical Froude number in layered fluids.

8.2.3. Flow over sinusoidal bed.

A third case is included for the purpose of checking and because of its relation to later discussion. The case is another demonstration of the generality of equation (8.15). We apply it to the interface of the flow system sketched in fig. 8.2, and get the relation
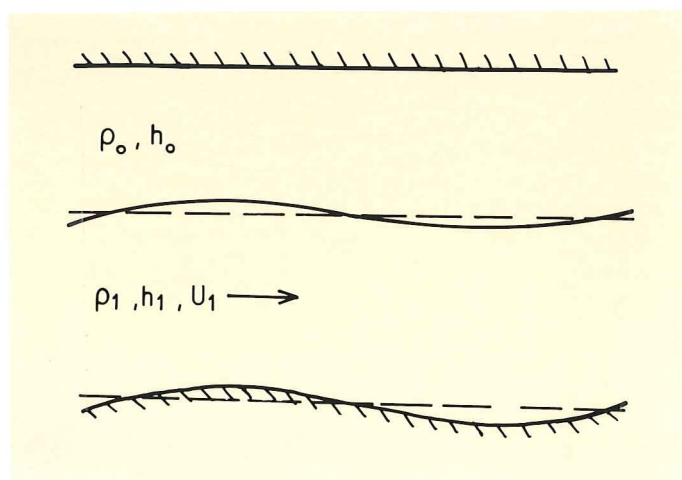
Fig. 8.2. Two layer flow over a sinusoidal bed. Definition sketch.

$$\rho_1 \left(1/\text{th } kh_1 - a_{21}/\text{sh } kh_1\right)U_1^2 = \Delta\rho g/k \tag{8.20}$$

having assumed stationary and stable flow ($c \equiv o$). The model is restricted to cases of no relative motion between the upper layer and the bed perturbation. Relation (8.20) may be rearranged in the following way

$$a_{21} = \left(F^2 - \Delta\rho\rho_1^{-1} \text{ th } kh_1/kh_1\right)F^{-2} \text{ ch } kh_1 \tag{8.20a}$$

showing that the interface is in phase with the bed when the paranthesis is positive, or when

$$F^2 > \Delta\rho\rho_1^{-1} \text{ th } kh_1/kh_1 \tag{8.21}$$

In the long wave limit (8.20a) gives that a_{21} is positive if F^2 is larger than $\Delta\rho/\rho_1$. We may also note that the only influence on the flow by the upper layer is through $\Delta\rho$. The free surface version of (8.20a) is obtained by simply setting $\rho_o \equiv 0$, and may be written

$$a_{21} = \left(F^2 - \text{th } kh_1/kh_1\right)F^{-2} \text{ ch } kh_1 \tag{8.22}$$

where the Froude number as before is defined by $F^2 = U_1^2/gh_1$. Formula (8.22) is readily seen to be equivalent to the relation given by Lamb (art. 246). The version (8.22) has a form more suitable for comparison with other parts of this work.

It is interesting to note that the relation

$$F^2 = \text{th } kh_1/kh_1 \tag{8.23}$$

again plays a central role. We have stated the problem – as in other relevant texts, f.ex. Lamb – as one of stationary and stable flow. Formula (8.23) comes out as a relation separating in-phase flow from (180°) out-of-phase flows, fig.8.3.
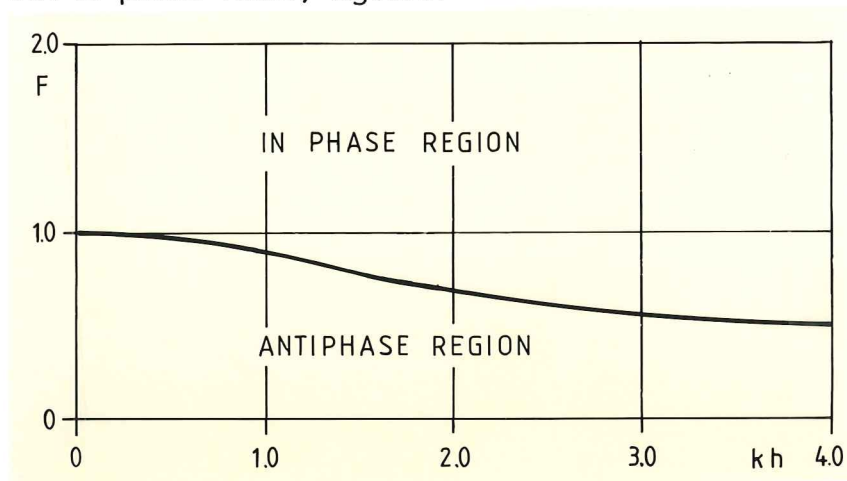
Fig. 8.3. Phase of amplitude ratio for free surface flow over sinusoidal bed.

One might want to include a purely imaginary frequency in this problem to discuss the interface stability. However, this would give us a stability relation of the type

$$\sigma_i = f \ (kh; F, a_{21}) \tag{8.24}$$

which does not serve satisfactorily as a stability result containing the undetermined amplitude ratio. It is thus clear that in formulating a stability problem properly by the present model, fixed boundaries should not be perturbed. A further remark about relation (8.23) should be made in view of the amplitude formula (8.22). Besides being a phase

separating relation it gives the wave length for a given flow (i.e. given F) for which the amplitude ratio (8.22) is zero. If the amplitude ratio is inversed, formula (8.23) is turned into a singularity relation.

8.2.4. Flow under a fixed sinusoidal boundary.

A final example is included as additional background for later discussion.
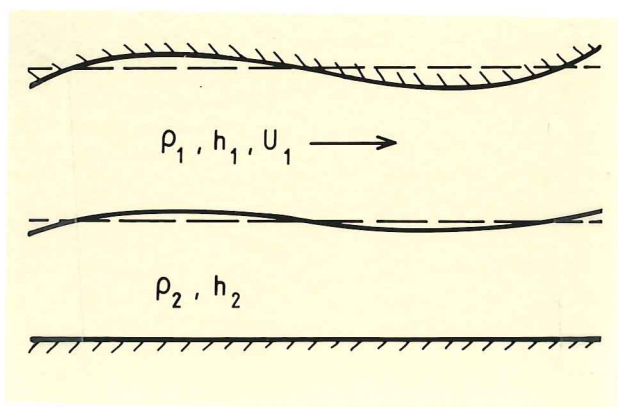
Fig. 8.4. Flow under sinusoidal boundary. Definition sketch.

The flow model is sketched in fig. 8.4. We assume, as in the previous example, that the flow is stationary and stable and that there is no motion of the lower fluid relative to the upper boundary perturbation. Equation (8.15) now gives

$$\rho_1(1/\text{th } kh_1 - a_{12}/\text{sh } kh_1)U_1^2 = \Delta\rho g/k \qquad (8.25)$$

for the interface. Solving for the amplitude ratio we get

$$a_{12} = (F^2 - \Delta\rho\rho_1^{-1} \text{ th } kh_1/kh_1)F^{-2} \text{ ch } kh_1 \qquad (8.26)$$

this relation is of the same type as (8.20a) or (8.22) the main difference being that the amplitude ratio on the left is inversed.

8.2.5. Final remarks on potential theory results for sinusoidal boundaries.

The way the hydrodynamic problems are formulated above leads to serious drawbacks of the results. One has been pointed out already: the inconclusiveness of the interfacial condition as to stability or instability.

In the case of a stationary single layer free surface flow over a sinusoidal bed it seems justified to ask whether such a flow really exists or not. Yih (1976) finds that the free surface becomes unstable by resonant interaction between different free surface modes.

However, Yih's model as well as the potential theory formulas disregard the shearing effects at the fixed boundaries, and their possible interaction with the free surface, which will be present in real fluids. It therefore seems to be an open question how to interpret relations like the ones shown in the two preceding subsections. A closer examination of shear effects at the bed and free surface interaction effects will be presented later in this report.

8.3. A further aspect of the generalised condition.

The generalised dynamic interfacial condition (8.15) may be written shortly

$$\alpha_{j-1} (c-U_{j-1})^2 + \alpha_j (c-U_j)^2 = \Delta\rho_j \, g/k \tag{8.27}$$

where the meaning of α_j and α_{j-1} is obvious. As a quadratic equation in the phase velocity it has the solution

$$c = \bar{U} \pm i\{\alpha_{j-1}\alpha_j\Delta U^2 - (\alpha_{j-1}+\alpha_j)\Delta\rho_j g/k\}^{\frac{1}{2}}/(\alpha_{j-1}+\alpha_j) \tag{8.28}$$

where $\bar{U} = (\alpha_{j-1} U_{j-1} + \alpha_j U_j)/(\alpha_{j-1} + \alpha_j)$. The stability boundary is then given by

$$\Delta U^2 k / \Delta \rho_j g = (\alpha_{j-1} + \alpha_j) / \alpha_{j-1} \alpha_j .$$

$$= \{ \rho_{j-1} \text{sh } kh_j (\text{ch } kh_{j-1} - a_{j-1,j})$$

$$+ \rho_j \text{sh } kh_{j-1} (\text{ch } kh_j - a_{j+1,j}) \} .$$

$$\cdot \{ \rho_{j-1} \rho_j (\text{ch } kh_{j-1} - a_{j-1,j})(\text{ch } kh_j - a_{j+1,j}) \}^{-1} \qquad (8.29)$$

This relation is of course not useful as a stability criterion as it depends on three unknown amplitudes. The most interesting aspect of (8.29) appears to be the strong influence on the stability boundary by the ratio between neighbouring amplitudes versus the hyperbolic cosine to the dimensionless layer thickness between them. The relations

$$a_{j-1,j} = \text{ch } kh_{j-1} \qquad (8.30)$$

$$a_{j+1,j} = \text{ch } kh_j \qquad (8.31)$$

in fact represent singular conditions in the above formula for the stability boundary.

9. THE FREE SURFACE - BED LAYER SYSTEM.

9.1. Specification of the system.

The hydrodynamic system to be considered initially in this chapter is sketched below, fig. 9.1.
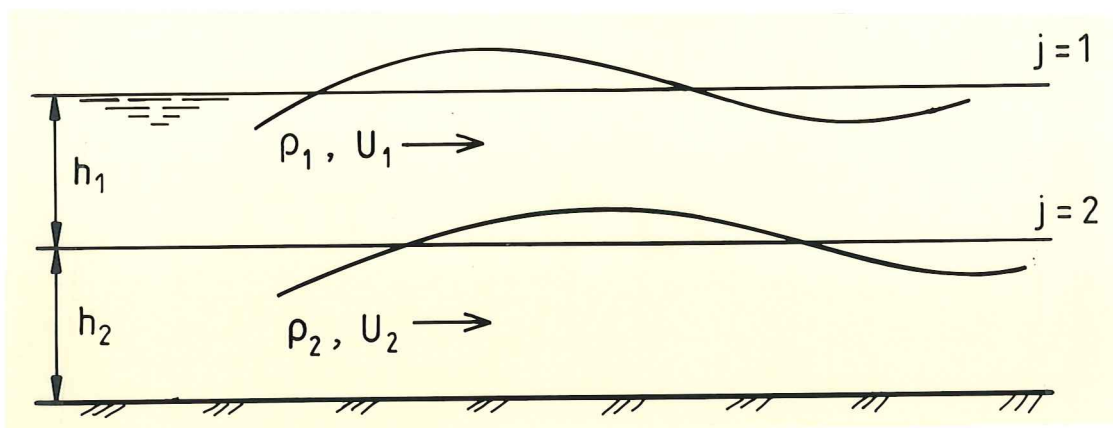
Fig. 9.1. Two-layer free surface system. Definition sketch.

In the terminology of chapter seven we are dealing with a three layer model with zero density of the upper layer, $\rho_0 = 0$. The system, is perturbed as shown, allowing generally a phase shift θ to exist between the two surfaces. This phase will in turn be determined by the system's mechanical conditions.

9.2. Stability condition.

We consider first the most general situation with finite depth of both layers. By use of (8.15) on the free surface and in turn on the interface, we get the two equations

$$(1/\text{th } kh_1 - a_{21}/\text{sh } kh_1)(c - U_1)^2 = g/k \qquad (9.1)$$

$$\rho_1(1/\text{th } kh_1 - a_{12}/\text{sh } kh_1)(c - U_1)^2$$

$$+ \rho_2(c - U_2)^2/\text{th } kh_2 = \Delta\rho \, g/k \qquad (9.2)$$

The eigenvalues of the system are now determined and will be discussed in the following.

9.2. The eigenvalue equation.

The system (9.1) – (9.2) is rewritten in a more traditional way for eigenvalue analysis

$$\{(c - U_1)^2/\text{th } kh_1 - g/k\}a_1 - \{(c - U_1)^2/\text{sh } kh_1\} \, a_2 = 0 \quad (9.3)$$

$$\{-\rho_1(c-U_1)^2/\text{sh } kh_1\}a_1 + \{\rho_1{}^*(c-U_1)^2 + \rho_2{}^*(c-U_2)^2$$

$$- \Delta\rho g/k\}a_2 = 0 \qquad (9.4)$$

The determinant of this homogeneous set of algebraic equations must be zero in order to have non-zero amplitude solutions. The determinantal equation is

$$\{\rho_1{}^*(c-U_1)^2 - \rho_1 g/k\}\{\rho_1{}^*(c-U_1)^2 + \rho_2{}^*(c-U_2)^2 - \Delta\rho g/k\}$$

$$= \rho_1{}^{*2}(c-U_1)^4/\text{ch}^2 kh_1 \qquad (9.5)$$

The term responsible for coupling in the system is the one on the right hand side of (9.5) and is seen to diminish rapidly for large values of the argument kh_1.

One conclusion is immediately reached on inspection of (9.5): Since all variables, except possibly c, are real, an identical equation exists for $\bar{c}$ – the complex conjugate of c. That is

$$\{\rho_1{}^*(\bar{c}-U_1)^2 - \rho_1 \ g/k\}\{\rho_1{}^*(\bar{c}-U_1)^2 + \rho_2{}^*(\bar{c}-U_2)^2 - \Delta\rho g/k\}$$

$$= \rho_1{}^{*2}(\bar{c}-U_1)^4/ \ ch^2 \ kh_1 \qquad (9.6)$$

So the conclusion is:

> To every eigenvalue solution there corresponds another eigen-value being the complex conjugate of the first. This result is trivially valid for purely real eigenvalues.

In the decoupled case $kh_1 \gg 1$ we are back to the two prototype one degree of freedom cases: the classical finite depth K-H internally, and the modified dispersion equation for neutral gravity waves on the free surface. This means that the decoupled system has either 4 real eigen-values or two real and two complex conjugate eigenvalues. Generally we will then have one unstable wave in the decoupled case for a given flow system. Esch, as reported by Le Blond and Mysak, found that this was the case in the coupled system as well, with a small density difference, the Boussinesq approximation being applied. There is no reason to expect this to be different in our system where the Boussinesq approximation is not necessary.

9.3. Transformed stability condition.

In a coordinate system following the lower layer the stability condition (9.5) is readily seen to transform into

$$\{\rho_1{}^* \ (\zeta-\Delta U)^2 - \rho_1 \ g/k\}\{\rho_1{}^*(\zeta-\Delta U)^2 + \rho_2{}^*\zeta^2 - \Delta\rho g/k\}$$

$$= \rho_1{}^{*2} \ (\zeta-\Delta U)^4/ch^2 kh_1 \qquad (9.7)$$

the new relative phase velocity ζ being defined by

$$\zeta = c - U_2 \qquad (9.8)$$

This form of the stability equation shows that the velocity "shear" $\Delta U = U_1 - U_2$ is determining for the system's stability and not the velocities U_1 and U_2 of the subject layers themselves, exactly as in the classical K-H case. Since (9.8) is a purely real transformation

$$\zeta_r = c_r - U_2$$

$$\zeta_i = c_i \qquad\qquad\qquad (9.9)$$

the stability problem is conserved by the transformation in the sense that the stability boundary $c_i = 0$ and generally the growth rate is conserved.

9.4. The thin sublayer limit.

9.4.1. The eigenvalue equation and the shear Froude number.

Starting from equation (9.7) we note that the bed layer depth is represented by $\rho_2{}^* = \rho_2/\text{th } kh_2$. For perturbations that are long compared to the bed layer thickness, which again is assumed much smaller than the main flow depth, the eigenvalue equation may now be rewritten

$$\{F^2(\xi-1)^2 - \text{th } kh_1/kh_1\}(r+1)F^2 \text{ th } kh_1 \ \xi^2 =$$

$$\{-F^4 \text{ th}^2 kh_1(\xi-1)^4 + (r+1)F^2(\text{th } kh_1/kh_1)(\xi-1)^2$$

$$- r \ (\text{th } kh_1/kh_1)^2\} \ kh_2 + O\{(kh_2)^2\} \qquad (9.10)$$

We have used the notations

$$r = \Delta\rho/\rho_1 = (\rho_2 - \rho_1)/\rho_1 \qquad\qquad (9.11)$$

$$\xi = \zeta/\Delta U = \zeta/(U_1 - U_2) \qquad\qquad (9.12)$$

and

$$F^2 = \Delta U^2/gh_1 \qquad\qquad (9.13)$$

The first two are obviously dimensionless versions of the density difference and the relative phase velocity. The last parameter, defined by (9.13), might be called a shear Froude number. The superscript ("dash") will be omitted in the following. The definition (9.13) should, however, be kept in mind.

9.4.2. The finite eigenvalue solutions.

Inspecting equation (9.10) we may reason as follows:
Assuming ξ to be of finite magnitude the square bracket terms on the right hand side are finite. Since the bracket is multiplied by kh_2, assumed small, the right hand side of the equation is small. The only way to satisfy the equation for finite ξ – values must then be by requiring that the left hand side square bracket should be small of order kh_2:

$$F^2(\xi-1)^2 - \text{th } kh_1/kh_1 = O\{kh_2\} \tag{9.14}$$

We obviously get the two solutions

$$\xi^{(1)} = F^{-1}\{F + (\text{th } kh_1/kh_1)^{\frac{1}{2}}\} + O\{kh_2\} \tag{9.15}$$

$$\xi^{(2)} = F^{-1}\{F - (\text{th } kh_1/kh_1)^{\frac{1}{2}}\} + O\{kh_2\} \tag{9.16}$$

We note that $\xi^{(1)}$, to a first approximation, is a real and always positive eigenvalue. The other eigenvalue, $\xi^{(2)}$, is also real. However, $\xi^{(2)}$ may be seen to become negative as well as positive. And, additionally, for perturbations close to satisfying

$$F^2 = \text{th } kh_1/kh_1 \tag{9.17}$$

(9.16) gives

$$\xi^{(2)} = O\{kh_2\} \tag{9.18}$$

which contradicts the finiteness assumption. Clearly the eigenvalue solution (9.16) is not valid in the vicinity of (9.17). This particular case will be treated separately in the following.

The solutions $\xi^{(1)}$ and $\xi^{(2)}$ may be found in a strictly analytical way by developing them from an asymptotic expansion based on the smallness of kh_2. The procedure is shown in appendix A and the result in formula (A-15). Since the "inspectional procedure" above gives the same solution it is considered good enough here, and no further analysis will be made, dealing with the finite eigenvalues. The analytical strength of the asymptotic expansion technique will be fully appreciated, however, when dealing with the small eigenvalues in the following.

The physical interpretation of $\xi^{(1)}$ and $\xi^{(2)}$ is clearly that they represent ordinary neutral surface waves. The wave corresponding to $\xi^{(1)}$ travels downstream on top of the basic flow. The $\xi^{(2)}$ wave travels in the opposite direction relative to the flow. However, relative to the (unknown) sublayer flow the $\xi^{(2)}$ wave travels upstream or downstream depending on whether th kh_1/kh_1 is larger or smaller than F^2. The same type of wave should also be able to propagate slowly upstream or downstream and even with zero rate relative to the sublayer. The eigenvalue solution for this case is, however, not given by (9.16). Reference is therefore made to the later special treatment.

10. SMALL EIGENVALUES.

10.1. Solution procedure.

In the following we will seek the small eigenvalues of our flow system. First we rewrite the complete eigenvalue equation for small depth of the sublayer

$$\{F^2(\xi-1)^2 - \text{th } kh_1/kh_1\}(r+1) \; F^2 \; \text{th } kh_1 \; \xi^2 =$$

$$- kh_2 \{F^4 \text{th}^2 kh_1 \; (\xi-1)^4 - (r+1) \; F^2(\text{th } kh_1/kh_1)(\xi-1)^2$$

$$+ r \; (\text{th } kh_1/kh_1)^2\} + O\{(kh_2)^2\} \tag{10.1}$$

A perturbation procedure based on the assumption

$$kh_2 \ll 1 \tag{10.2}$$

will be used to solve this equation for the small eigenvalues. Inspection of (10.1) reveals that small eigenvalues will be of order $(kh_2)^{\frac{1}{2}}$. We therefore choose this as the basic perturbation parameter for the development:

$$\epsilon = (kh_2)^{\frac{1}{2}} \tag{10.3}$$

The small eigenvalues are now sought as an asymptotic series

$$\xi = \xi_1\epsilon + \xi_2\epsilon^2 + \xi_3\epsilon^3 + \cdots \tag{10.4}$$

10.2. The growth rate solution.

The details of the mathematical development may be followed by reading appendix A. We shall take the solution found there directly into consideration. The first approximation is given by equation (A – 20) as

$$\xi^{(3,4)} = \pm\, i\{F^4 - (r+1)F^2 cth\ kh_1/kh_1 + r/(kh_1)^2\}^{\frac{1}{2}}$$

$$\cdot\ \{(r+1)(F^2 - th\ kh_1/kh_1)F^2 cth\ kh_1\}^{-\frac{1}{2}}(kh_2)^{\frac{1}{2}}$$

$$+\ O\{kh_2\}$$

$$=\ i\ \xi_i^{(3,4)} + O\{kh_2\} \tag{10.5}$$

Alternatively the solution may be written as

$$\xi_i^2{}^{(3,4)} = \{F^2 - f_1(kh_1,r)\}\{F^2 - f_2(kh_1,r)\}\ \cdot$$

$$\cdot\ \{F^2 - f_3(kh_1)\}^{-1}F^{-2}\{cth\ kh_1\ (r+1)\}^{-1}\ \cdot\ kh_2$$

$$+\ O\{(kh_2)^2\} \tag{10.6}$$

where

$$f_1(kh_1,r) = \tfrac{1}{2}(r+1)\ cth\ kh_1/kh_1$$

$$+\{(r+1)^2(cth\ kh_1/kh_1)^2/4 - r/(kh_1)^2\}^{\frac{1}{2}} \tag{10.7}$$

$$f_2(kh_1,r) = \tfrac{1}{2}(r+1)cth\ kh_1/kh_1$$

$$-\{(r+1)^2(cth\ kh_1/kh_1)^2/4 - r/(kh_1)^2\}^{\frac{1}{2}} \tag{10.8}$$

$$f_3\ (kh_1) = th\ kh_1/kh_1 \tag{10.9}$$

10.3. Stability interpretation.

The formulas (10.6) – (10.9) now allow a stability interpretation, remembering that a positive $\xi^2{}_i$ means instability while a negative $\xi^2{}_i$ means neutrality of the considered flow. One should also note that the function $f_3(kh_1) = th\ kh_1/kh_1$ for all finite values of the arguments lies between $f_1(kh_1,r)$ and $f_2(kh_1,r)$.

The growth rate formula (10.6) is dominated by the proportionality factor kh_2, which is by assumption small. Thus, when the flow system is subject to perturbations that are long, as assumed, it will basically exhibit a weak instability as determined by this factor. A drawback of the result is that the sublayer thickness h_2 is unknown. We have even no firm basis for claiming it to be a constant. What can be said concerning the physical meaning of this is that if the wave number k varies more than h_2 then the shorter perturbations are more unstable than the longer ones. Consequently the shorter perturbations in the long wave range should be observable before the longer ones, if observable at all. For this reason the instability also is termed progressive.

The other main aspect of our stability result (10.6) is the growth rate dependence on the main flow variables F, kh_1 and r.
Obviously the conditions

$$F^2 = f_1(kh_1, r) \tag{10.10}$$

and

$$F^2 = f_2(kh_1, r) \tag{10.11}$$

are stability limits since the growth rate is zero on them with an instability region on one side and a neutral region on the other.
The solution

$$F^2 = f_3(kh_1) = \text{th } kh_1/kh_1 \tag{10.12}$$

is, however, not a stability boundary in the same sense. The growth rate formula (10.6) should not be applied in the neighbourhood of (10.12) since the smallness assumption for the solution is violated. The stability solution for perturbations of (10.12) is treated separately in the following. At this stage we conclude by noting that (10.12) marks a transition zone between an unstable $\{F, kh_1\}$ region below and a neutral region above.

The following figure 10.1 illustrates the stability result (10.6) by showing the different regions with the stability boundaries (10.10-11) and the transitional relation (10.12) drawn. Figure 10.2. shows the growth rate squared ξ^2_i and magnified by the factor $1/kh_2$ for $kh_1 = 1.0$ and $r = 0.5$. The strongest growth rate appears to be found just below the curve (10.12).

Again it is emphasized that the solution as illustrated does not apply close to (10.12). This particular case is discussed in detail in section 10.6 in the following. An example illustration of how the growth rate generally is distributed in the $F - kh_1$ plane is shown in fig. 10.3.
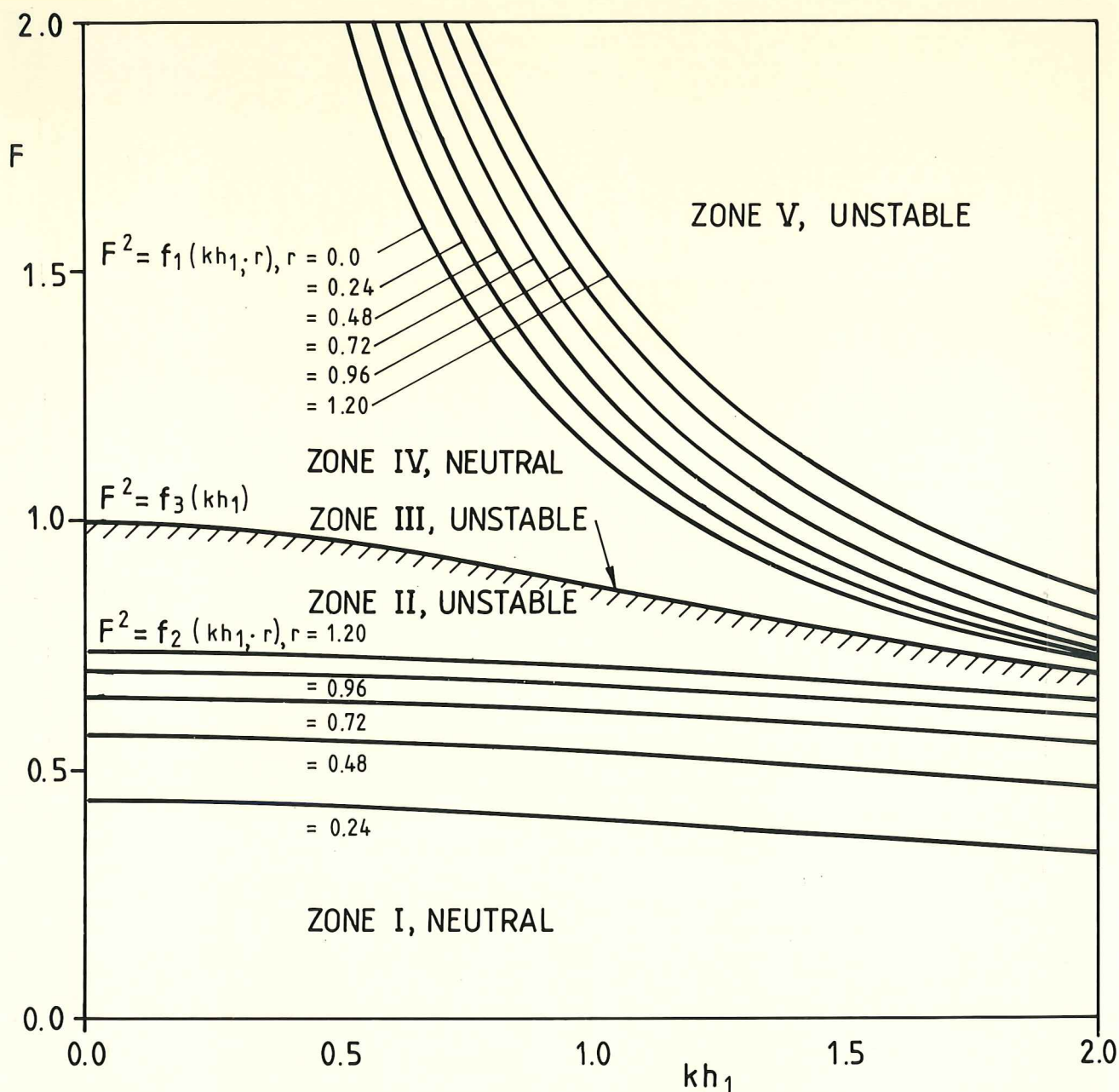
Fig 10.1. Stability regions in $F - kh_1$ plane for a free surface – thin sublayer system. The density parameter $r = \Delta\rho/\rho_1$ is varied in steps of 0.24 from 0.0 to 1.20. The shaded curve is $F^2 = \tanh kh_1/kh_1$, while the lower curve in the upper group ($r = 0.0$) is $F^2 = \coth kh_1/kh_1$. The shaded zone is one of stronger instability.

Fig.10.2. Variation of magnified growth rate with shear Froude number. The illustration case is drawn for $kh_1 = 1.0$ and $r = 0.5$. Asymptiotic value for large F is $(r+1)^{-1}$ th kh_1.

Fig.10.3. Curves of constant magnified growth rate in the $F - kh_1$ diagram for the case $r = 0.25$.

10.4. Two special cases.

10.4.1. The hydraulic limit.

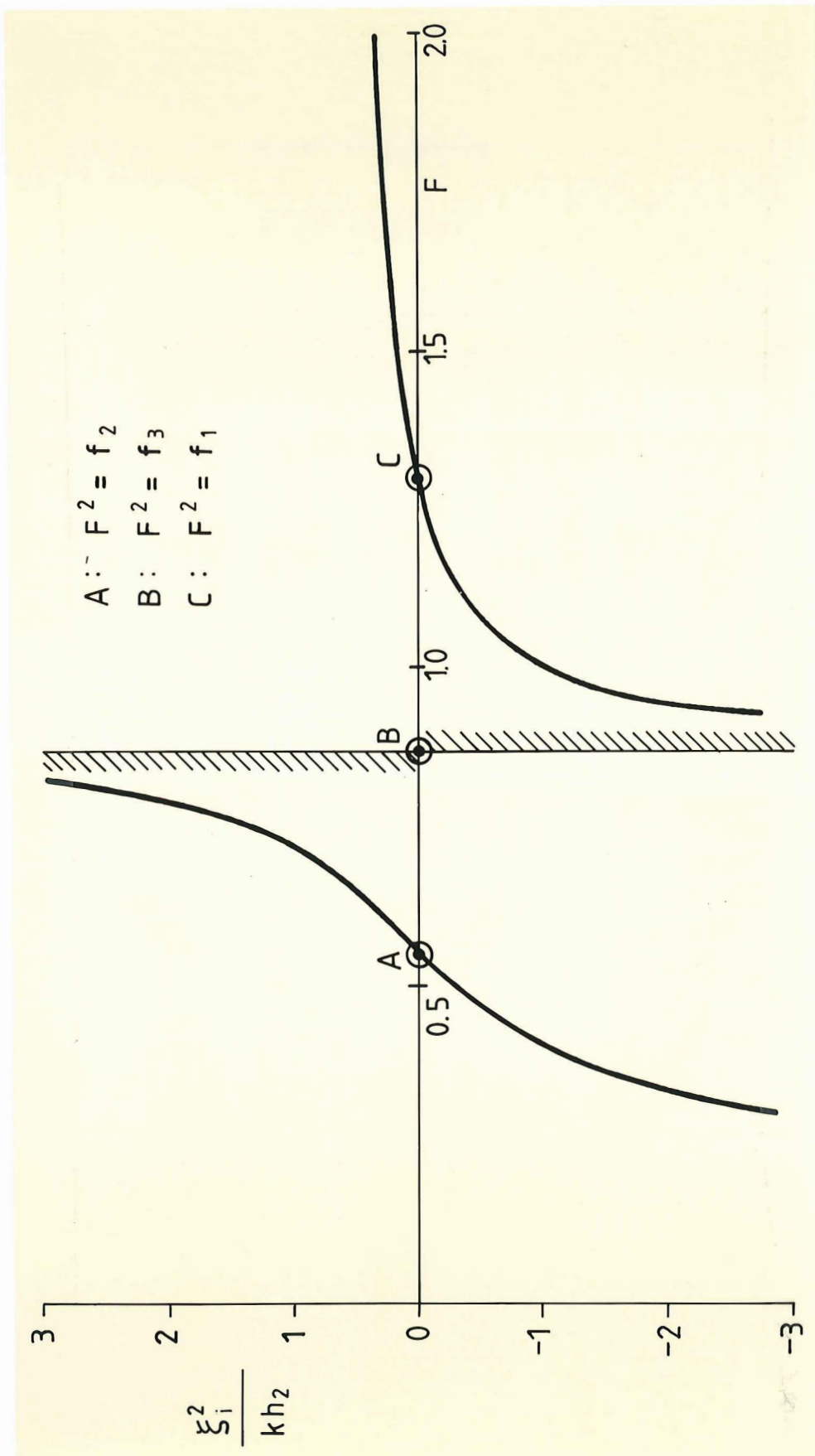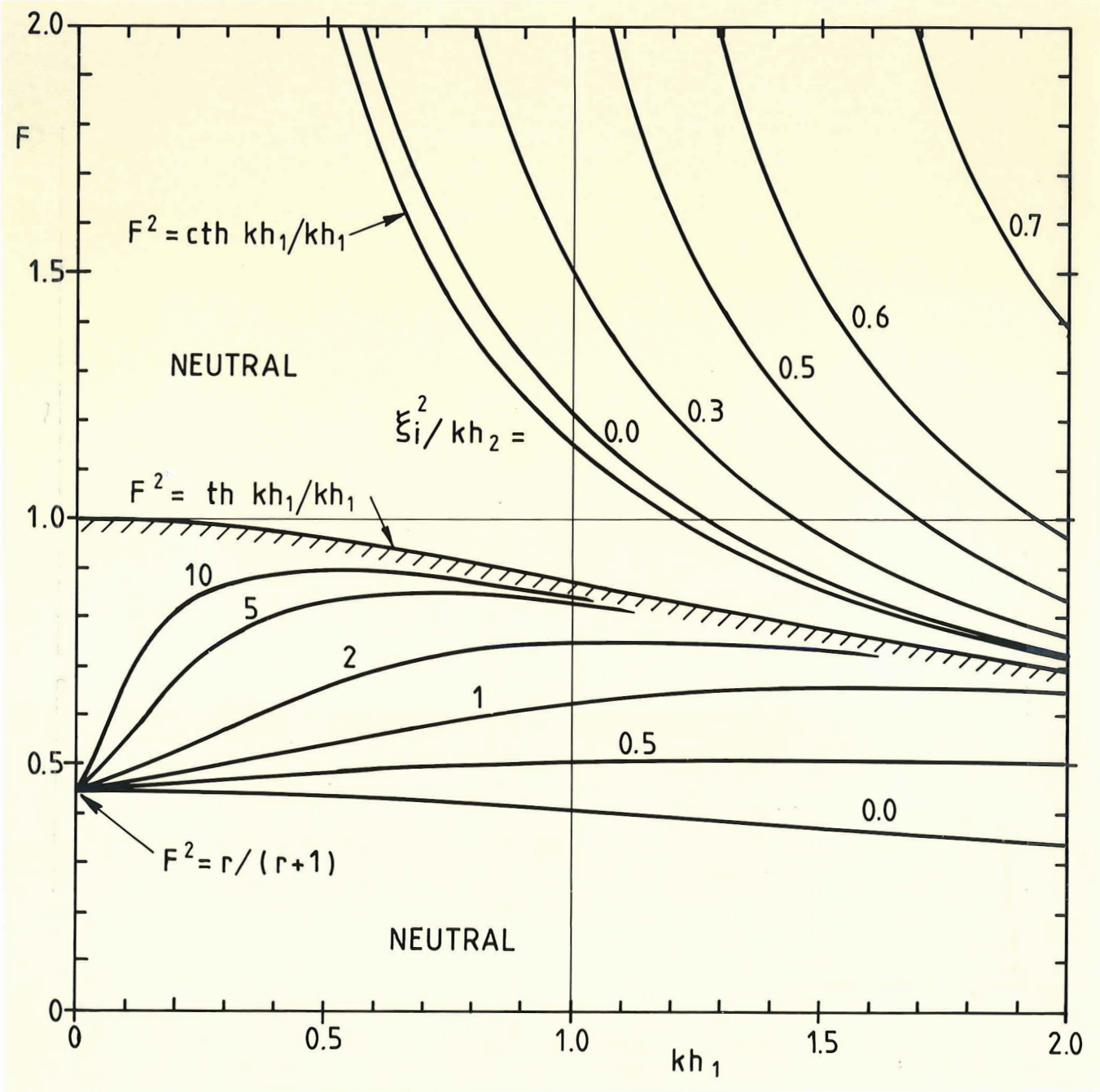For long wave perturbations the stability result (10.5) is easily seen to give the limit relation

$$\xi_i^2 = - \{F^2 - r/(r+1)\}\{F^2-1\}^{-1} F^{-2} h_2/h_1$$

$$+ \text{H.O.T.} \tag{10.13}$$

which indicates stability properties as follows

$$1 < F^2 \qquad \text{neutral}$$

$$r/(r+1) < F^2 < 1 \qquad \text{unstable} \tag{10.14}$$

$$F^2 < r/(r+1) \qquad \text{neutral}$$

Again we should not allow F to approach 1.0 in the above formula. It may be noted that the growth rate formula (10.13) is independent of wave length.

10.4.2. Homogeneous flow.

This is the case where $r=0$ or no density difference exists between the bed layer and the main flow, the case of homogeneous water flow being included. Formula (10.5) now gives

$$\xi_i^2 = \{F^2 - \text{cth } kh_1/kh_1\}\{F^2 - \text{th}_1/kh_1\}^{-1} \text{ th } kh_1 \cdot kh_2$$

$$+ \text{H.O.T.} \tag{10.15}$$

The flow is consequently stabilitywise characterised as

$$\text{cth } kh_1/kh_1 < F^2 \qquad\qquad\qquad \text{unstable}$$

$$\text{th } kh_1/kh_1 < F^2 < \text{cth } kh_1/kh_1 \qquad \text{neutral}$$

$$F^2 < \text{th } kh_1/kh_1 \qquad\qquad\qquad \text{unstable} \qquad\qquad (10.16)$$

One may further note the limiting cases of small and large Froude numbers given by

$$\xi_i^2 = \text{cth } kh_1 \cdot kh_2, \qquad F<<1,0 \qquad\qquad (10.17)$$

and

$$\xi_i^2 = \text{th } kh_1 \cdot kh_2, \qquad F>>1,0 \qquad\qquad (10.18)$$

The magnified growth rate formula (10.15) may be illustrated as a function of F as shown in fig. 10.4 below
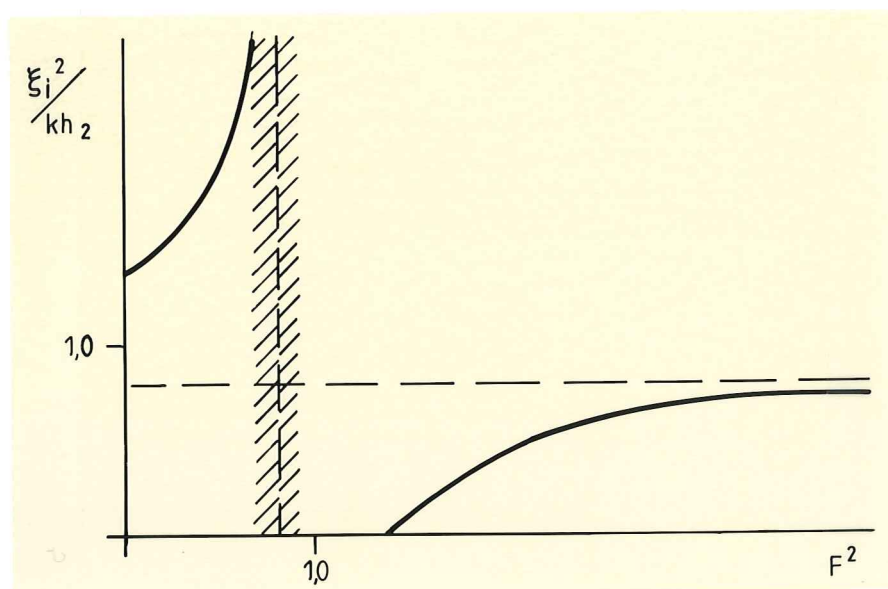

Fig.10.4. Magnified Growth rate varying with Froude number for homogeneous flow.

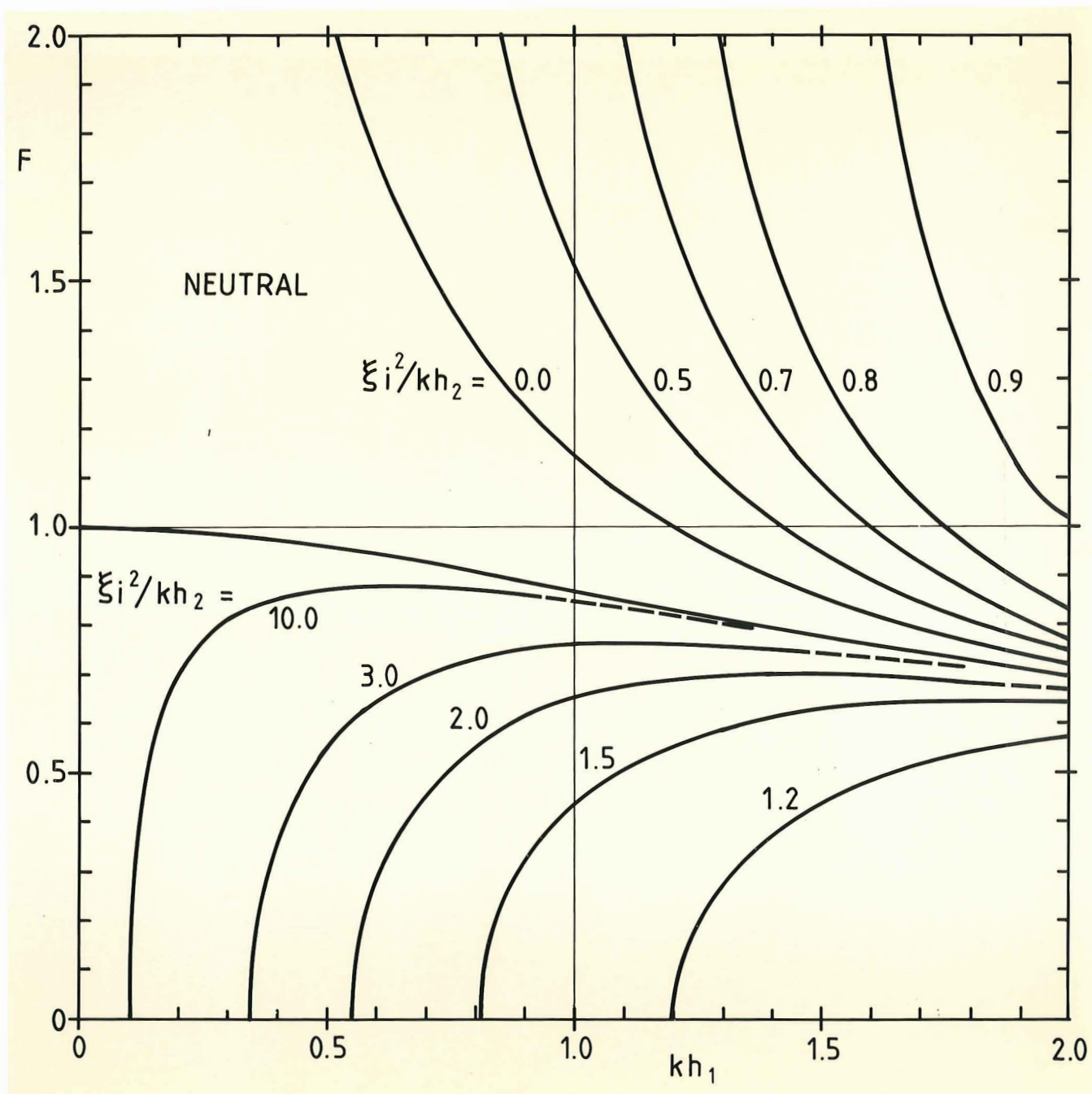In the following figure 10.5. the lines of constant magnified growth rate in the F - kh$_1$ plane are shown.

Fig.10.5. Curves of constant magnified growth rate in the F - kh$_1$ diagram for the case r = 0.

10.5. Propagation.

10.5.1. Finite eigenvalue case.

The two finite eigenvalues $\xi^{(1)}$ and $\xi^{(2)}$ given by (9.15) and (9.16) are the propagation velocities of two ordinary free surface wawes, one propagating with the flow and the other against it, as pointed out at the end of section 9.4.2.

10.5.2. Small eigenvalue case.

The stability solution (10.5) or (10.6) should be interpreted as propagation rate formulas for perturbations that are neutral. The result is now more logically written

$$\xi_r^2 = -\{F^2-f_1\}\{F^2-f_2\}\{F^2-f_3\}^{-1} \; F^{-2}\text{th } kh_1 \cdot kh_2$$

$$+ \text{ H.O.T.} \tag{10.19}$$

These perturbations will not be generated by the present instability mechanism and are in this sense of less interest.

Of more interest is the question about the propagation rate of the unstable perturbations, since they are more likely to be observed in reality. Since the result (10.5) now is a purely imaginary eigenvalue, the propagation rate to the approximation $(kh_2)^{\frac{1}{2}}$ is zero. In order to get a quantitive expression for it the small eigenvalue solution then has to be developed to a higher order of approximation. This development is again shown in appendix A. Taking the result into direct consideration as given by (A-24) we have

$$\xi^{(3,4)} = \pm \, i \, \xi_i^{(3,4)} + \{F^4 - 2F^2\text{th } kh_1/kh_1 + (kh_1)^{-2}\}.$$

$$.\{(r+1)(F^2-\text{th } kh_1/kh_1)^2\text{cth } kh_1\}^{-1}.kh_2$$

$$+ \, O\{(kh_2)^{3/2}\} \tag{10.20}$$

The term of order kh_2 is seen to have the following characteristics

- it is common to both of the eigenvalues (+ or − sign in $(kh_2)^{\frac{1}{2}}$ term)
- it is real
- it is positive for all values of the arguments kh_1 or r.

This term obviously has to be interpreted as the propagation rate of the unstable perturbations. It says then that all unstable perturbations propagate downstream. This result should also be excluded from the neighbourhood of (10.12).

10.6. The case $F^2 = \text{th } kh_1/kh_1$.

10.6.1. One finite eigenvalue.

The solution procedure is found in appendix A. Equation (A-28) gives the finite eigenvalue solution as

$$\xi^{(1)} = 2 + O\{kh_2\} \qquad (10.21)$$

which clearly is the one for neutral surface waves propagating downstream, now with the double velocity of the free stream velocity, approximately. This solution also follows directly from the more general finite-value result (9.15).

The result (9.16) is now invalid and should be replaced by the first of the following solutions.

10.6.2. Small eigenvalues.

The mathematical treatment of the actual case in appendix A results in the three eigenvalue solution (A-36, 37, 38). One solution is real, i.e. that of a neutral wave:

$$\xi^{(2)}_r = -\{(r+1) \text{ sh } 2kh_1\}^{-1/3}(kh_2)^{1/3} + \text{H.O.T.} \qquad (10.22)$$

$$\xi_{i}^{(2)} = 0 + \text{H.O.T.} \tag{10.23}$$

The negative sign shows upstream propagation.

Another eigenvalue is given as:

$$\xi_{r}^{(3)} = \tfrac{1}{2}\{(r+1)\ \text{sh}\ 2kh_{1}\}^{-1/3}(kh_{2})^{1/3} + \text{H.O.T.} \tag{10.24}$$

$$\xi_{i}^{(3)} = \tfrac{1}{2}\sqrt{3}\{(r+1)\text{sh}\ 2kh_{1}\}^{-1/3}(kh_{2})^{1/3} + \text{H.O.T.} \tag{10.25}$$

expressing downstream propagation by the positive $\xi_{r}^{(3)}$ and instability by the positive $\xi_{i}^{(3)}$.

The last eigenvalue expresses an (asymptotically) stable perturbation:

$$\xi_{r}^{(4)} = \xi_{r}^{(3)} \tag{10.26}$$

$$\xi_{i}^{(4)} = -\xi_{i}^{(3)} \tag{10.27}$$

and confirms the earlier finding of eigenvalues in our problem occurring as complex conjugate pairs.

All three eigenvalues above are seen to be of order $(kh_{2})^{1/3}$. This follows from the fact that our present analysis is performed for perturbations satisfying exactly the condition $F^2 = f_3(kh_1) = \text{th}\ kh_1/kh_1$. There is no reason, however, not to expect a gradual transition from the above solution to the two finite plus the two $O\{(kh_2)^{\frac{1}{2}}\}$ solutions found earlier when the perturbation is allowed to pass through the whole range of conditions. This range includes points well above $F^2 = f_3(kh_1)$ as well as points in the vicinity of and exactly on this relation plus finally points well below it.

The essential stability result found here then is that the flow is weakly unstable of order $(kh_{2})^{1/3}$ on

$$F^2 = f_3(kh_1) \tag{10.12}$$

The unstable perturbations propagate downstream.

The exact location of the transition boundary between the unstable region below and at (10.12) and the neutral region above is not given by the present analysis. The conclusion is, however, that it is located in the vicinity of and just above (10.12). One may thus consider (10.12) as a first approximation to this boundary.

The growth rate limit when approaching (10.12) from below is thus given by (10.25). For comparison with fig. 10.2, the "magnified growth rate" then has the limiting value

$$\xi_i^{(3)2}/kh_2 = (3/4)\{(r+1)sh\ 2kh_1\}^{-2/3}(kh_2)^{-1/3} \qquad (10.28)$$

11. AMPLITUDE RATIO SOLUTIONS.

11.1. Finite eigenvalue case.

It is readily verified by substitution of the eigenvalue solution (9.14) into equations (9.1) and (9.2), or equations (11.2) and (11.3) below, that the amplitude ratio associated with the two finite eigenvalues in question is given by

$$a_{21} = O\{kh_2\} \qquad (11.1)$$

Mathematical details are found in appendix B. This result is simply another expression for the fact that the two finite eigenvalues give, to a first order of approximation, neutral gravity waves with a vertical motion going to zero at the bed.

11.2. Small eigenvalue case.

Equations (9.1) and (9.2) are now rewritten in the following form

$$a_{21}^{(I)} = \{F^2(\xi-1)^2 - th\ kh_1/kh_1\}F^{-2}\ ch\ kh_1\ (\xi-1)^{-2} \quad (11.2)$$

$$a_{12}^{(II)} = \{F^2(\xi-1)^2 - r\ th\ kh_1/kh_1\}F^{-2}\ ch\ kh_1\ (\xi-1)^{-2}$$

$$+ (\rho_2^*/\rho_1^*)\ ch\ kh_1\ \xi^2(\xi-1)^{-2} \qquad (11.3)$$

The superscript (I) refers here to the free surface dynamic condition while superscript (II) refers to the dynamic condition on the interface. Remembering now that ξ is a small eigenvalue

$$\xi = \xi_r + i\xi_i = O\{kh_2\} + i\ O\{(kh_2)^{\frac{1}{2}}\} \qquad (11.4)$$

by (10.5) and (10.20), we may develop $a_{21}^{(I)}$ or $a_{21}^{(II)}$ as shown in appendix B. In order to achieve a unique amplitude ratio, it is essential that the last term in (11.3) is included and developed by

using (11.4). The mathematical procedure may be followed in appendix B, leading to the result

$$a_{21} = \{F^2 - \text{th } kh_1/kh_1\}F^{-2} \text{ ch } kh_1 + O\{(kh_2)^{\frac{1}{2}}\} \qquad (11.5)$$

It is remarkable from (11.1) and (11.5) that

- finite eigenvalues give small amplitude ratios.
- small eigenvalues give finite amplitude ratios.

The result (11.5), generally finite, is not valid along $F^2 = \text{th } kh_1/kh_1 = f_3(kh_1)$, being developed for eigenvalues with this restriction. Amplitude ratio solutions along $F^2 = f_3(kh_1)$ are developed in the last part of appendix B and will be commented on in the following.

We may note from (11.5) that away from the condition $F^2 = f_3(kh_1)$ the amplitude ratio is positive above and negative below it, corresponding to in phase and 180° out of phase perturbations respectively.

One may also note that the result (11.5) to first order of approximation is identical to the potential theory result (8.22). However, the essential difference is that (11.5) is developed for a weakly unstable interfacial mode while (8.22) is for a fixed sinusoidal bed.

11.3. Two special amplitude ratios.

The weakly unstable mode with the finite amplitude ratio (11.5) may be further examined for conditions giving amplitude ratios of $\pm$ unity. After some algebraic manipulation we find

$$a_{21} = \pm 1 : \quad F^2 = \text{sh } kh_1 \text{ (ch } kh_1 \pm 1)^{-1}/kh_1 \qquad (11.6)$$
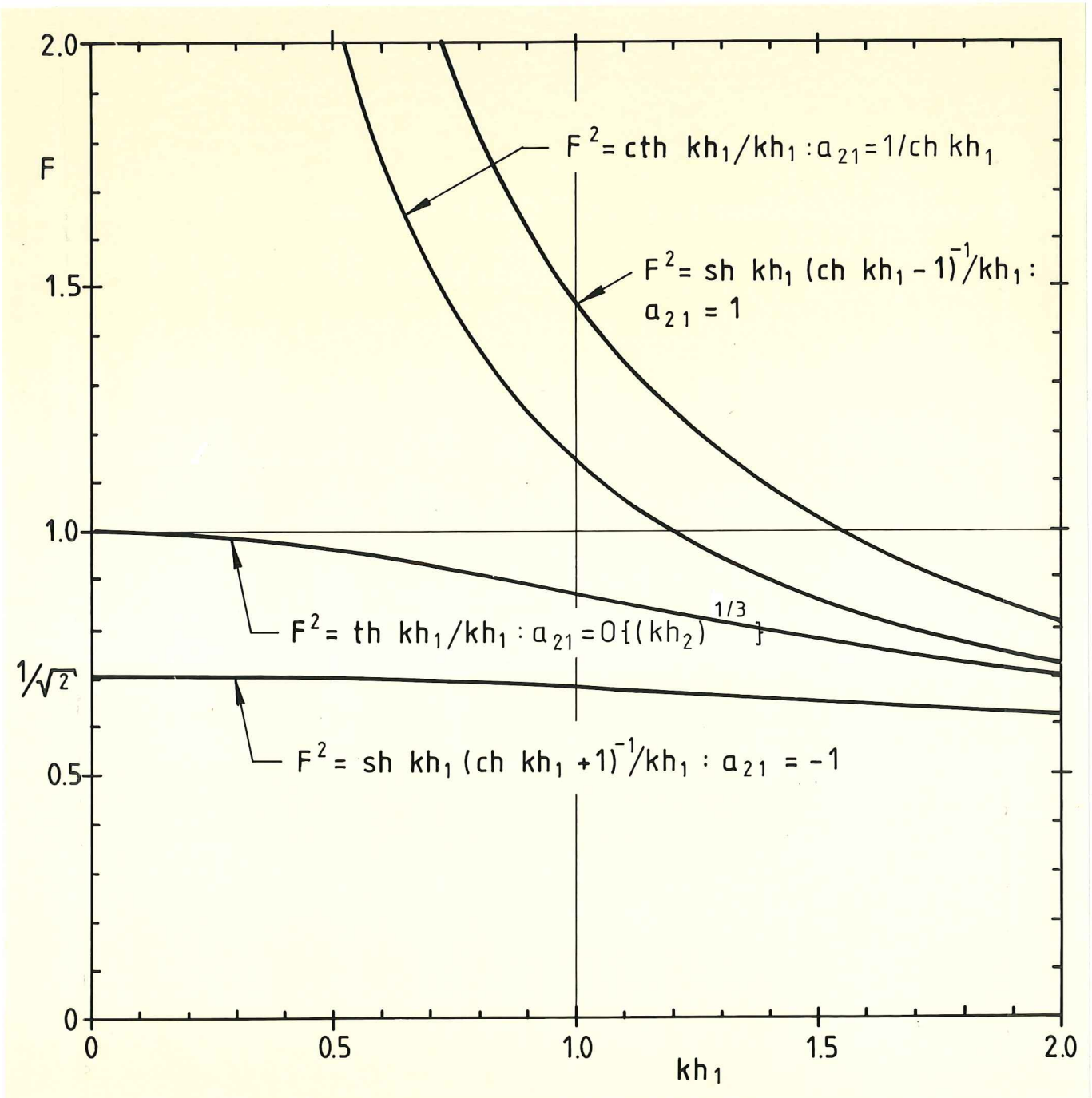
Fig. 11.1. Location of particular unstable mode amplitude ratios in the
F – kh$_1$ plane, to first approximation.

The result (11.6) plus the easily confirmed result for the same (now neutral) mode

$$a_{21} = 1/\text{ch } kh_1 \qquad (11.7)$$

when existing, along $F^2 = \text{cth } kh_1/kh_1$, are shown in fig. 11.1.

11.4. Amplitude ratio at stability boundaries.

An explicit solution for the amplitude ratio may be found by assuming $\xi = 0$ in (11.2) and (11.3). Hereby the solution is restricted to the conditions in the immediate vicinity of the upper and lower stability boundaries. The solution is easily found to be

$$a_{21} = -\tfrac{1}{2}r^{-1}(1-r)\{1\pm(1+4r(1-r)^{-2} \text{ ch}^{-2}kh_1)^{\tfrac{1}{2}}\}\text{ch } kh_1 \qquad (11.8)$$

with the hydraulic limiting approximation

$$a_{21} = -\tfrac{1}{2}r^{-1}(1-r)\{1\pm(1+4r(1-r)^{-2})^{\tfrac{1}{2}}\} \qquad (11.9)$$

or

$$a_{21}^+ = - r^{-1} \qquad (11.10)$$

and

$$a_{21}^- = 1.0 \qquad (11.11)$$

Here plus sign refers to the lower stability boundary while minus refers to the upper.

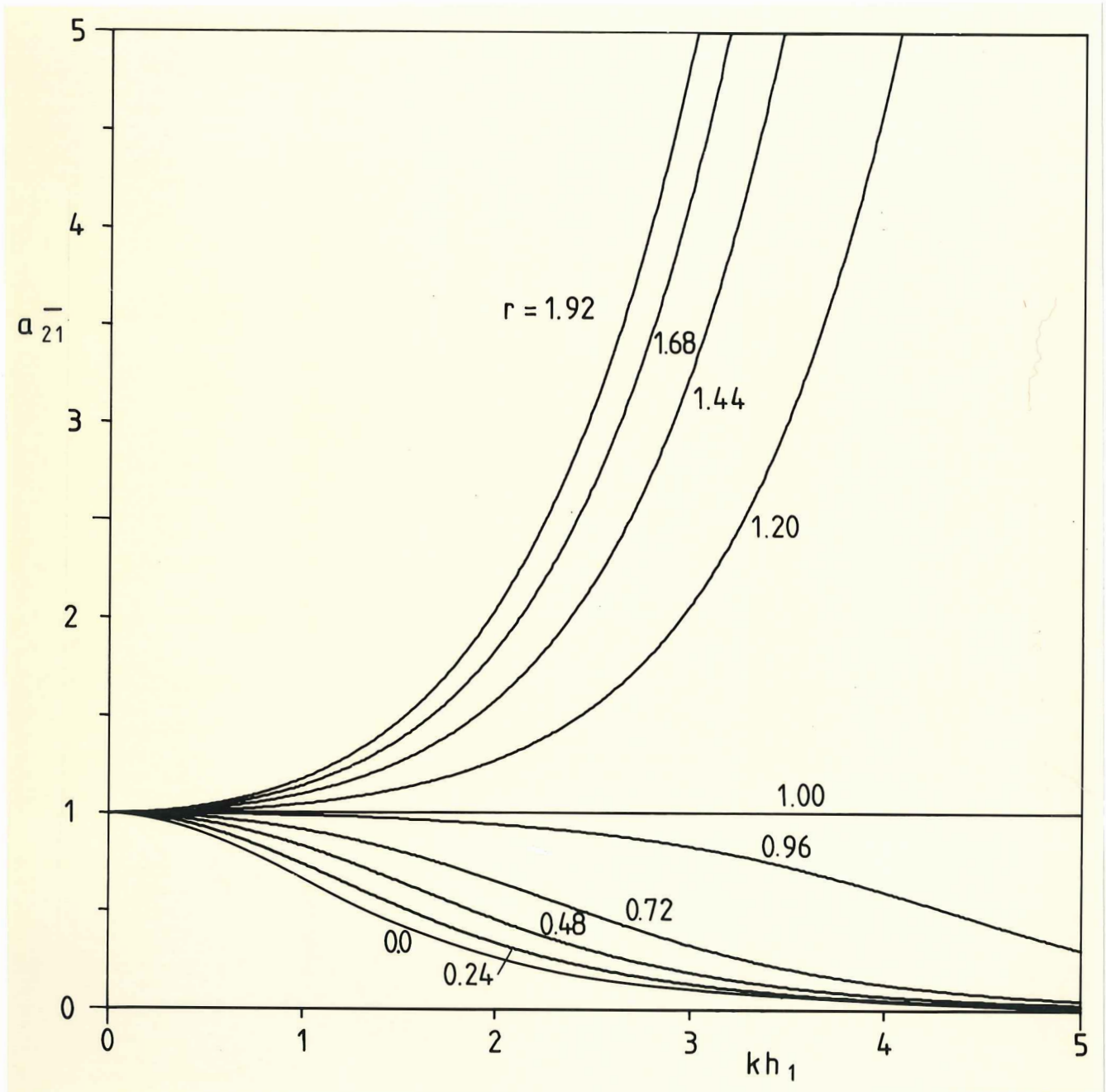The above solutions are illustrated in the following figures 11.2 and 11.3.

Fig 11.2. Amplitude ratio in thin sublayer – free surface flow system corresponding to upper stability boundaries in fig. 10.1.
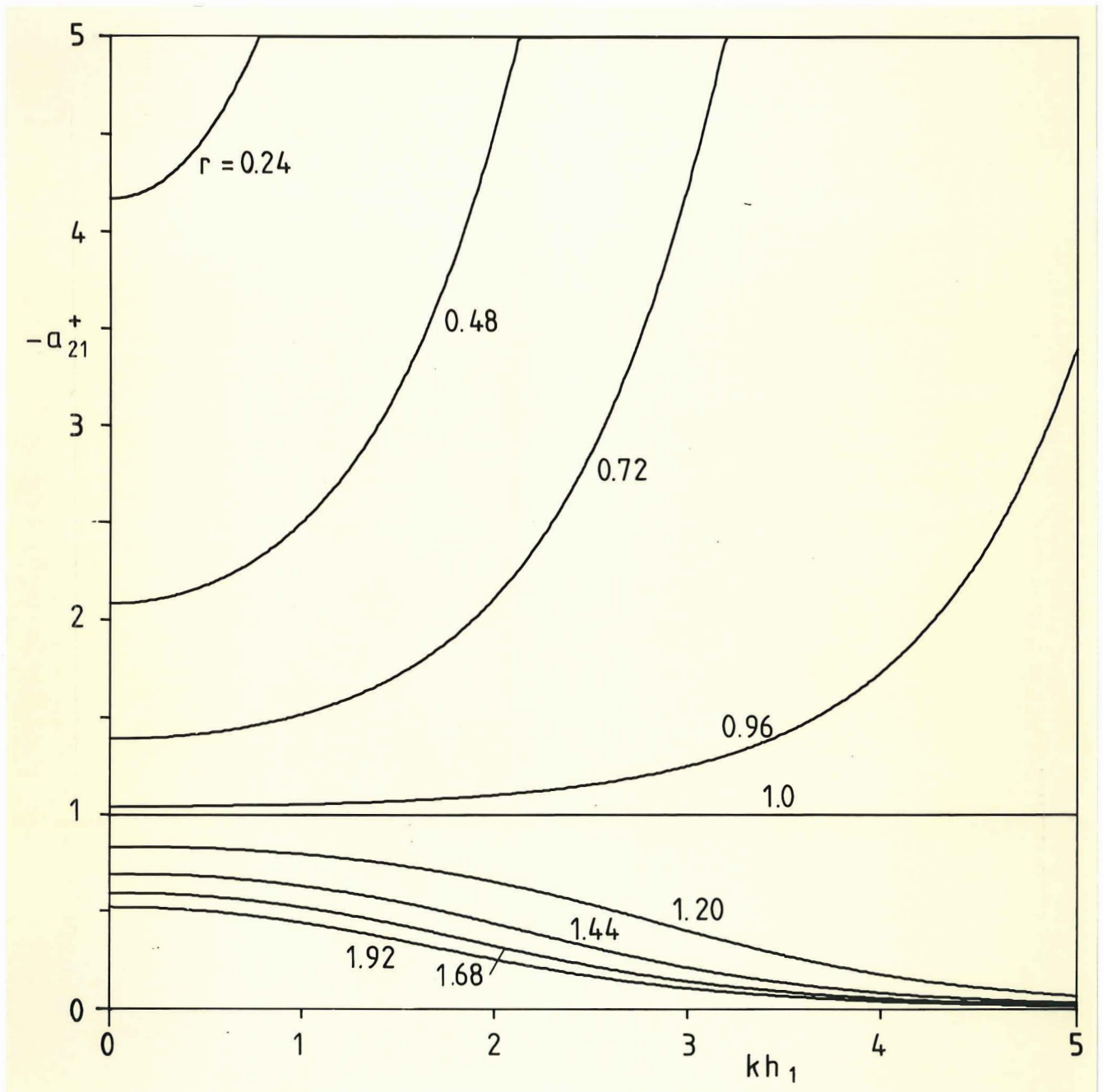
Fig 11.3. Amplitude ratio in thin sublayer-free surface flow system corresponding to lower stability boundaries in fig 10.1.

11.5. Transitional amplitude ratio.

The amplitude ratios found so far do not apply along the transitional relation

$$F^2 = \text{th } kh_1 / kh_1 \qquad (11.11)$$

The case is treated mathematically in appendix B with the result for the three small eigenvalues

$$a_{21}^{(n+2)} = 2 \text{ ch } kh_1 \text{ } e^{-i2n\pi/3} \{(r+1)\text{sh } 2kh_1\}^{-1/3} (kh_2)^{1/3}$$

$$+ O\{kh_2\}^{2/3}\}, \quad n=0,1,2 \qquad (11.12)$$

The superscript (n+2) now refers to the respective eigenvalue solution given in (10.22-27). In particular the neutral eigenvalue (10.22-23) has an amplitude ratio given by $n = 0$, or

$$\text{arg } a_{21}^{(2)} = \theta_{21}^{(2)} = 0 \qquad (11.13)$$

which means that the perturbation on the free surface is in phase with the one on the shear interface.
On the other hand the unstable mode gives an amplitude ratio phase difference given by

$$\text{arg } a_{21}^{(3)} = \theta_{21}^{(3)} = -2\pi/3 \qquad (11.14)$$

The interpretation of this result in the physical plane is obviously as shown in the following figure.
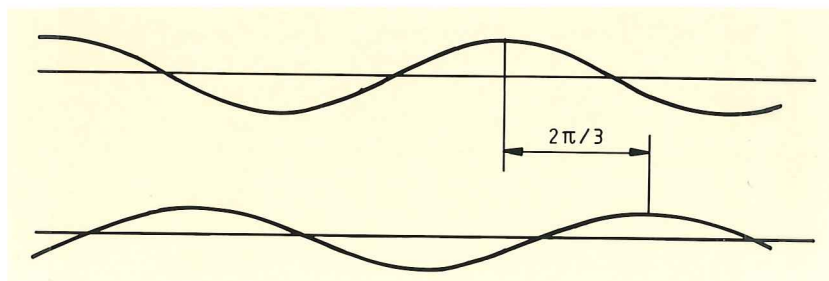
Fig. 11.4. Transitional phase relationship of amplitude ratio for the
unstable mode.

11.6. Summary of eigenvalue and amplitude ratio results.

The number of results gained in the two preceding chapters on eigen-
values and associated amplitude ratios are numerous. For full infor-
mation on them the only way is to go into the text. An overall presen-
tation in terms of order of magnitude and phase relationships for the
different cases is given in the following table 11.1. A main conclusion is
that the free surface influences the bed layer stability strongly as
illustrated by the figures 7.4 and 10.1.

Table 11.1. An order of magnitude summary of eigenvalue analysis results.

I : $F^2 < f_2(kh_1,r)$
II : $f_2(kh_1,r) < F^2 < f_3(kh_1)$
III : $F^2 = f_3(kh_1)$
IV : $f_3(kh_1) < F^2 < f_1(kh_1,r)$
V : $f_1(kh_1,r) < F^2$
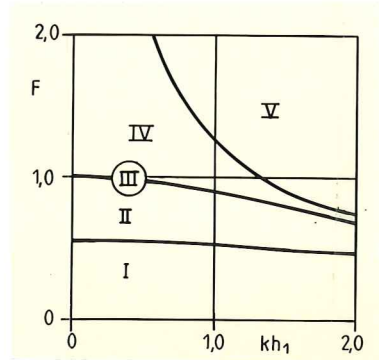
	j	I	II	III	IV	V
$O\{\xi_r^{(j)}\}$	1	+1	+1	+1	+1	+1
	2	-1	-1	$-(kh_2)^{1/3}$	+1	+1
	3	$-(kh_2)^{\frac{1}{2}}$	$+kh_2$	$+(kh_2)^{1/3}$	$-(kh_2)^{\frac{1}{2}}$	$+kh_2$
	4	$+(kh_2)^{\frac{1}{2}}$	$+kh_2$	$+(kh_2)^{1/3}$	$+(kh_2)^{\frac{1}{2}}$	$+kh_2$
$O\{\xi_i^{(j)}\}$	1	0	0	0	0	0
	2	0	0	0	0	0
	3	0	$+(kh_2)^{\frac{1}{2}}$	$+(kh_2)^{1/3}$	0	$+(kh_2)^{\frac{1}{2}}$
	4	0	$-(kh_2)^{\frac{1}{2}}$	$-(kh_2)^{1/3}$	0	$-(kh_2)^{\frac{1}{2}}$
$O\{|a_{21}^{(j)}|\}$	1	kh_2	kh_2	kh_2	kh_2	kh_2
	2	kh_2	kh_2	$(kh_2)^{1/3}$	kh_2	kh_2
	3	1	1	$(kh_2)^{1/3}$	1	1
	4	1	1	$(kh_2)^{1/3}$	1	1
$\theta_{21}^{(j)}$	1	0	0	0	0	0
	2	0	0	0	0	0
	3	$-\pi$	$-\pi$	$-2\pi/3$	0	0
	4	π	π	$-2\pi/3$	0	0

11.7. Final remarks on the stability model.

So far the proposed stability model is analysed mathematically. Physical interpretation of the results are done only to a limited extent. Even if the model is purely hydrodynamical its relevance to pure water channel flow will not be discussed as part of this work, in spite of the fact that the question about this relevance is interesting enough. The model has been proposed and developed with sedimentary flow and sand wave generation as the target. The discussion of the preceding stability model as a possible generating mechanism for granular bed waves will then be the subject of the remaining part of this report.

PART III

THE GENERATION OF SAND WAVES AS A K-H TYPE OF
INSTABILITY.

INCLUDING:

- DESCRIPTION AND RESULTS OF A LIMITED SET OF QALITATIVE
  EXPERIMENTS

- A QALITATIVE COMPARISON OF EXPERIMENTAL RESULTS AND
  THEORY

- A SUMMARY OF THE WORK

12. SOME QUALITATIVE EXPERIMENTS.

12.1. Purpose

The bed layer stability results developed in the preceding chapters are of course of limited interest by themselves. The comparison between stability behaviour as predicted by the theory on the one hand and actual physical stability behaviour on the other is the only way to possibly improve on this.

To supplement earlier experimental work as summarised in part I of this report with observations motivated directly by the preceding theory a limited number of qualitative experiments are performed. The sand bed particle distribution, the flow rate, the flow depth and the resulting sand wave lengths are grossly determined. There is, however, no attempt made to do measurements of flow or sand movement in any detail. The emphasis is in stead put on visualisation of phenomena occurring as part of the sand wave form generation process. The visualisation includes the character of the free surface, the main flow, the internal exitation or "degree of in-stability" and the behaviour of the bed forms.

Observing instability phenomena in the near bed region and interaction with the free surface is naturally of central importance in the present exper-imental approach.

After a presentation of the test rig, the equipment used, the sand particle distribution and the test procedure, the observations will be considered.

12.2. Experimental set up.

The flume used is shown drawn in fig. 12.1. All measures are given in meters.
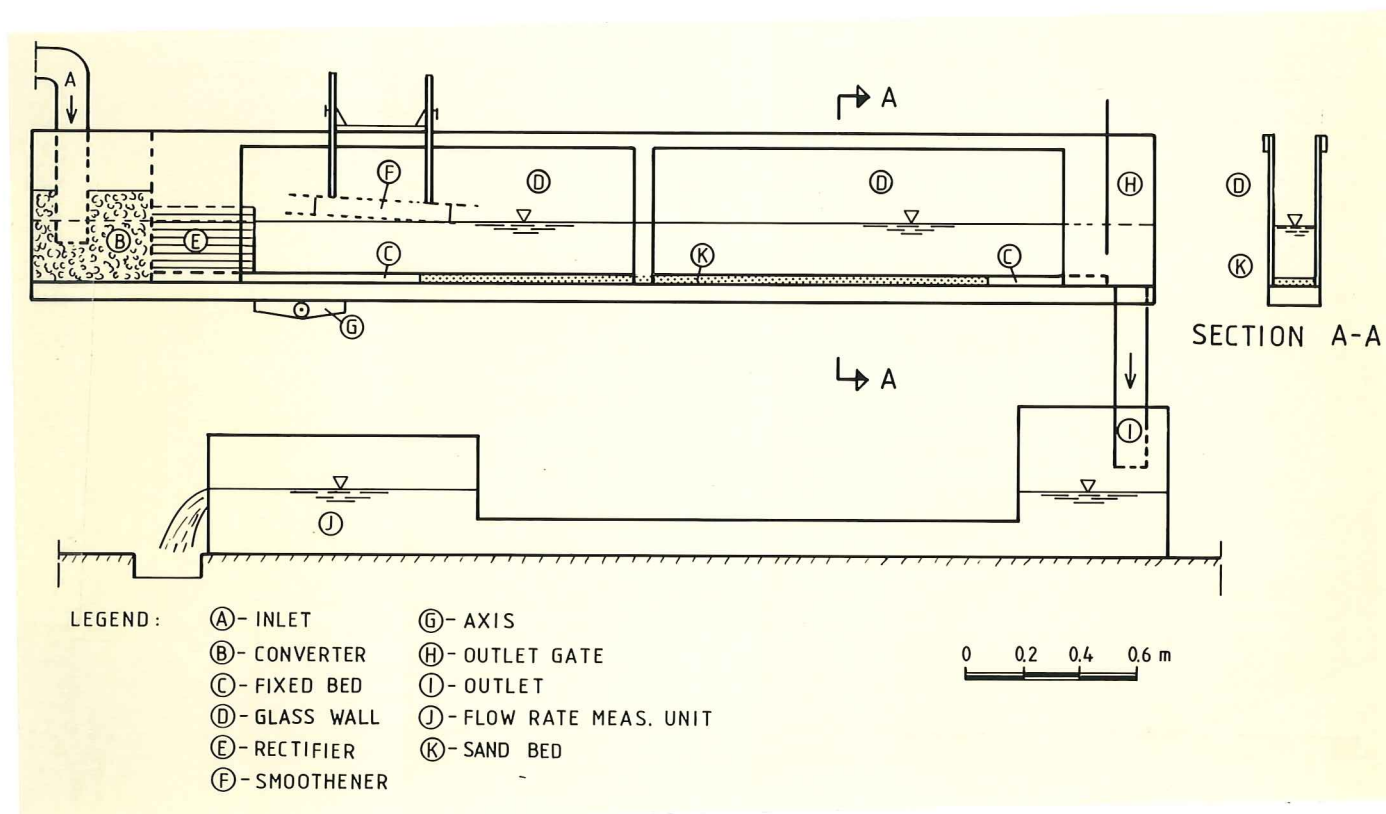
Fig. 12.1. Test flume used for experiments on sand wave form generation.

A 3 cm deep and 15 cm wide sand bed extends in all experiments 1.90 m over the central part of the flume. The flow and sand bed phenomena are visualised by placing a white colored wall with a 5 cm x 5 cm square grid in black behind the rear glass wall of the test flume. The visual obser-vations are made from one side of the flume looking perpendicularly through the flow. With a white screen as background the bed profile as well as the free surface form and sediment flow phenomena are observed. In addition all tests are recorded on video tape providing a unique possibility of repeated observations. All photographs shown in the following are reproduced from the video recordings.

12.3. Sand material.

The sand material used for the tests is represented here by the particle
distribution curves in fig. 12.2. Two slightly different sands are used, as
shown.
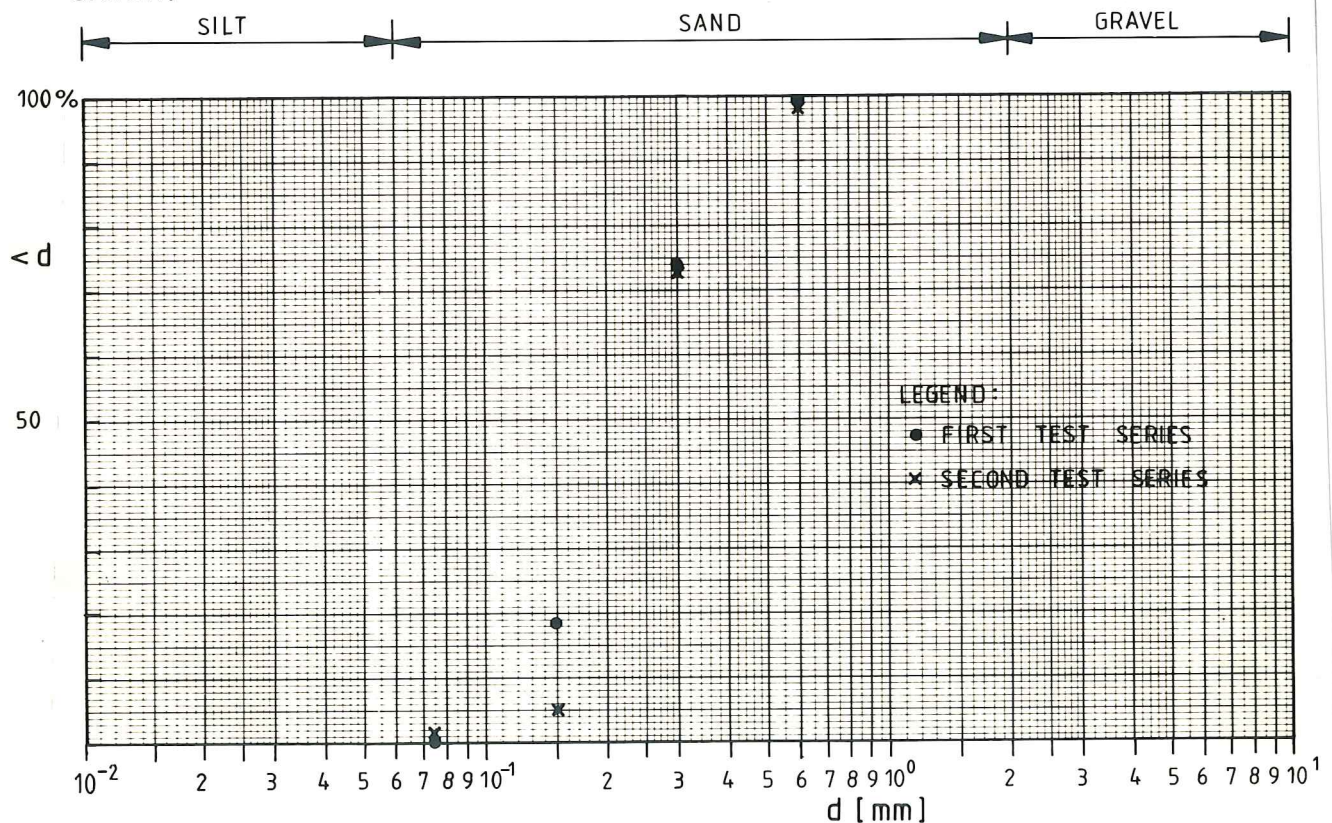
Fig. 12.2. Particle distribution for test sands.

12.4. Test procedure.

The basic parameter varied in the tests is the main flow Froude number.
While the water flow transport rate is kept constant at 5.4 l/s the Froude
number is varied over the range 0.3 - 0.8 by regulating the outlet gate of
the flume. For Froude numbers larger than 0.5 a slight slope of the flume
is applied. One single test is run with the reduced transport rate 1.6 l/s,
namely that for F = 1.1, visualising a case of antidune development. The
correspondence between the Froude - number and the flow depth in all
experiments except the antidune test is shown in fig. 12.3.

A second series of experiments was run after studying the visual record-
ings from the first series. The second series covered the more limited
Froude number range 0.5 - 0.7, and was run to focus somewhat differently
on the phenomena seen. The applied sand was approximately the same as in
the first series, see fig. 12.2, while all other test conditions were kept the
same. The photographic material shown in the following is partly from the
first and partly from the second series.

Each test is started from a small velocity and high water level (F < 0.2),
and then accelerated up to the wanted Froude number by opening the outlet
gate, the gate being properly calibrated in advance. The Froude number
referred to is defined by mean velocity and total depth and to be the one
at the initial stage of bed wave development. As will be seen the flow
conditions including the Froude - number changes as a result of the
development of the sand waves.
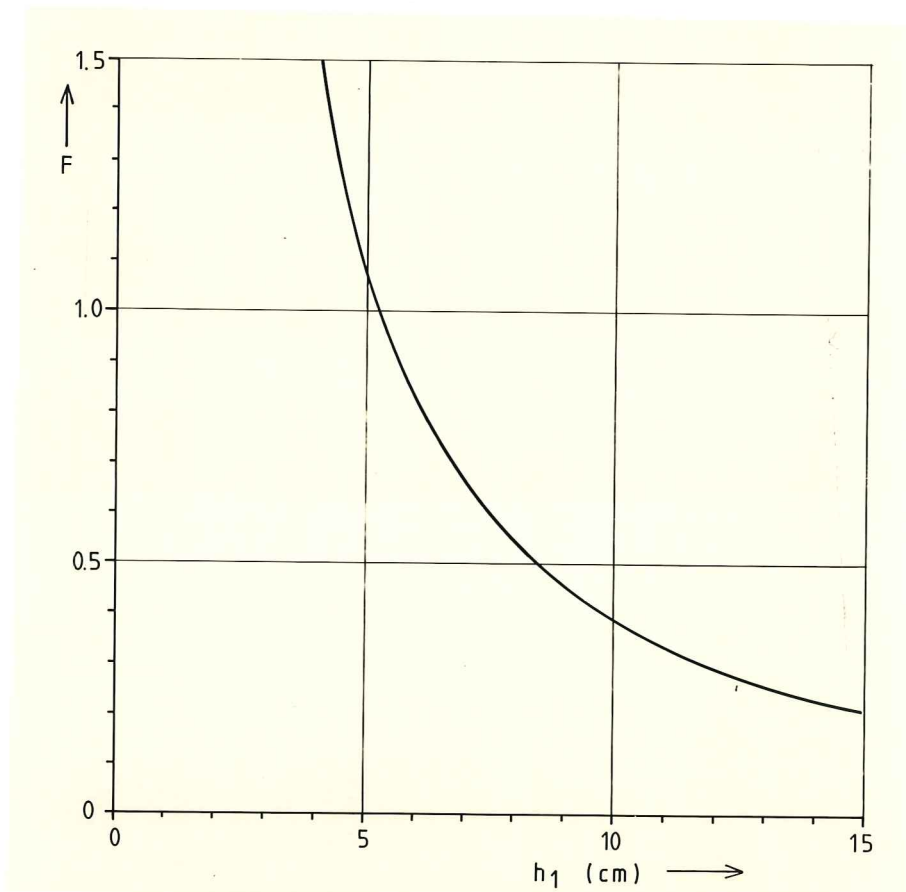
Fig. 12.3. Correspondence between Froude number and water depth in
        lower regime tests.

13. THE LOWER REGIME INSTABILITY.

13.1. A progressive instability.

A test for F = 0.4 shows very clearly the progressive character of the bed waves. The first photograph below is taken at an early stage in the development of wave forms while the second is taken several minutes later in the same test.

a.)

b.)

Fig. 13.1. The wave length of bed forms increase during their formation; a: early stage, b: later stage, F = 0.4.

It is clear from fig. 13.1. that there has been a considerable increase (about three times) in the bed wave length from stage a to stage b. If the two stages are plotted in the $F - kh_1$ diagram, we find the development
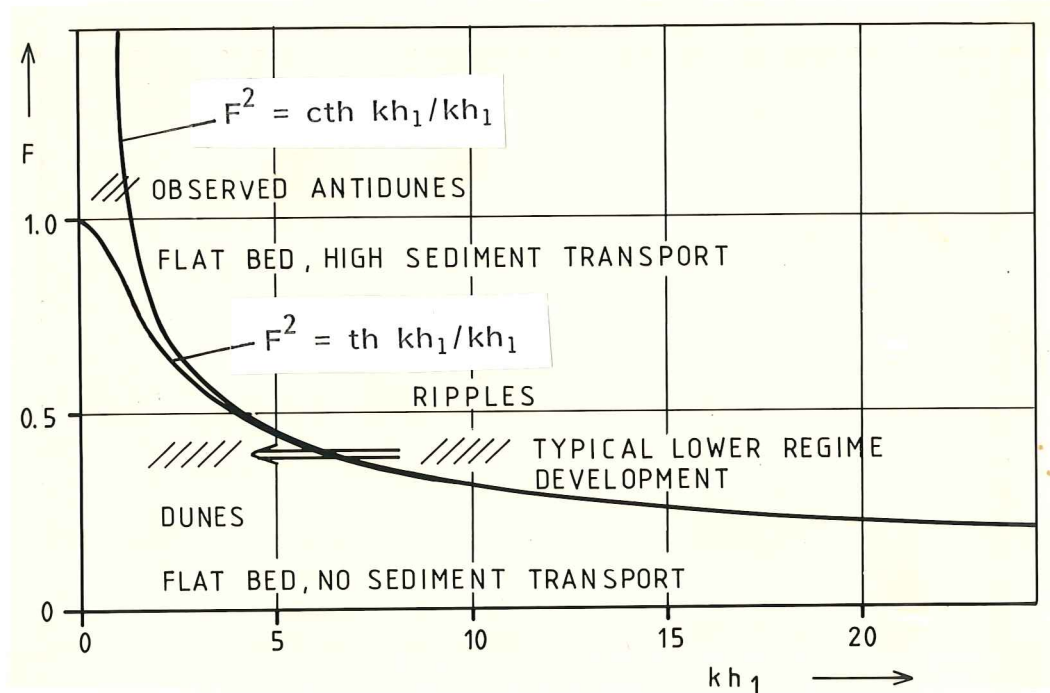
Fig. 13.2. The progression of bed wave forms for the $F = 0.4$ test, plotted in the $F - kh_1$ diagram. Later antidune observation is also shown.
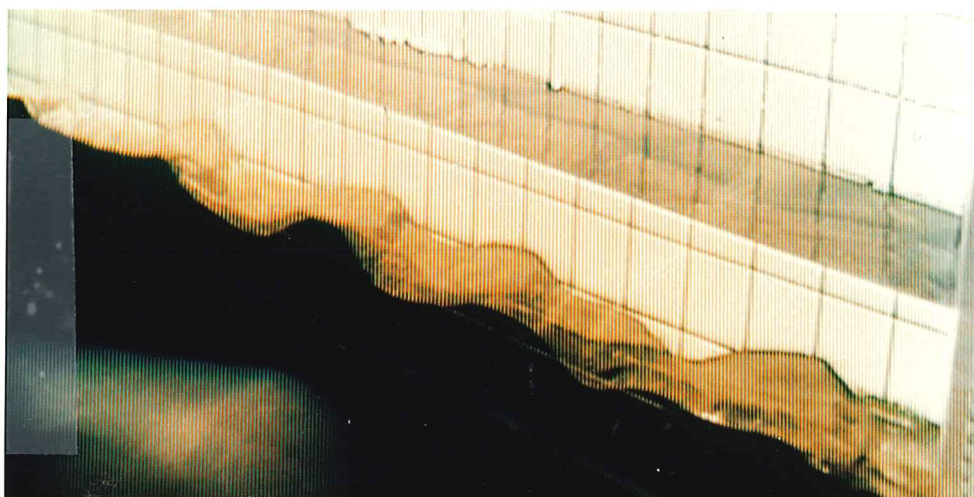
located as shown in fig. 13.2. The first sand waves seen are located in the upper unstable region of the $F - kh_1$ diagram. Their wave length is roughly about half of the water depth, i.e. in absolute measure about 7.5 cm. They can not be seen to interact with the free surface. Fig. 13.1 also confirms the generally agreed high degree of regularity and two-dimensionality of the first waves seen.

Thus in total the first waves seem to fall well within the definition of ripples, as given in the nomenclature of section 2.1.
The later stage sand waves are less unique in size and wavelength than the first waves. However, their wavelength fall within a reasonably short range, indicated in fig. 13.2. These waves are clearly seen to be located in the lower unstable region of the $F - kh_1$ diagram. The shape of these later waves are not typically that of dunes. We also see that the interaction with

the free surface is still small. It should be made clear that these later waves are not the final ones. A further increase in wave length was seen during this test.

This feature of progressive occurrence, though emphasized by some writers, is not generally acknowledged in the literature as the basic feature of bed wave development as it really seems to be. In all experiments performed in the lower range the bed waves showed this same progressive character. The observed bed waves as given by Kennedy in fig. 3.5 should now be reconsidered with this bed wave property in mind.

Both the early waves and the later waves propagate slowly downstream, as did all other sand waves for the subcritical flow tests. The propagation velocity was extremely small (a few centimeters per minute), i.e. orders of magnitude smaller than the free stream velocity.

The growth rate was also small. However, no experimental determination of it was made. Also when judging growth rate as well as propagation rate, one should keep in mind the continuous change in wave length from shorter to longer, as pointed out.

Between the early waves and the later waves shown, an intermediate stage of higher disorder is observed. This stage is considered separately in the following.

13.2. The intermediate stage.

It was mentioned in the previous section that at a stage of development (progression) of the bed forms they show a strongly irregular, rapidly changing 3-dimensional pattern while the fluid interior appear to be more excited than before or afterwards. The fotographs in figs. 13.3 a and b are both from this stage of a $F = 0.5$ test.

a.)
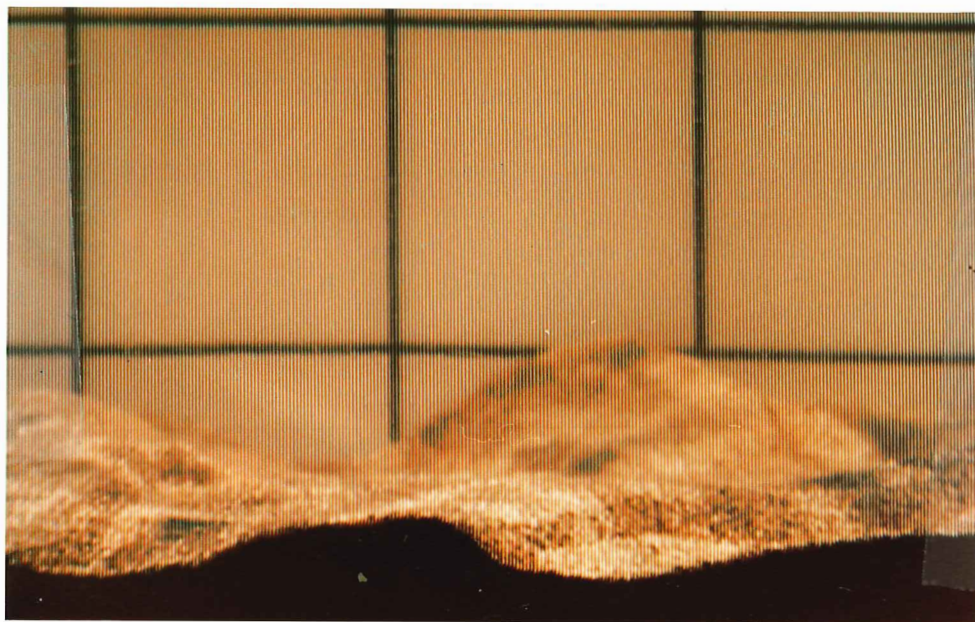
b.)

Fig. 13.3. Excited flow phase in F = 0.5 test with irregular 3D bed wave
forms (a), and "lift up" (b).

The "lift up" phenomenon is a peculiar one and is focused on by Jackson (1976) and discussed by him in light of the "bursting" phenomena observed in fixed bed channel flow. The phenomenon was observable in the present tests only during the excited intermediate st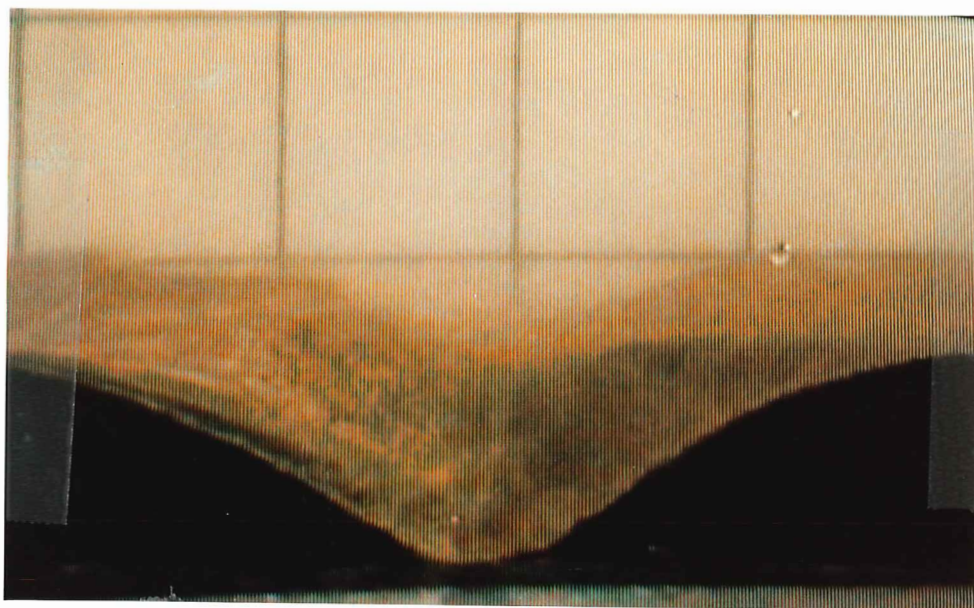age of bed form development and not observable at all for some Froude numbers. A suggestion more than an explanation is the following:

In view of the progressive character of the bed form development the boundary layer will "lead" this development. At a certain stage the boundary layer perturbation will just have reached underneath the transitional (phase shift) condition $F^2 = \text{th } kh_1/kh_1$, while the bed forms remain as developed outside. The bed topography forces the in-phase relation on the free surface, while the unstable perturbation at the boundary layer is in an out-of-phase state versus the free surface causing the "lift up".

The "lift up" phenomenon is not a dominating one, at least not on laboratory scale, and a wider discussion of it is hardly justified in the present context.

13.3. The amplitude ratio development.

The tests confirmed earlier findings with respect to the phase relationship for dunes, i.e. stable wave forms in the lower regime interacting with the free surface, in that the dunes and the free surface are basically 180° out of phase with each other. The classical potential theory for flow over a sinusoidal bed as described in chapter 8, equation (8.22), is in fact successful on this point.

A more interesting observation of amplitude ratio is to follow its development during a test. An even more convincing demonstration of the progressive character of the instability than by development of wave lengths, as followed in section 13.1, is given by the amplitude phase development. The photographs in figure 13.4 below are all from a F=0.5 test. Fotograph "a" is taken at an early stage where the wave form is in the upper instability region and the amplitudes are seen to be of in-phase type. Fotograph "b" is taken at the transitional stage, approximately, where the downstream wave form is seen still to be of in-phase type while going upstream the wave forms are gradually lengthening and gradually altering phase. It

should be remarked here that in all tests there was a clear tendency towards that the upstream end of the test section was "leading" the development. This is clearly an effect of local test conditions, which will be commented on later.

The final bed forms observed during this test were as shown in photograph "c", having the typical dune shape and an antiphase amplitude ratio.

a.)
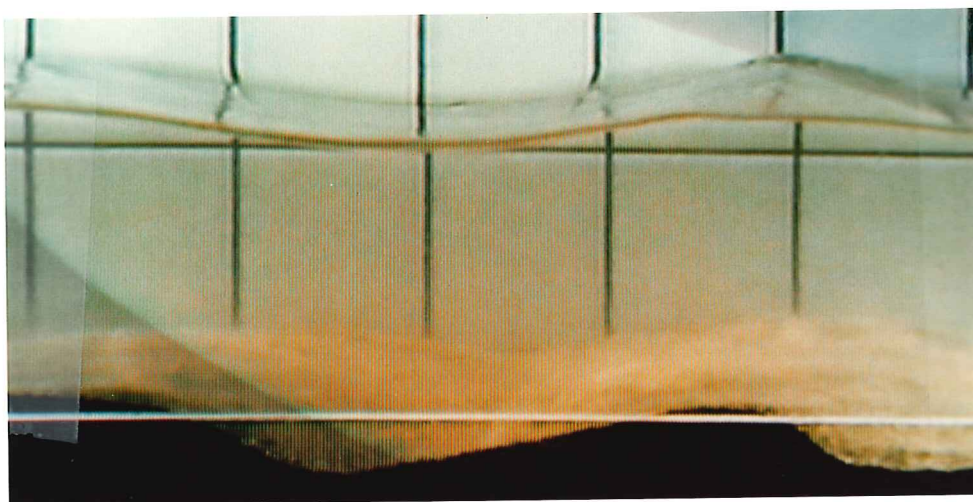
b.)
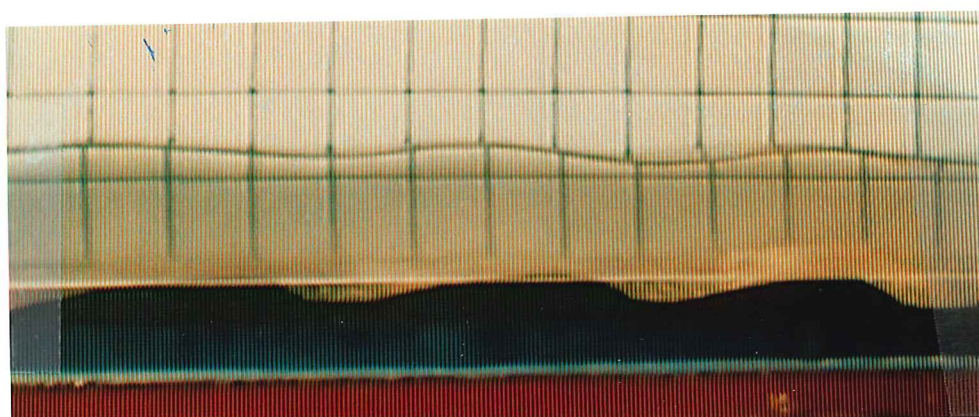
c.)
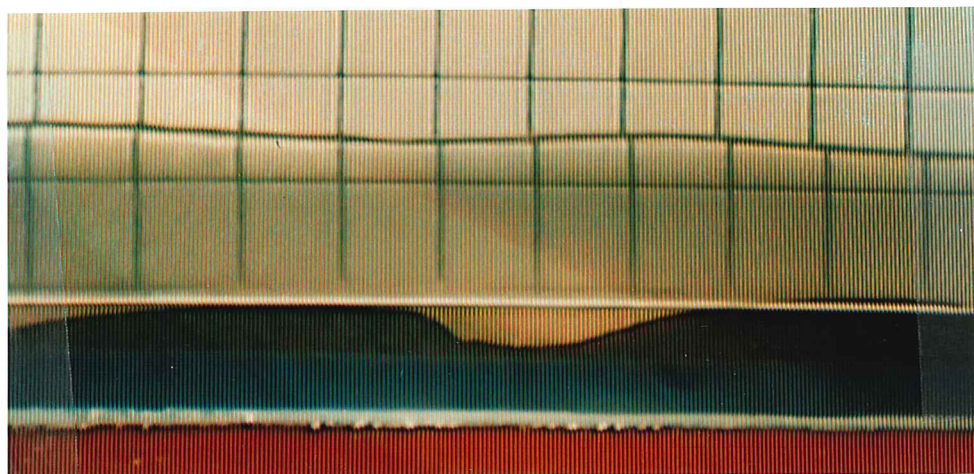
Fig. 13.4. Amplitude and phase development during an F = 0.5 test.
a: early stage, b: transitional stage, c: final stage.

The message from the above photographs is clearly this: The instability
responsible for the sand wave forms seen start up in the upper unstable
region with little or no interaction with the free surface (depending on F).
Gradually it develops towards longer wave lengths and stronger free
surface interaction. The phase shifts gradually from the potential theoretic
0° above to approximately 180° below the transitional condition as is again
predicted by potential theory.

From the point of view of the present theoretical model for bed layer stabil-
ity it may be remarked that the above observations compare relatively well
with the theoretical results. As presented in table 11.1 the phase of the
unstable eigenvalue $\theta^{(3)}_{21}$ shifts from zero above the transitional condition
to $- 2\pi/3$ right at it and into $-\pi$ below the condition.
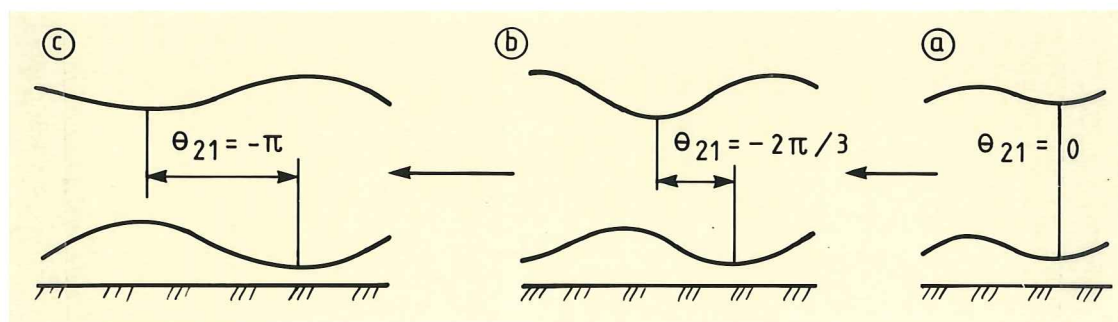
Fig. 13.5. Development of unstable perturbation according to the present
theory. a: upper unstable region.
b: transitional,
c: lower unstable region.

13.4. Superposed ripples.

A series of extra tests were performed for the only purpose of repeating
earlier test while doing the photographic job differently. A basic lesson to
be learnt from this is that the repeatability of such tests is not a matter of
a rough approach to test conditions. Even if the flow conditions were
repeated and controlled as exactly as possible the behaviour of the bed, in
fact essential parts of the lower region bed forms development, was
different from that in the first tests. The only parameter that could be
identified as slightly different from earlier was the sand particle
distribution. The content of the finer particles was less in the extra series,
as shown in figure 12.2.

The first part of the bed forms development was very similar to what we
had seen the first time. However, the stable dune pattern as shown in fig.
13.4.c was not obtained. In stead a continuously changing pattern of short
length wave forms (ripples) were seen existing together with larger dune -
like wave forms, as shown on the following picture, fig. 13.6.

Fig. 13.6. Ripples superposed on larger dune-like bed forms.

Such superposed ripples were not observed at all in the first series of tests. It is not intended to give any explanation of this here. We just point out what might be an essential point here, namely that the finer particle content of the bed sand influences the density profile of the flow. Hence the whole levelling of the lower instability region is altered, with reference to figure 10.3. One should expect the development at the bed to be different depending on approaching the zero growth rate limit, i.e. F^2 below $r/r+1$, or not, i.e. F^2 above this value.

13.5. Transition. Flat bed.

The transitional bed configuration consists of a partly flat bed, partly low-amplitude ("washed-out") dunes or ripples, according to the ASCE classification of section 2.1. The Froude number is typically in the range 0.8 - 1.0. The state of flat bed appears to be an ultimate state for this transitional configuration, i.e. F just below 1.0. The literature interpretes the flat bed as a stable configuration for the bed.

One test was run for F=0.8 to observe the typical features of the bed, the surface and the flow. The bed features were of low amplitude, of in-phase type, i.e. upper unstable region, propagated quickly downstream in comparison to the propagation velocities seen usually, and were accompanied by a high sediment transport rate. The ultimate state of flat bed is known also to be accompanied by a high sediment transport rate.

Again referring to figure 10.3 it should be noticed that the shear layer at the bed is strongly unstable for all wave lengths of the lower unstable region. Further it appears that the instability increases when the transition condition $F^2 = \text{th } kh_1/kh_1$ is approached from the lower side. In other words: we are faced with a situation where the traditional concept of bed stability is standing in sharp contrast to the state of stability of the shear layer just above the bed.

We have for this same reason – a strong lower region instability close to $F^2 = \text{th } kh_1/kh_1$ – used the term "transitional condition" about it, and will continue to do so.

13.6. The antidune test.

One single case of antidune generation was run. The flow rate was reduced from 5.4 l/s for the lower regime tests to 1.6 l/s in the antidune test. The Froude number was 1.1.

The bed waves generated corresponded to earlier descriptions of antidunes in that they
- occurred in groups of two or three waves
- in their first stage were almost nonprogressive but moving with increasing still small velocity upstream as they grew larger
- collapsed, particularly the front wave in the group, at a certain stage whereafter the growth and propagation development was more or less repeated
- had an in-phase relationship to the free surface
- were located in zone IV (fig. 10.1) of the $F - kh_1$ diagram.

14.   THEORY VERSUS EXPERIMENTS.

14.1.   An important remark.

It should be kept clearly in mind that the stability model discussed in
chapters 9 - 11 is a purely hydrodynamic one, i.e. strictly not one of
bed waves at all. It is therefore highly justified to ask about the
relevance of such a limitation. The present chapter will deal with this
and some other questions of basic nature, and of relevance to the
stability problem under discussion. Besides this a summary of agreement-
/disagreement results is given.

14.2. Nature of bed perturbation and erosion equation.

The erosion equation, orginally established by Exner, was met several times
in part I of this report, reading

$$\frac{\partial q_t}{\partial x} + (1-n) \frac{\partial n_3}{\partial t} = 0 \qquad\qquad (14.1)$$

where q_t is total horisontal sediment flux, n is bed porosity and n_3 the
bed perturbation.

The erosion equation expresses mathematically that horizontal gradients
in total sediment flux exist for one single reason namely an increase or
decrease of the sediment bed wave. In other words it excludes other
reasons for horizontal flux gradients.

Operating on total horizontal sediment flux the erosion equation is a
vertically integrated relation. This again means that it is basically an
equation for a hydraulic type of analysis.

A third aspect of the erosion equation is also emphasized, namely that
it is one of sediment continuity. The sediment bed is in other words
represented solely by a nondynamic relation in earlier analysis. A
continuity requirement of this type is of course part of a complete

analytical treatment. But in search for a responsible hydrodynamic instability the coupling to a "passive" bed is believed to be less important than the shear flow or free surface effects. On the other hand, when asking about the actual result over some time of such an instability, this coupling is likely to be most important. This point is further focused on by the following reasoning:

A perturbation of a sediment flow close to the bed will be subject to a "solidification" once it exists. By the term "solidification" we think about the settling of grains to form part of the underlying, from now on wavy bed. This property is solely one of granular beds, in opposition to fixed channel beds, and may be a key effect in the realisation of the bed wave development as a long term gradually changing process.

14.3. A comment on pure water flow and the maximum growth rate criterion.

The same basic hydrodynamic instability in pure water flow over a flat bed will more likely be dominated by phenomena of a more well defined wave length. This system is without the solidification effect and therefore more likely to give way for the perturbations of maximum growth rate. This, on the other hand, is to say that the maximum growth rate criterion does not apply in the case of bed wave development, at least not in its most simple version, leading to one particular wave length to be observed. The progressive character of bed wave development, which is considered by the author as an empirical fact, stands clearly in opposition to such a criterion.

14.4. Theory and experiments compared.

The alternative way to consider bed wave development is suggested by the chapter 9 - 11 theory, which in the same type of terminology might be called a small growth rate progressive process. In this respect the present theory and experiments seemingly agree. When looking further into the theoretical details we conclude by stating general agreement on the following points

- small propagation velocity
- small growth rate
- finite wave length
- significant instability effect of free surface.

One may further note that the K – H instability works without a free surface but then with a restricted instability range. Again this is in general agreement with well established experimental knowledge.

Amplitude ratios and phase relationships between bed and free surface are in broad terms observed as given by the theory. Threedimensional effects and peculiar phenomena like "lift up" are not included in the above statement.

A remarkable point is the seeming experimental confirmation of the high growth rate suddenly met just underneath the condition $F^2 = \text{th } kh_1/kh_1$ during progression from shorter to longer waves.

The fact that the interpretation of the subject instabilities is most meaningfully done in the $F – kh_1$ plane – a general agreement exists on this point – is by itself a strong indication of a K – H type of instability.

The above statements are general and qualitative. The experiments performed as part of this work do not allow stronger specific conclusion. Therefore the most important conclusion is the generally promising comparison between theory and experiments for lower range events. Improvements are certainly needed on ripple and antidune aspects.

15. LIMITATION OF THE PRESENT ANALYSIS. SUGGESTIONS FOR FURTHER WORK.

15.1. The analytical model.

15.1.1. Basic flow modelling.

A.J. Raudkivi in his stimulating 1983 paper proposes a basic velocity profile of approximately the same simplicity as the one applied here. The difference is a linearly decreasing velocity profile in the lower layer in Raudkivi's model, while the present model applies a concentrated velocity shear at a distance h_2 from the bed.
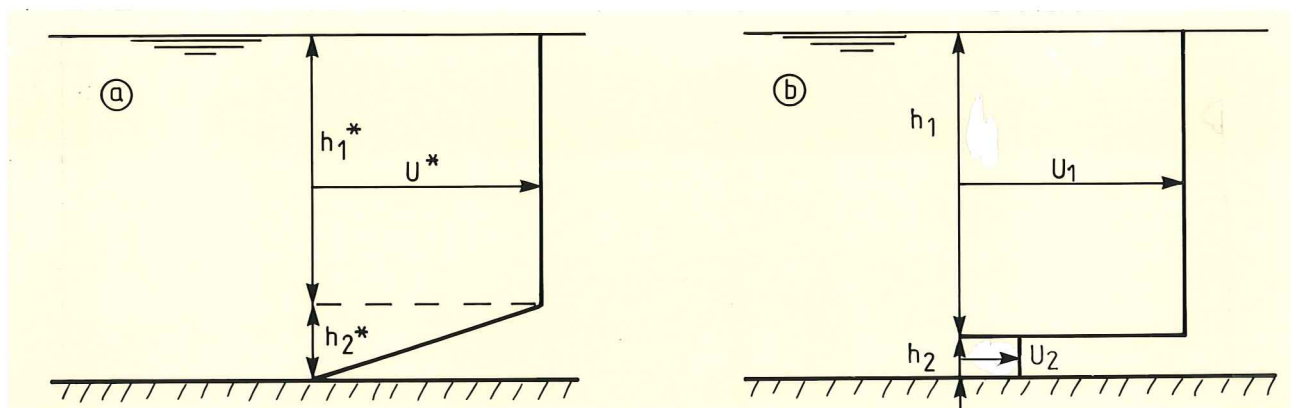
Fig. 15.5. Basic flow velocity profiles. a: Suggested by Raudkivi, b: present model.

The essential feature of bed shear is then included in both but modelled somewhat differently. The present model is chosen for analytic convenience. In any case a proper matching of the basic flow with the boundary layer at the bed is needed for a measure for h_2^* in model a as well as for h_2 in model b. A further comparison will have to await a stability analysis based on profile a.

15.1.2. Stability model development.

The present stability model suffers from a noncomplete description close to the transitional condition. Completeness here requires a continuous description of growth and propagation rates as well as amplitude ratio and phase when passing through. It seems possible to do this, once h_2 is given, by computerised eigenvalue analysis.

15.1.3. Sediment flow modelling.

The admittedly most serious limitation of the present stability model, considered as one for bed wave development, is the modelling of the sediment flow and the absence of erosional effects. This, it is the author's belief, accounts for the lack of success in explaining all aspects of the antidune behaviour. And a natural next step to take in further theoretical work along the present line would be to include the erosion effects in the analysis. Besides this a more complete modelling of the sedimentcarrying boundary layer at the bed should be attempted.

15.2. Experimental limitations.

The experimental rig used in the present qualitative tests of course has certain limitations. The flume is 15 cm wide and the wall boundary layers must be expected to have a slight influence on the flow conditions. The width is further smaller than the longest wave forms developed and may reduce the impression of threedimensionality of the bed features.

Another limitation of the test flume lies in its limited length plus arrangements at the upstream and downstream end of the test section. The upstream bottom edge at the beginning of the sand bed section tended to act as a local disturbance, and the development of bed waves usually started here. A flume dedicated to this type of tests would certainly have to be designed different from the one used in these respects.

15.3. Future experimental work.

It is emphasized that the subject studied here is one where theory and experiment should go "hand in hand". As in all hydrodynamic stability work the experimentation suggested by theoretical developments should be done with the best equipment available and under the most well controlled conditions possible. Along this way future steps towards improved understanding and description of bed waves should be taken. The number of tests to be made is likely to be high. However, the importance of the subject and the intriguing phenomena involved should guarantee strong efforts.

Among the topics emerging from this work will be a systematic variation of sand particle distribution, particularly the finer part, and observation of the accompanying development process. This will be a large experimental work by itself.

Refinements, experimentally as well as theoretically, should be the subject of critical judgement since no refinement is justified by itself. There obviously is a need to tie the flow instability problem stronger to the bed stability problem. Equipment for spatial correlation of flow disturbances (fluctuations) thus seems justified in future experimental work. Hereby a determination of wave lengths or correlation lengths is made possible. And this should be followed by an interpretation in $F - kh_1$ diagram.

A reinterpretation of the involved Froude number is desirable. The hydraulic way of stability analysis is conclusively invalid. A simple consequence of this is that experimental work should be undertaken to improve the understanding of the Froude number as a truly hydrodynamic parameter. This should be part of a work also aiming at further insight into the bed layer character, interaction with the free surface included.

16. SUMMARY AND FINAL REMARKS.

16.1. The granular bed stability problem.

The subject has developed from a stage of poor understanding and primitive theoretical description some decades ago, through a period of high analytical and experimental activity, up to the present day status where much empirical knowledge is available and where the analytical models have been refined considerably but still without offering a satisfactory explanation for the development of bed waves. The type of instability responsible for this development has not been convincingly demonstrated by any of the previous theories.

The most serious drawbacks of existing theories are:

- dependance on empirical and not generally valid relations for the sediment transport which need themselves separate theories for their own existence, and
- use of concepts and "laws" of developed flow providing a full decoupling from the basic hydrodynamic stability problem of the flow and obscuring the type of instability acting.

Experimentalists have been forced back to pure shear flow studies or single grain behaviour in shear flow. A full treatment and understanding of granular bed phenomea is very likely not possible without a simultaneous and fully valid handling of the flow stability problem.

16.2. The K – H mechanism and its relevance to the bed wave problem.

The earlier attempts in applying the K – H mechanism have, fully justified, been met with serious objections. On this basis the K-H instability seems to have been considered generally invalid in the analysis of granular bed stability.

Being aware of the limitations of the K – H theory and by using the generalisation of the K – H model as established, an analytical tool

considerably more useful than earlier one-degree-of-freedom formulas is now at hand. When applied to a system with bed shear and free surface several of the basic features of sand waves are demonstrated:

- small propagation velocity
- small growth rate
- finite wave length
- free surface instability effect
- acting without a free surface
- gradual development from shorter to longer waves

In addition specific results of K - H theory in this system seems to be supported by observations i.e. amplitude ratio and phase develpment. A sudden increase in instability of the flow during the gradual development from shorter to longer waves is predicted by the theory and seems to have a physical counterpart. The antidune development is not satisfactorily met by the present K - H model, nor is the development of ripples.

16.3. Final remarks.

Not only the antidune and ripple cases but indeed the whole subject calls for further theoretical and experimental work. The present work primarily points out a way of approach that seems to justify some optimism. In proceeding along the lines suggested the aim should be not only an improved description of the bed waves as roughness elements. Equally important is it to gain an extended understanding and improved calculational basis for the erosion, transportation and aggregation processes of granular materials.

If the belief of the author is justified, the present work may serve as a first step in this direction. And in the whole picture of sedimentary processes the bed waves will then prove to be limiting events or a materialisation of an asymptotically weak hydrodynamic instability, not necessarily all the way of K - H type, where the flow shear close to the bed as well as the main flow and a possible free surface all play essential roles in their generation.

REFERENCES.

ALLEN, J.R.L., 1968:   "Current ripples". North Holland Publishing Company, Amsterdam.

ANDERSON, A.G., 1953: "The characteristics of sediment waves formed by flow in open channels". Proc. third midw. Conf. in fluid mech., Minneapolis, pp. 329-395.

BENJAMIN, T.B., 1957: "Wave formation in laminar flow down an inclined plane". J. Fl. Mech. Vol.2, pp. 554 - 574.

BETCHOV, R. AND CRIMINALE, W.O., 1967: "Stability of parallel flows". Academic press, New York.

BRUUN, P. AND GERRITSEN, F., 1960: "Stability of coastal inlets". North Holland Publ. Comp.

BRUUN, P. 1966:   "Stability of coastal inlets, Vol. 2, Tidal inlets and littoral drift", Universitetsforlaget, Trondheim.

COMMITTEE ON SEDIMENTATION, TASK FORCE ON BED FORMS IN ALLU-VIAL CHANNELS; 1966: "Nomenclature for bed forms in alluvial channels". J. ASCE, Hy 3, pp. 51 - 64.

EINSTEIN, H.A. AND HUON LI, 1956: "The Viscous Sublayer Along a Smooth Boundary", ASCE, J. Eng. Mech. Div., Vol. 82, no. em 2.

EINSTEIN, H.A. AND CHIEN, N., 1955: "Effects of Heavy Sediment Concentration Near the Bed on Velocity and Sediment Distribution". U.S. Army Corps Engrs., Missouri River Div., Rep. Sediment. ser. no. 8.

ENGELUND, F., 1970:   "Instability of erodible beds". J.F. Mech., Vol. 42, No 2, pp. 225 - 244.

ENGELUND, F. AND FREDSØE, J., 1971: "Threedimensional stability analysis of open channel flow over an erodible bed". Nordic Hydrology, II, pp. 93 - 108.

ENGELUND, F. AND FREDSØE, J., 1974: "Transition from dunes to plane bed in alluvial channels". Series paper 4, inst. hydrod. and hydr. Eng., Lyngby, Denm.

ENGELUND, F. AND FREDSØE, J., 1982: "Sediment ripples and dunes". Ann, Rev. Fl. Mech., Vol. 14, pp. 13 - 37.

ENGELUND, F. AND HANSEN, E., 1972: "A monograph on sediment transport". Tekn. Forl., Copenhagen.

ENGELUND, F.A. AND HANSEN, E., 1966: "Investigations of flow in alluvial streams". Acta Polytechnica Scandinavica, Civ. Eng. and Bldg. Constr. Series no. 35, Copenhagen.

EXNER, F.M., 1925: "Über die Wechselwirkung zwischen Wasser und Geschiebe in Flussen". Sitzungsberichte der Akademie der Wissenschaften, Heft 3 - 4, Wien.

FREDSØE, J., 1979: "Unsteady flow in straight alluvial streams: Modification of individual dunes". J.FL. Mech., Vol. 91, part 3, pp. 497 - 512.

FREDSØE, J., 1981: "Unsteady flows in straight alluvial streams. Part2. Transition from dunes to plane bed". J. FL. Mech., Vol. 102, pp. 431 - 453.

FREDSØE, J., 1974: "On the development of dunes in erodible channels." J. FL. Mech., Vol. 64, Part I, pp. 1 - 16.

GRADOWCZYK, M.H., 1968: "Wave propagation and boundary instability in erodible - bed channels". J. FL. Mech., Vol. 33, Part1, pp. 93 - 112.

GRASS, A.J., 1974: "Transport of fine sand on a flat plate bed: Turbulence and suspension mechanics".Euromech. Coll. 48, Inst. Hydrodyn. and Hydraulic Eng., Tech. Univ. Denm., Lyngby, pp. 33 - 34.

GREENHILL, A.G., 1887: "Wave motion in hydrodynamics". Amer. J. of Math., Vol. 9, pp. 62 - 112.

GUY, H.P., SIMONS, D.B. AND RICHARDSON, E.V., 1966: " Summary of alluvial channel data from flume experiments 1956 - 61. U.S. Geological Survey, professional paper no. 462 - I, Governm. Print. off., Wash DC.

HAYASHI, T., 1970: " Formation of dunes and antidunes in open channels". J. ASCE, Hy2, pp. 357 - 366.

JACKSON, R.G., 1976: "Sedimentological and fluid dynamic implications of the turbulent bursting phenomenon in geophysical flows. J.FL. Mech., Vol. 77, part 3, pp. 531 - 560.

KENNEDY, J.F., 1963: "The mechanics of dunes and antidunes in erodible bed channels". J. FL. Mech., Vol. 16, part 4, pp. 521 - 544.

KENNEDY, J.F., 1969: "The formation of sediment ripples, dunes and antidunes". Ann. Rev. FL. Mech. Vol. 1, pp.- 147-168.

KNAPP, D.F. AND ROACHE, P.J., 1968: "A combined visual and hot - wire investigation on boundary layer transition". AIAA J., Vol. 6, pp. 29 - 36.

LAMB, H., 1932:   "Hydrodynamics". Cambridge Univ. Press.

LE BLOND, P.H. AND MYSAK, C.A., 1978: "Waves in the ocean". Elsevier oceanography series.

LEVI, E., 1981:   "An oscillatory approach to turbulence". Iutam symp. on turb. shear flows, Toulouse, pp. 348 – 358. ED.: R. Michel, J. Cousteix and. R. Houdeville, Springer.

LIN, C.C., 1967:   "The theory of hydrodynamic stability". Cambridge Monogr. Mech. and Appl. Math.

LIU, H-K., 1957:   "Mechanics of sediment ripple formation". J. ASCE, Hy 2, paper 1197.

LYSNE, D.K., 1969:   "Movement of sand in tunnels". J. ASCE, Hy 6, pp. 1835 – 1846.

MOLLO - CHRISTENSEN, E., 1971: " Physics of turbulent flow". AIAA J., Vol. 9, no. 7, pp. 1217 - 1228.

NYCHAS, S.G., HERSHEY, H.C. AND BRODKEY, R.S., 1973: "A visual study of turbulent shear flow". J. Fl. Mech, Vol. 61, part 3, pp. 513 - 540.

RAUDKIVI, A.J., 1966:   "Bed forms in alluvial channels". J. Fl. Mech., Vol. 26, part 3, pp. 507 - 514.

RAUDKIVI, A.J., 1967:   "Loose boundary hydraulics". Pergamon Press.

RAUDKIVI, A.J., 1983:   "Thoughts on ripples and dunes". Journ. of Hydraulic Research, 21, no. 4.

REYNOLDS, A.J., 1965:   "Waves on the erodible bed of an open channel". J. Fl. Mech., Vol. 22, part 1, pp. 113 - 133.

REYNOLDS, A.J., 1976:   "A decade's investigation of the stability of erodible stream bed". Nordic hydrology, Vol. 7, pp. 161 - 180.

RICHARDS, K.J., 1980:   "The formation of ripples and dunes on an erodible bed". J. Fl. Mech., Vol. 99, part 3, pp. 597 - 618.

SHIRASUNA, T., 1973:   "Formation of sand waves". Proc. 15 Congr.IAHR, pp. 107 - 114.

SUMER, B.M. AND DEIGAARD, R.M. 1981: "Particle motions near the bottom in turbulent flow in an open channel. Part 2." J. Fl. Mech no. 109, pp. 311.

YALIN, M.S., 1977:   "Mechanics of sediment transport". Pergamon Press.

YIH, C-S., 1976:   "Instability of surface and internal waves". Adv. Appl. Mech., Vol. 16, pp. 369 – 419.

YIH, C-S., 1980:   "Stratified flows". Academic Press.

APPENDIX A

ASYMPTOTIC EXPANSION OF EIGENVALUES

A-1. THE FINITE EIGENVALUE SOLUTION.

Starting with the eigenvalue equation

$$\{F^2(\xi-1)^2 - th\ kh_1/kh_1\}(r+1)\ F^2 th\ kh_1 \cdot \xi^2 =$$

$$- kh_2\ \{F^4\ th^2 kh_1(\xi-1)^4 - (r+1)\ F^2(th\ kh_1/kh_1)(\xi-1)^2$$

$$+ r(th\ kh_1/kh_1)^2\} + O\{(kh_2)^2\} \tag{A-1}$$

we will search the eigenvalues developed as an asymptotic expansion based on the smallness requirement $kh_2 \ll 1$. First we rewrite the above equation in a more tractable form as

$$\{\alpha(\xi-1)^2 + \beta\}\ \xi^2 = kh_2\ \{\gamma(\xi-1)^4 + \delta(\xi-1)^2 + \kappa\} \tag{A-2}$$

$$+ O\{(kh_2)^2\}$$

where the new symbols have the obvious definitions

$$\alpha = (r+1)F^4 th\ kh_1$$

$$\beta = -(r+1)F^2 th^2 kh_1/kh_1$$

$$\gamma = -F^4 th^2 kh_1$$

$$\delta = (r+1)F^2 th\ kh_1/kh_1$$

$$\kappa = -r(th\ kh_1/kh_1)^2 \tag{A-3}$$

The expansion parameter is defined as

$$\varepsilon = (kh_2)^{\frac{1}{2}} \tag{A-4}$$

and the eigenvalue expansion then is formulated by

$$\xi = \xi_0 + \xi_1\epsilon + \xi_2\epsilon^2 + \xi_3\epsilon^3 + - - - \tag{A-5}$$

From this we get the following derived expansions for higher powers of ξ:

$$\xi^2 = \xi_0^2 + 2\xi_0\xi_1\epsilon + (2\xi_0\xi_2 + \xi_1{}^2)\epsilon^2 + O\{\epsilon^3\}$$

$$\xi^3 = \xi_0^3 + 3\xi_0^2\xi_1\epsilon + 3\xi_0(\xi_0\xi_2 + \xi_1{}^2)\epsilon^2 + O\{\epsilon^3\}$$

$$\xi_4 = \xi_0^4 + 4\xi_0^3\xi_1\epsilon + 2\xi_0^2(2\xi_0\xi_2 + 3\xi_1{}^2)\epsilon^2 + O\{\epsilon_3\} \tag{A-6}$$

Hereby the eigenvalue equation (A-2) may be developed into

$$\xi_0^2 \{\alpha\xi_0^2 - 2\alpha\xi_0 + \alpha + \beta\}$$

$$+ \xi_0\xi_1\{4\alpha\xi_0^2 - 6\alpha\xi_0 + 2(\alpha + \beta)\} \epsilon$$

$$+ \{2\alpha\xi_0^2(2\xi_0\xi_2 + 3\xi_1{}^2) - 6\alpha\xi_0(\xi_0\xi_2 + \xi_1{}^2)$$

$$+ (\alpha + \beta)(2\xi_0\xi_2 + \xi_1{}^2)\}\epsilon^2$$

$$= \{\gamma\xi_0^4 - 4\gamma\xi_0^3 + (6\gamma+\delta)\xi_0^2 - 2(2\gamma+\delta)\xi_0 + \gamma + \delta + \kappa\}\epsilon^2$$

$$+ O\{\epsilon^3\} \tag{A-7}$$

The first term in the above expansion is of order ϵ^0 and determines the possible finite solutions for ξ:

$$\xi_0^2 \{\alpha\xi_0^2 - 2\alpha\xi_0 + \alpha + \beta\} = 0 \tag{A-8}$$

Here a double root is obviously

$$\xi_0^{(3,4)} = 0 \tag{A-9}$$

so that the two corresponding eigenvalues must be sought as higher order terms in the expansion. The two remaining roots of (A-8) are given by

$$\alpha \xi_0^2 - 2\alpha \xi_0 + \alpha + \beta = 0 \qquad\qquad (A-10)$$

or

$$\xi_0^{(1,2)} = 1 \pm (-\beta/\alpha)^{\frac{1}{2}}$$

$$= F^{-1}\{F \pm (th\ kh_1/kh_1)^{\frac{1}{2}}\} \qquad\qquad (A-11)$$

so determined provided $\xi_0 \neq 0$. This means that the possibility that $\xi_0 = 0$ given by the minus sign in (A-11) should be excluded from the solution.

We proceed a little further in finding higher order corrections to the finite eigenvalues (A-11). From the term of order ϵ in (A-7) we have

$$\xi_0 \xi_1 \{4\alpha \xi_0^2 - 6\alpha \xi_0 + 2(\alpha+\beta)\} = 0 \qquad\qquad (A-12)$$

Since ξ_0 now is different from zero and given by (A-11) the only solution to (A-12) is

$$\xi_1 = 0 \qquad\qquad (A-13)$$

which means that the finite eigenvalues have no correction terms of order $(kh_2)^{\frac{1}{2}}$. The ϵ^2 term in (A-7) may be used to determine a possible correction term of order kh_2. It is easily seen that the term is

$$\xi_2 = \{\gamma \xi_0^4 - 4\gamma \xi_0^3 + (6\gamma+\delta)\xi_0^2 - 2(2\gamma+\delta)\xi_0 + \gamma + \delta + \kappa\}.$$

$$\cdot \{4\alpha \xi_0^2 - 6\alpha \xi_0 + 2(\alpha+\beta)\}^{-1} \xi_0^{-1} \qquad\qquad (A-14)$$

where $\xi_1 = 0$ has now been used. A further development of ξ_2 by substitution of expressions for $\xi_0, \alpha, \beta, \gamma, \delta$ and κ will not be performed. In general the finite eigenvalues may then be written

$$\xi^{(1,2)} = F^{-1}\{F \pm (th\ kh_1/kh_1)^{\frac{1}{2}}\} + O\{kh_2\} \qquad\qquad (A-15)$$

where the second eigenvalue (minus sign) should not be allowed to approximate zero.

A-2. SMALL EIGENVALUES.

The determination of the small eigenvalues of equation (A-1) is most effectively performed by the direct (i.e. $\xi_o = 0$) expansion

$$\xi = \xi_1 \epsilon + \xi_2 \epsilon^2 + \xi^3 \epsilon^3 + \xi_4 \epsilon^4 + - - -$$

$$\xi^2 = \xi_1^2 \epsilon^2 + 2\xi_1\xi_2\epsilon^3 + (\xi_2^2 + 2\xi_1\xi_3)\epsilon^4 + - - -$$

$$\xi^3 = \xi_1^3 \epsilon^3 + 3\xi_1^2\xi_2\epsilon^4 + - - -$$

$$\xi^4 = \xi_1^4 \epsilon^4 + - - - \tag{A-16}$$

where as before $\epsilon = (kh_2)^{\frac{1}{2}}$. Development of the rewritten eigenvalue equation (A-2) now gives

$$(\alpha + \beta)\xi_1^2\epsilon^2$$

$$+ \{-2\alpha \ \xi_1^2 + 2(\alpha + \beta)\xi_2\}\xi_1\epsilon^3 =$$

$$(\gamma + \delta + \kappa)\epsilon^2$$

$$-2(2\gamma + \delta)\xi_1\epsilon^3 + O\{\epsilon^4\} \tag{A-17}$$

The ϵ^2 terms now determine a first approximation to the small eigenvalues by

$$(\alpha + \beta)\xi_1^2 - (\gamma + \delta + \kappa) = 0 \tag{A-18}$$

or

$$\xi_1^2 = (\gamma + \delta + \kappa)(\alpha + \beta)^{-1} \tag{A-19}$$

When (A-3) is used for substitution we find

$$\xi_1^{(3,4)} = \pm \, i\{F^4 - (r+1)F^2\text{cth } kh_1/kh_1 + r/(kh_1)^2\}^{\frac{1}{2}}.$$

$$\cdot \{(r+1)(F^2 - \text{th } kh_1/kh_1)F^2\text{cth } kh_1\}^{-\frac{1}{2}} \qquad (A-20)$$

This eigenvalue term may be purely imaginary or real depending on the variables in the brackets.

Proceeding to the terms of order ε^3 in (A-17) we determine the next term in the eigenvalue expansion by

$$\{-2\alpha\,\xi_1^2 + 2(\alpha + \beta)\xi_2 + 2(2\gamma+\delta)\}\xi_1 = 0 \qquad (A-21)$$

or, since $\xi_1 \neq 0$:

$$\xi_2 = \{\alpha\,\xi_1^2 - (2\gamma+\delta)\}(\alpha+\beta)^{-1}$$

$$= \{\alpha(\kappa-\gamma) - \beta(2\gamma+\delta)\}(\alpha+\beta)^{-2} \qquad (A-22)$$

when (A-19) is used. By the definitions (A-3) this gives the solution

$$\xi_2^{(3,4)} = \{F^4 - 2F^2\text{th } kh_1/kh_1+(kh_1)^{-2}\}.$$

$$\cdot \{(F^2 - \text{th } kh_1/kh_1)^2(r+1)\text{cth } kh_1\}^{-1} \qquad (A-23)$$

It is easily seen that both solutions $\xi_2^{(3,4)}$ are real and positive for all values of the variables involved.

As in the finite eigenvalue case we may proceed to higher order terms by first calculating ξ_3 from ε^4 terms in (A-17) and so on. We conclude by inspecting (A-17) that this can easily be done. We will, however, stop the development of the small eigenvalues at this stage. The solution so far developed then is

$$\xi^{(3,4)} = \pm i\{F^4 - (r+1)F^2\text{cth } kh_1/kh_1 + r/(kh_1)^2\}^{\frac{1}{2}}.$$

$$\cdot \; \{(r+1)(F^2 - \text{th } kh_1/kh_1)F^2\text{cth } kh_1\}^{-\frac{1}{2}} \cdot (kh_2)^{\frac{1}{2}}$$

$$+ \; \{F^4 - 2F^2\text{th } kh_1/kh_1 + 1/(kh_1)^2\} \; \cdot$$

$$\cdot \; \{(r+1)(F^2 - \text{th } kh_1/kh_1)^2\text{cth } kh_1\}^{-1} \cdot kh_2$$

$$+ \; O\{(kh_2)^{3/2}\} \tag{A-24}$$

The solution is not valid close to the condition where

$$F^2 = \text{th } kh_1/kh_1 \tag{A-25}$$

where the smallness requirement is contradicted. This case is considered separately in the following.

A-3. THE CASE F^2 = th kh_1/kh_1.

This case is investigated by starting from the following rewritten form of the eigenvalue equation (A-2):

$$\alpha(\xi-2)\xi^3 = kh_2\{\gamma(\xi-1)^4 + \delta(\xi-1)^2 + \kappa\} \tag{A-26}$$

where the parameters are defined as

$$\alpha = -\beta = (r+1)F^4 \text{ th } kh_1$$

$$\gamma = -F^4 \text{ th}^2 kh_1$$

$$\delta = (r+1) F^4$$

$$\kappa = -r F^4 \tag{A-27}$$

Inspection of (A-26) gives the finite solution

$$\xi^{(1)} = 2 + O\{kh_2\} \tag{A-28}$$

This is seen to be exactly the same solution as the one (positive root) found before in (A-15).

Inspection of (A-26) also leads to the following perturbation parameter

$$\varepsilon = (kh_2)^{1/3} \tag{A-29}$$

when small eigenvalues are searched.

The small eigenvalues are now searched by developing ξ as

$$\xi = \xi_1\varepsilon + \xi_2\varepsilon^2 + \xi_3\varepsilon^3 + --- \tag{A-30}$$

The developed powers ξ^2, ξ^3 and ξ^4 are found as before. After introduction of the developed forms in (A-26) we can write the eigenvalue equation as

$$- 2\alpha\, \xi_1^3 \epsilon^3 + \alpha\, \xi_1^2 (\xi_1^2 - 6\xi_2)\epsilon^4 =$$

$$(\gamma + \delta + \kappa)\epsilon^3 - 2(2\gamma+\delta)\xi_1\epsilon^4 + O\{\epsilon^5\} \qquad \text{(A-31)}$$

The terms of order ϵ^3 now give the solution

$$\xi_1^3 = -(\gamma + \delta + \kappa)(2\alpha)^{-1} \qquad \text{(A-32)}$$

which after introduction of (A-27) and some simplification gives the three first order eigenvalues as

$$\xi^{(n+2)} = e^{i(3-2n)\pi/3}\{(r+1)\text{sh } 2kh_1\}^{-1/3}\ (kh_2)^{1/3}$$

$$+ O\{(kh_2)^{2/3}\}\ ,\ n = 0,1,2 \qquad \text{(A-33)}$$

They obviously have the same first order absolute value

$$|\xi^{(n+2)}| = \{(r+1)\text{sh } 2kh_1\}^{-1/3}\ (kh_2)^{1/3} \qquad \text{(A-34)}$$

but separate arguments

$$\arg\ \{\xi^{(n+2)}\} = \pi/3,\ \pi,\ 5\pi/3 \qquad \text{(A-35)}$$

respectively. They are located in the ξ – plane as shown in the following figure
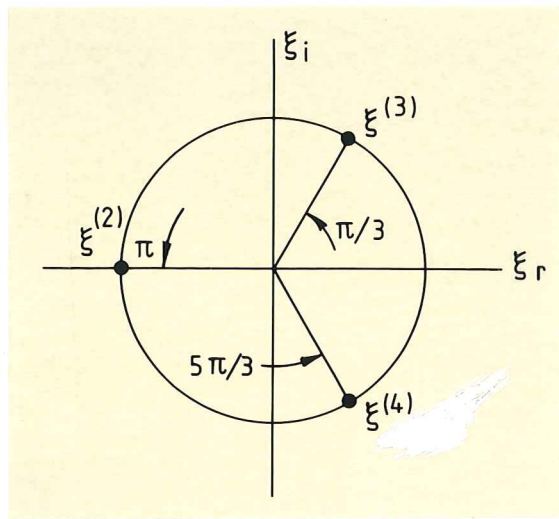
Fig.A-1. Eigenvalue solution in phase velocity plane for the case
$F^2 = $ th kh_1/kh_1.

One of the eigenvalues $\xi^{(2)}$, is real while the two others are complex conjugate.

For the purpose of physical interpretation we consider real and imaginary parts of the three eigenvalues. It is easily confirmed that the resulting formulas are

$$\xi_r^{(2)} = - \{(r+1)\text{sh } 2kh_1\}^{-1/3} (kh_2)^{1/3}$$

$$\xi_i^{(2)} = 0 \tag{A-36}$$

$$\xi_r^{(3)} = \tfrac{1}{2} \{(r+1)\text{sh } 2kh_1\}^{-1/3} (kh_2)^{1/3}$$

$$\xi_i^{(3)} = \tfrac{1}{2} \sqrt{3} \{(r+1)\text{sh } 2kh_1\}^{-1/3} (kh_2)^{1/3} \tag{A-37}$$

$$\xi_r^{(4)} = \xi_r^{(3)}$$

$$\xi_i^{(4)} = - \xi_i^{(3)} \tag{A-38}$$

Going back to (A-31) we may determine the next term in the development of small eigenvalues from the ε^4 coefficient as

$$\alpha \, \xi_1^4 - 6\alpha \, \xi_1^2 \xi_2 = 2(2\gamma+\delta)\xi_1 \qquad\qquad (A-39)$$

or

$$\xi_2 = \{2(2\gamma+\delta) + \alpha \, \xi_1^3\}(6\alpha \, \xi_1)^{-1} \qquad\qquad (A-40)$$

This is fully determined by the parameters α, γ, δ and κ together with the ξ_1 solution. We will not pursue the development of (A-40), but just conclude that the term generally exists for all three eigenvalues under discussion. We have then found the three small eigenvalues as

$$\xi^{(n+2)} = e^{i(3-2n)\pi/3}\{(r+1)\text{sh } 2kh_1\}^{-1/3} \, (kh_2)^{1/3}$$

$$+ \, O\{(kh_2)^{2/3}\}, \; n = 0,1,2 \qquad\qquad (A-41)$$

APPENDIX B

AMPLITUDE RATIO CALCULATIONS

B-1. FINITE EIGENVALUES.

With reference to chapter 11 the following developments are intended to give the details in calculating the final amplitude ratio (11.1). Starting by substitution of (9.14) into (11.2), we get

$$a_{21}^{(I)} = \text{ch } kh_1 \{\text{th } kh_1/kh_1 + O\{kh_2\}^{-1}\{Okh_2\}$$

$$= O\{kh_2\} \tag{B-1}$$

It is obvious that this includes both of the finite eigenvalues $\xi(1)$ and $\xi(2)$.

For the sake of control we also develop the alternative or interface amplitude ratio formula (11.3) for the same eigenvalues:

$$a_{12}^{(II)} = \text{ch } kh_1 \{(1-r) \text{ th } kh_1/kh_1 + O\{kh_2\}\} \cdot$$

$$\cdot \{\text{th } kh_1/kh_1 + O\{kh_2\}\}^{-1}$$

$$+ \text{ch } kh_1 \; \rho_2\rho_1^{-1} \text{ th } kh_1\{\text{th } kh_1/kh_1 + O\{kh_2\}^{-1}F^2\xi^2/kh_2$$

$$= (1-r)\text{ch } kh_1 + (1+r)\text{ch } kh_1 \cdot kh_1 \; F^2\xi^2/kh_2$$

$$+ O\{kh_2\} \tag{B-2}$$

We note that the term with kh_2 in the denominator is large, since ξ is finite while the first term is finite and the other terms are small. The last formula may now be inverted for comparison with (B-1), since $a_{12} \equiv a_{21}^{-1}$ by definition. This leads to

$$a_{21}^{(II)} = \{(1-r) + kh_1 \; F^2\xi^2/kh_2 + O\{kh_2\}\}^{-1}/\text{ch } kh_1$$

$$= \{kh_1 \text{ ch } kh_1 \; F^2\xi^3\}^{-1} \cdot kh_2 + O\{(kh_2)^2\} \tag{B-3}$$

This is then the explicit expression for the result (11.1)

B-2. SMALL EIGENVALUES.

The small eigenvalue case is treated in a similar way as the previous one. The amplitude ratio to be considered first is the one given by equation (11.2)

$$a_{21}^{(I)} = F^{-2}(\xi-1)^{-2} \text{ ch } kh_1 \{F^2(\xi-1)^2 - \text{th } kh_1/kh_1\} \quad (B-4)$$

which for eigenvalues satisfying $\xi = O\{(kh_2)^{\frac{1}{2}}\}$ obviously gives

$$a_{21}^{(I)} = F^{-2} \text{ ch } kh_1 \{F^2 - \text{th } kh_1/kh_1\} + O\{(kh_2)^{\frac{1}{2}}\} \quad (B-5)$$

It seems not obvious that formula (11.3) should give the same result as (B-5). A closer examination will therefore be given. According to (11.3) we should have

$$a_{12}^{(II)} = F^{-2}(\xi-1)^{-2} \text{ ch } kh_1 \{F^2(\xi-1)^2 - r \text{ th } kh_1/kh_1\}$$

$$+ \text{ ch } kh_1 (r+1) \text{ th } kh_1 (kh_2)^{-1} \xi^2(\xi-1)^{-2} \quad (B-6)$$

Again $\xi = O\{(kh_2)^{\frac{1}{2}}\}$, and by relation (10.20)

$$\xi^2 = -\xi_i^2 + O\{(kh_2)^{3/2}\} \quad (B-7)$$

Further substitution of formula (10.8)(repeated here)

$$\xi_i^2 = \{F^4 - (r+1)F^2 \text{ cth } kh_1/kh_1 + r/(kh_1)^2\} \cdot$$

$$\cdot \{(F^2 - \text{th } kh_1/kh_1)F^2 \text{ cth } kh_1(r+1)^{-1}\}kh_2 \quad (B-8)$$

for ξ_i^2 leads to

$$a_{12}^{(II)} = F^{-2} (F^2 - \text{th } kh_1/kh_1)^{-1} \text{ ch } kh_1 F^4(1-\text{th}^2 kh_1)$$

$$+ O\{(kh_2)^{\frac{1}{2}}\}$$

$$= F^2(F^2 - \text{th } kh_1/kh_1)^{-1} \text{ ch } kh_1 + O\{(kh_2)^{\frac{1}{2}}\} \quad (B-9)$$

And finally this result may be inverted, remembering that $a_{21} = a_{12}^{-1}$, to give

$$a_{21}^{(II)} = F^{-2} \text{ ch } kh_1(F^2 - \text{th } kh_1/kh_1) + O\{(kh_2)^{\frac{1}{2}}\} \quad (B-10)$$

which is seen to be identical to (B-5). Again it should be remembered that the small eigenvalue solution is not valid at the transition condition $F^2 = \text{th } kh_1/kh_1$. The corresponding amplitude ratio solution should be treated specially as was the eigenvalue solution. This is done in the following.

B-3. THE CASE $F^2 = $ th kh_1/kh_1.

The finite eigenvalue case is included in the results (B-1) and (B-3). We therefore go to the three small eigenvalues for particular evaluation of the amplitude ratio along the condition $F^2 = $ th kh_1/kh_1.

From the free surface equation (B-4) we get

$$a_{21} = F^{-2} \text{ ch } kh_1 \{F^2 - (1-\xi)^{-2} \text{ th } kh_1/kh_1\}$$

$$= F^{-2} \text{ ch } kh_1 \{F^2 - \text{th } kh_1/kh_1 - 2\xi \text{ th } kh_1/kh_1\} + \cdots$$

$$= - 2 \text{ ch } kh_1 \ \xi + \cdots \tag{B-11}$$

Corresponding to the three eigenvalues (A-33) we now get the three amplitude ratios as

$$a_{21}^{(n+2)} = - 2 \text{ ch } kh_1 \ e^{i(3-2n)\pi/3}\{(r+1)\text{sh } 2kh_1\}^{-1/3}(kh_2)^{1/3}$$

$$+ O\{(kh_2)^{2/3}\}, \quad n = 0,1,2 \tag{B-12}$$

All three are of the same order in kh_2, namely

$$a_{21}^{(n+2)} = O\{(kh_2)^{1/3}\}, \quad n = 0,1,2 \tag{B-13}$$

It is emphasized that the superscript $(n+2)$ now refers to the respective eigenvalue found in App. A.

We also note that two of the amplitude ratios are complex. Their locations in an Argand diagram for amplitude ratios are as shown in the following figure.
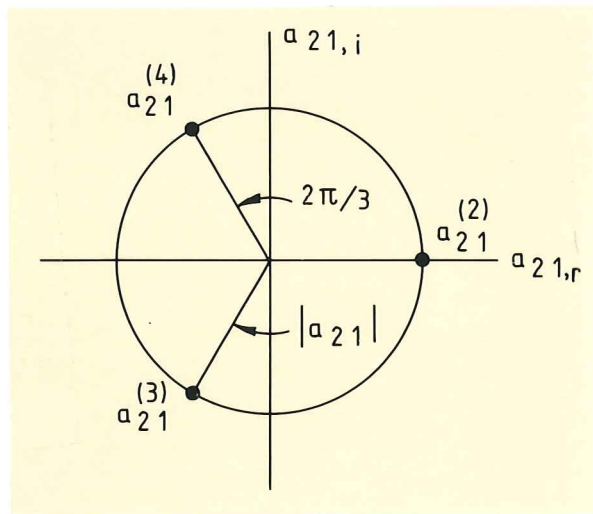
Fig.B-1. Amplitude ratio solutions for the case $F^2 = $ th kh_1/kh_1.

In particular the phase differences defined at the end of section 8.1 are given as

$$\theta_{21}^{(2)} = 0$$

$$\theta_{21}^{(3)} = -2\pi/3$$

$$\theta_{21}^{(4)} = 2\pi/3 \qquad\qquad (B-14)$$

It is easily confirmed that the interface equation (B-6) gives exactly the same result for the amplitude ratio. The last term in (B-6) is the significant one being of order $(kh_2)^{-1/3}$. By inversion we have

$$a_{21} = \{(r+1)\text{sh } kh_1 \ \xi^2\}^{-1} \ . \ kh_2 + \text{H.O.T.}$$

$$= -2 \text{ chkh}_1 \ \xi + \text{H.O.T.} \qquad\qquad (B-15)$$

by using that $\xi^3 = -\{(r+1)\text{sh } 2kh_1\}^{-1} \ . \ kh_2$.

Higher order terms, H.O.T. in the short notation of (B-15), are not shown explicitly here. Besides this the result (B-15) is identical to (B-11) from the free surface equation.